

# Magnetic Tweezers Based Force Spectroscopy Studies of the Structure and Dynamics of Nucleosomes and Chromatin

Proefschrift

ter verkrijging van

de graad van Doctor aan de Universiteit Leiden,

op gezag van Rector Magnificus prof.mr. P.F. van der Heijden,

volgens besluit van het College voor Promoties

te verdedigen op donderdag 1 oktober 2009

klokke 13:45 uur

door

**Maarten Christiaan Kruithof**

geboren te Andernach (Duitsland),

in 1980

**Promotiecommissie**

Promotor: Prof. Dr. T. Schmidt  
Co-promotor: Dr. Ir. J. van Noort  
Overige Leden: Prof. Dr. N. Dekker  
Prof. Dr. M. Noteborn  
Prof. Dr. J. van Ruitenbeek  
Prof. Dr. H. Schiessel  
Dr. R. Seidel  
Dr. G. Wuite

Casimir PhD Series, Delft-Leiden, 2009-10

ISBN 978-90-8593-057-0

An electronic version of this thesis can be found at <https://openaccess.leidenuniv.nl>

Dit werk wordt financieel gesteund door de Nederlandse Organisatie voor Wetenschappelijk Onderzoek (NWO).

This thesis is dedicated to my son Chris.



---

# CONTENTS

<b>1</b>	<b>Introduction</b>	<b>1</b>
1.1	DNA Compaction by Nucleosomes . . . . .	4
1.2	Single Molecule Force Spectroscopy . . . . .	4
1.3	Magnetic Tweezers . . . . .	5
1.4	Nucleosome and Chromatin Properties . . . . .	6
1.5	Overview of the Thesis . . . . .	7
	Bibliography . . . . .	8
<b>2</b>	<b>Sub-Piconewton Dynamic Force Spectroscopy Using Magnetic Tweezers</b>	<b>11</b>
2.1	Introduction . . . . .	12
2.2	Materials and Methods . . . . .	13
2.3	Validation of the method . . . . .	15
2.4	Energy analysis . . . . .	20
2.5	Dynamic force spectroscopy on nucleosome-nucleosome interactions . . . . .	21
2.6	Conclusion . . . . .	23
	Bibliography . . . . .	23

<b>3</b>	<b>Hidden Markov Analysis of Nucleosome Unwrapping Under Force</b>	<b>25</b>
3.1	Introduction . . . . .	26
3.2	The Probability Distribution of the End-To-End distance of a DNA-Bead System	28
3.3	Brownian Dynamics Simulations . . . . .	30
3.4	Analysis of Mono-nucleosome Unwrapping Under Force . . . . .	33
3.5	Structural Implications . . . . .	36
3.6	Conclusion . . . . .	38
3.7	Appendix: The Effect of Camera Filtering on the Measured Height Fluctuations of a Bead in a Trap . . . . .	40
	Bibliography . . . . .	45
<b>4</b>	<b>Single Molecule Force Spectroscopy Reveals a Highly Compliant Helical Folding for the 30 nm Chromatin Fiber</b>	<b>49</b>
4.1	Introduction . . . . .	51
4.2	Results . . . . .	52
4.3	Discussion . . . . .	66
	Bibliography . . . . .	72
<b>5</b>	<b>Thermal Fluctuations of Neighbouring Nucleosomes increase Nucleosome Stability</b>	<b>77</b>
5.1	Introduction . . . . .	78
5.2	A Model for a Single Nucleosome Under Force . . . . .	79
5.3	The Effect of Thermal Motion on Wrapping Dynamics . . . . .	83
5.4	Comparison With Experiments on Mononucleosomes . . . . .	84
5.5	Contributions of Neighbouring Nucleosomes . . . . .	85
5.6	Second Turn Unwrapping . . . . .	87
5.7	Rupture Forces Depend on Force Fluctuations . . . . .	88
5.8	Conclusion . . . . .	90
	Bibliography . . . . .	90

<b>Summary</b>	<b>95</b>
<b>Samenvatting</b>	<b>97</b>
<b>Curriculum Vitae</b>	<b>101</b>
<b>List of Publications</b>	<b>103</b>





---

---

# CHAPTER 1

---

## Introduction

Living organisms are built from a large number of cells. These cells continuously respond to signals from outside and inside the cell by producing various kinds of proteins. The blueprints of all proteins are stored in genes. In eukaryotic cells, genes are carried in chromosomes, threadlike structures in the nucleus of a cell that become visible when the cell, upon dividing condenses these structures (Fig. 1.1a). The typical X shape of the completely condensed chromosomes becomes visible when they are isolated from a cell in mitosis (Fig. 1.1b). Chromosomes consist of two parts: DNA, carrying the genetic information of the cell and proteins. The protein components of chromosomes function largely to package and control the long DNA molecules. Recently it has become clear that the dynamics of DNA compaction are vital for the function of a cell. The size of a polymer in solution is generally given by the radius of gyration, which is, for a biological polymer such as DNA, given by  $R = \sqrt{Lp/3}$  with  $L$  its contour length and  $p$  its persistence length, known to be about 50 nm for DNA. Without compaction, the radius of gyration of the 2 meters of DNA in a human cell would be around 180  $\mu\text{m}$  and would never fit into a cell nucleus which has a typical radius of several micrometers. Furthermore, DNA is compacted even more at each cell division when chromosomes have to be divided between the two new daughter cells. This packing has to be done in an orderly fashion so that the chromosomes can be replicated correctly at each cell division. On the other hand, DNA needs to be accessed for the expression of genes. Genes can be controlled by regulation of the compaction of DNA. For a complete understanding of the regulation of

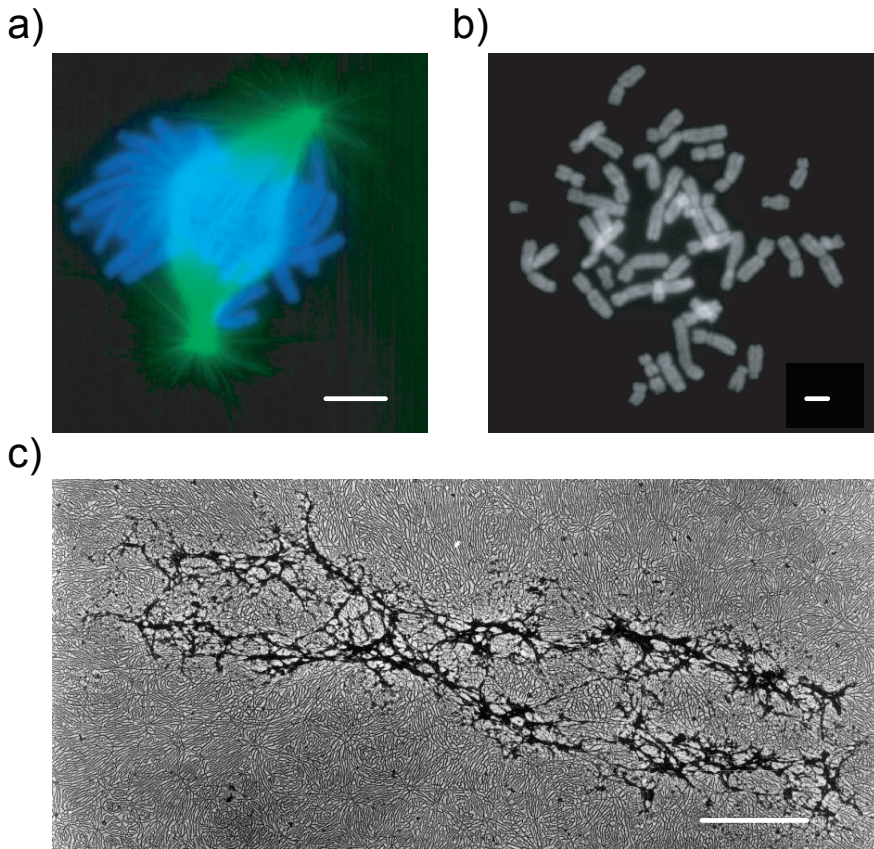


Figure 1.1: *Chromosomes in eukaryotic cells. All scale bars are 2  $\mu\text{m}$ . (a) A fluorescence image of a cell during mitosis, the mitotic spindles are shown in green and the chromosomes in blue. (b) Fully condensed chromosomes extracted from an eukaryotic cell, showing the well known X shape. (c) An electron microscopy image of a chromosome where all proteins are denatured [1]. The chromosome scaffold (black) and the uncondensed DNA (grey) are visible.*

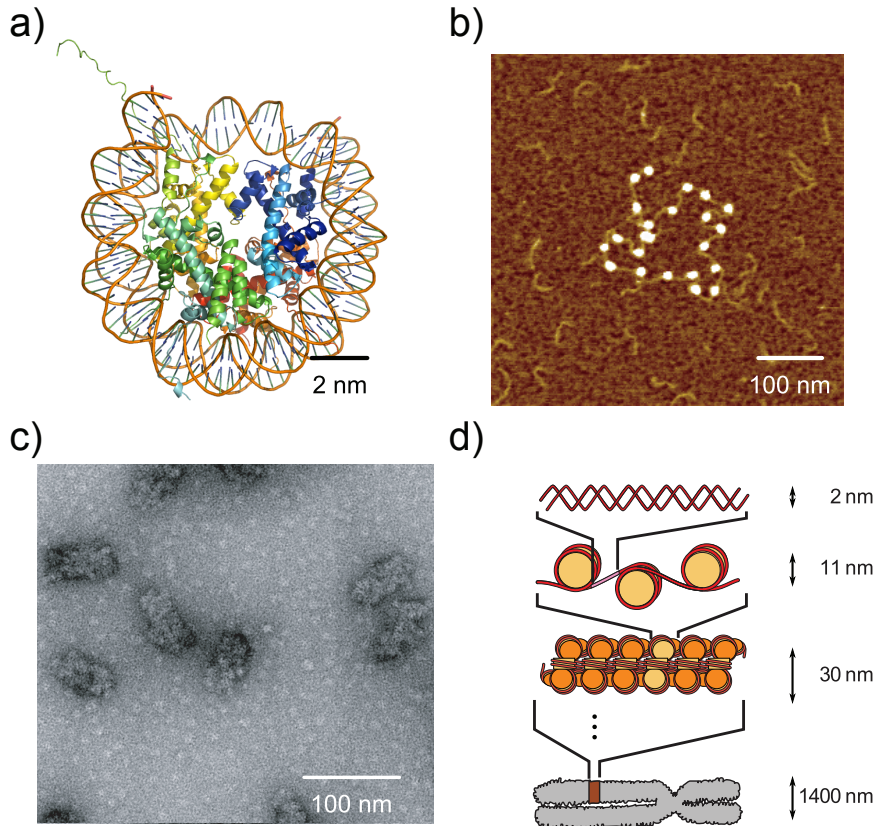


Figure 1.2: Nucleosomes and their organisation in eukaryotic cells. (a) The nucleosome crystal structure shows 147 base pairs of DNA wound in 1.65 turns around a histone octamer [2]. (b) An atomic force microscopy image of 23 nucleosomes on a single DNA molecule. This is known as the beads-on-a-string configuration. (c) Chromatin fibers of 65 nucleosomes as imaged by electron microscopy. The nucleosomes are folded in the so called 30 nm fiber [3]. (d) A schematic overview of chromosome folding. The DNA is wound around histone octamers, forming nucleosomes, which are regularly spaced on the DNA. In vitro, at physiological salt conditions, these arrays fold into a 30 nm fiber. After several, as of yet unknown, higher order folding steps, the DNA folds into a chromosome.

DNA compaction, we need to understand, at molecular detail, not only the structure but also the dynamics of this compaction.

## 1.1 DNA Compaction by Nucleosomes

At the first level, DNA is compacted by specific proteins, called histones. When these proteins are denatured, the DNA inside a chromosome expands dramatically, as depicted in Fig. 1.1c, indicating that the compaction and thus accessibility of DNA is regulated by these proteins. The histone DNA complex consists of eight histone proteins (dimers of H2A, H2B, H3 and H4) that wrap 147 bp of DNA in a helical fashion (Fig. 1.2a) [2]. The histone-DNA complex is called a nucleosome. Nucleosomes are regularly spaced along the DNA. When deposited on a surface from low ionic strength buffers, nucleosome arrays appear as beads-on-a-string like structures (Fig. 1.2b). A fifth species of histone proteins, called linker histones (H1 and H5), also play a role in the DNA compaction. They are known to constrict the DNA exiting the nucleosome, thereby stabilizing the structure of the nucleosome. Nucleosomes are spaced typically 10 – 90 bp by linker DNA [4]. *In vitro*, under physiological conditions nucleosome arrays fold into compact fibres, called chromatin, with a diameter of about 30 nm (Fig. 1.2c) [5–7]. A schematic overview of this DNA compaction is shown in Fig. 1.2d. Although the general structure of DNA compaction is known, the exact structure of the 30 nm fiber and the dynamics of the wrapping of DNA into nucleosomes, remain elusive despite three decades of intense research [7–9].

## 1.2 Single Molecule Force Spectroscopy

In this thesis, single molecule force spectroscopy is used to study the dynamic properties of nucleosomes and chromatin. It is especially suited to determine properties such as the forces and energies at which the chromatin structure is disrupted. In a typical force spectroscopy experiment, shown in Fig. 1.3a, a force is applied to a molecule of interest, usually DNA or RNA, and the extension of the molecule is measured. Force spectroscopy can be divided into two categories. In force clamp experiments the molecule of interest is stretched at a constant force to observe transient behavior of the molecule itself or proteins interacting with the molecule. In dynamic force spectroscopy experiments the position of the end of the molecule is changed during the experiments, to probe the energy landscape of the molecule of interest. The force can be applied using a magnetic bead and an external pair of magnets (magnetic tweezers), a latex bead and a focused laser beam (optical tweezers) or an atomic force microscopy tip. The

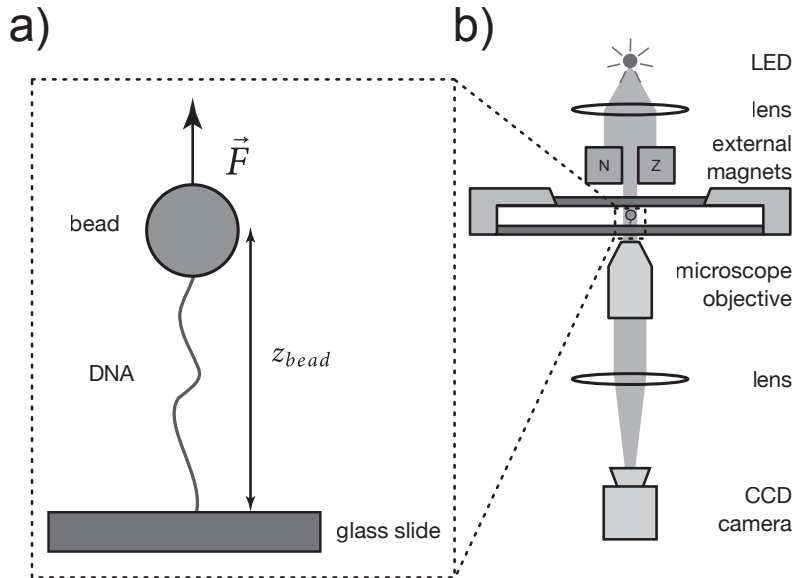


Figure 1.3: *Schematic overview of a force spectroscopy experiment. (a) A DNA molecule is attached to a bead on one end and to a glass slide on the other end. The molecule is stretched by an external force  $F$  and the height of the bead,  $z_{bead}$  is measured. (b) A schematic overview of the magnetic tweezers setup. Two external magnets apply a force to the magnetic beads in the sample. The bead is imaged on a CCD camera with an objective and a lens. A LED is used as the light source.*

dynamic range of these three force spectroscopy techniques is 0.05–30 pN for magnetic tweezers, 1–100 pN for optical traps and 10–1000 pN for the atomic force microscope. Hydrophobic and electrostatic forces dominate the interaction between nucleosomes in chromatin and between DNA and histones. These forces are in the order of several piconewtons, which makes magnetic tweezers the most suitable candidate for the force spectroscopy experiments on chromatin.

### 1.3 Magnetic Tweezers

In this thesis we used magnetic tweezers as a tool to perform force spectroscopy experiments. For these experiments we need to be able to apply a force to a molecule and quantify this force. We also need to be able to measure the extension of the molecule. Using two external magnets and a magnetic bead which is anchored to a molecule attached to the glass slide we can apply a force to the molecule as is depicted in Fig. 1.3b. The bead is imaged using a microscope

objective on a CCD camera (Fig. 1.3b). The three dimensional position of the bead is calculated from this image, with an accuracy of  $3 \text{ \AA}/\sqrt{\text{Hz}}$ , using home built software. The extension of the molecule can be calculated from the position of the bead and the applied force is calculated from the height of the bead  $z$  and the variance of the motion of the bead in the lateral direction  $\langle \Delta x^2 \rangle$  using equipartition

$$F = \frac{k_b T z}{\langle \Delta x^2 \rangle},$$

with  $k_b$  Boltzmann's constant and  $T$  the temperature.

## 1.4 Nucleosome and Chromatin Properties

Cui and Bustamante [10] were the first to investigate chromatin fibers purified from chicken blood with force spectroscopy using optical tweezers. They found that at forces higher than 20 pN the chromatin structure is irreversibly modified by the removal of histone cores from the native chromatin. Bennink *et al.* [11] investigated chromatin that was formed on  $\lambda$ -DNA from *Xenopus* egg extract. They found distinct steps of 65 nm, at forces between 20 and 40 pN, which they attribute to the unwrapping of DNA from the nucleosome. Brower-Toland *et al.* [12] studied artificial fibers where the nucleosomes were exactly positioned. They found that DNA unwraps from the nucleosome in two steps, at low forces ( $\sim 6$  pN) 25 nm of DNA releases from the nucleosome and at high forces ( $> 20$  pN) another 25 nm unwraps. If the high force was maintained for a long time, the histones would dissociate from the DNA. More recently, Pope *et al.* [13] calculated the energy barrier for unwrapping DNA from nucleosomes in chromatin fibers created from  $\lambda$ -DNA and *Xenopus* egg extract. They found an energy barrier of approximately  $25 k_b T$  for the unwrapping of 30 nm of DNA from a nucleosome at forces exceeding 15 pN, indicating that the second turn of DNA wound around the nucleosome is very tightly bound. A more detailed study by Mihardja *et al.* [14] on single nucleosomes showed that the first turn of DNA starts to unwrap at 2 pN and the second turn at 7 pN. Furthermore, they found that nucleosome is indeed a very stable structure, as exemplified by the lifetime of the fully wrapped state (2500 s) compared to the lifetime of the one turn unwrapped state (0.02 s). These experiments show that at forces larger than several pN the DNA starts to unwrap from the histone core. At lower forces the nucleosome-nucleosome interactions, which have a reported interaction energy of  $3.4 k_b T$  [10], are broken. In conclusion we know that when stretching chromatin, first the nucleosome-nucleosome interactions are disrupted, with a reported energy of  $3.4 k_b T$ , then the DNA unwraps from the nucleosome in two steps of approximately 25 nm .

## 1.5 Overview of the Thesis

**Dynamic Force Spectroscopy using Magnetic Tweezers.** In chapter 2 we introduce dynamic force spectroscopy for magnetic tweezers. The magnetic force in these experiments is calibrated from the magnet position. This allows us to apply and detect forces in real-time. We found that viscous drag dominates the motion of the magnetic bead at low forces. We analyzed the effects of the bead size, DNA contour length, DNA persistence length and magnet velocity on the drag, leading to the conditions under which the drag does not interfere with the measurements. Using this method we have reduced the measurement times by two orders of magnitude compared to traditional quasi-static force spectroscopy. We used this method to measure the transient interactions of sub saturated chromatin fibers.

**Forced Extension of Mononucleosomes.** In chapter 3 we measured the spontaneous wrapping and unwrapping of DNA from nucleosomes under constant force. We analyzed the resulting time traces using a hidden Markov model. We calculated the probability density of DNA under force and used this probability density in the hidden Markov analysis. This increased the accuracy of the step detection compared to a normal probability distribution especially at small stepsizes compared to the thermal motion of the bead. We were able to extract lifetimes of the wrapped and unwrapped state of the nucleosome. Furthermore we found that the angle from which the DNA extension exits the nucleosome affects the probability distribution of the DNA and we were able to extract this angle before and after unwrapping.

**Forced Extension of Chromatin.** In chapter 4 we used magnetic tweezers to probe the mechanical properties of a single, well-defined array of 25 nucleosomes. When folded into a 30 nm fibre, representing the first level of chromatin condensation, the fibre stretched like a Hookian spring. The extensive linear stretching of the fiber pointed to a solenoid as the underlying topology of the 30 nm fibre. Surprisingly, we found that linker histones do not affect the length or stiffness of the fibres, but stabilize fibre folding. We also were able to measure the nucleosome-nucleosome stacking energy and found it to be five times higher than previously reported.

**The Effect of Tether Stiffness on Nucleosome Stability.** In chapter 5 we investigated the discrepancy between the unwrapping force found between single nucleosome and chromatin fiber experiments, where the fiber unwraps at a much higher force than the single nucleosome. We found that the asymmetric energy landscape of nucleosome unwrapping and the force fluctuations in tethered particle experiments decreases the lifetimes of the wrapped and unwrapped state significantly. We also found that the stiffness of the DNA surrounding the nucleosome is largely responsible for the decrease in lifetime. The difference in stiffness of the DNA surrounding a single nucleosome and a nucleosome in a fiber explains the large differ-

ence in unwrapping force that is observed between force spectroscopy experiments on fibers and mononucleosomes.

## Bibliography

- [1] J. R. Paulson and U. K. Laemmli, "The structure of histone-depleted metaphase chromosomes," *Cell*, vol. 12, pp. 817–28, Nov 1977.
- [2] K. Luger, A. W. Mäder, R. K. Richmond, D. F. Sargent, and T. J. Richmond, "Crystal structure of the nucleosome core particle at 2.8 Å resolution," *Nature*, vol. 389, pp. 251–60, Sep 1997.
- [3] A. Routh, S. Sandin, and D. Rhodes, "Nucleosome repeat length and linker histone stoichiometry determine chromatin fiber structure," *Proc. Natl. Acad. Sci. U.S.A.*, vol. 105, pp. 8872–7, Jul 2008.
- [4] J. Widom, "A relationship between the helical twist of dna and the ordered positioning of nucleosomes in all eukaryotic cells," *Proc. Natl. Acad. Sci. U.S.A.*, vol. 89, pp. 1095–9, Feb 1992.
- [5] F. Thoma, T. Koller, and A. Klug, "Involvement of histone h1 in the organization of the nucleosome and of the salt-dependent superstructures of chromatin," *J Cell Biol*, vol. 83, pp. 403–27, Nov 1979.
- [6] J. Widom and A. Klug, "Structure of the 300Å chromatin filament: X-ray diffraction from oriented samples," *Cell*, vol. 43, pp. 207–13, Nov 1985.
- [7] P. J. J. Robinson and D. Rhodes, "Structure of the '30 nm' chromatin fibre: a key role for the linker histone," *Curr Opin Struct Biol*, vol. 16, pp. 336–43, Jun 2006.
- [8] J. Widom, "Toward a unified model of chromatin folding," *Annual review of biophysics and biophysical chemistry*, vol. 18, pp. 365–95, Jan 1989.
- [9] D. J. Tremethick, "Higher-order structures of chromatin: the elusive 30 nm fiber," *Cell*, vol. 128, pp. 651–4, Feb 2007.
- [10] Y. Cui and C. Bustamante, "Pulling a single chromatin fiber reveals the forces that maintain its higher-order structure.," *Proc. Natl. Acad. Sci. U.S.A.*, vol. 97, pp. 127–32, Jan 2000.
- [11] M. Bennink, S. H. Leuba, G. H. Leno, J. Zlatanova, B. G. de Groot, and J. Greve, "Unfolding individual nucleosomes by stretching single chromatin fibers with optical tweezers.," *Nat. Struct. Biol.*, vol. 8, pp. 606–10, Jun 2001.



- [12] B. D. Brower-Toland, C. L. Smith, R. C. Yeh, J. T. Lis, C. L. Peterson, and M. D. Wang, “Mechanical disruption of individual nucleosomes reveals a reversible multistage release of dna,” *Proc. Natl. Acad. Sci. U.S.A.*, vol. 99, pp. 1960–5, Feb 2002.
- [13] L. H. Pope, M. Bennink, K. A. van Leijenhorst-Groener, D. Nikova, J. Greve, and J. F. Marko, “Single chromatin fiber stretching reveals physically distinct populations of disassembly events,” *Biophys. J.*, vol. 88, pp. 3572–83, Feb 2005.
- [14] S. Mihardja, A. Spakowitz, Y. Zhang, and C. Bustamante, “Effect of force on mononucleosomal dynamics,” *Proc. Natl. Acad. Sci. U.S.A.*, vol. 103, pp. 15871–6, Oct 2006.



---

---

## CHAPTER 2

---

# Sub-Piconewton Dynamic Force Spectroscopy Using Magnetic Tweezers<sup>1</sup>

### Abstract

We introduce a simple method for dynamic force spectroscopy with magnetic tweezers. This method allows application of sub-piconewton force and twist control, by calibration of the applied force from the height of the magnets. Initial dynamic force spectroscopy experiments on DNA molecules revealed a large hysteresis that is caused by viscous drag on the magnetic bead and which will conceal weak interactions. Using smaller beads this hysteresis is sufficiently reduced to reveal intra-molecular interactions at sub-piconewton forces. Compared to typical quasi-static force spectroscopy a significant reduction of measurement time is achieved, allowing the real time study of transient structures and reaction intermediates. As a proof of principle nucleosome-nucleosome interactions on a sub-saturated chromatin fiber were analyzed.

---

<sup>1</sup>This chapter is based on the article: *Sub-piconewton Dynamic Force Spectroscopy Using Magnetic Tweezers* M. Kruithof, F. Chien, M. de Jager and J. van Noort, *Biophysical Journal*, 94 (6) 2343 - 2348

## 2.1 Introduction

To probe the mechanics of biomolecules at the single molecule level a variety of force spectroscopy techniques have been developed. This includes Optical Tweezers (OT), Magnetic Tweezers (MT), and Atomic Force Microscopy (AFM) [1]. With these techniques the energy landscape of biological bonds can generally be resolved accurately by applying an increasing force on a molecule and measuring its extension in time. Evans and Ritchie showed that careful analysis of the rupture force as a function of the force loading rate reveals both the interaction distance and the energy barrier of a molecular bond [2]. The energy dissipated by the rupture can be quantified from the hysteresis in a Force-Distance (F-D) cycle. For such dynamic force spectroscopy experiments OT and AFM are well suited as they both combine a position trap with nanometer resolution manipulation. However, the high spring constants of these traps in combination with the Brownian fluctuations limit the force accuracy of these techniques to approximately 1 pN for OT and 10 pN for AFM.

In contrast, MT, comprising a pair of permanent magnets in combination with a paramagnetic bead can be characterized as force clamps as they do not fix the position of the trapped bead but the applied force. The effective stiffness of the trap depends on the compliance of the polymer that tethers the bead to the surface. The applied force is calculated from the Brownian motion of the bead using equipartition theory. As a consequence of the high compliance of the tether, forces down to 10 fN are experimentally accessible, as shown by Strick et al. for example [3]. MT also clamp and constrain the rotation of the bead, giving a unique handle on DNA topology, for example. These features have made MT an indispensable tool to reveal many of the mechanical properties of DNA and DNA interacting proteins like topoisomerases, helicases, and chromatin remodellers [4]. Unfortunately, as a consequence of the small effective spring constant of these molecules at small forces and the large viscous damping of the bead, accurate quantification of the Brownian motion is time consuming and extends up to tens of minutes per force point. As a consequence, MT can typically only be operated in quasi-static force mode, where a series of force points needs to be acquired to obtain a full F-D profile [5].

In this paper we introduce dynamic force spectroscopy for MT. Here the magnetic force is calibrated to the magnet position. From this relation the applied force is calculated while the bead position is detected in real-time. A major advantage of dynamic force spectroscopy using MT compared to OT and AFM is that a sub-pN range of forces become accessible which are relevant in many biological applications. Moreover, measurement times are reduced by two orders of magnitude compared to traditional quasi-static force spectroscopy. This strong reduction of measurement time significantly relieves instrumentation drift issues commonly associated with MT experiments. Transient interactions that readily dissociate upon extended periods of increased force can now be measured with the highest accuracy. The artifacts that

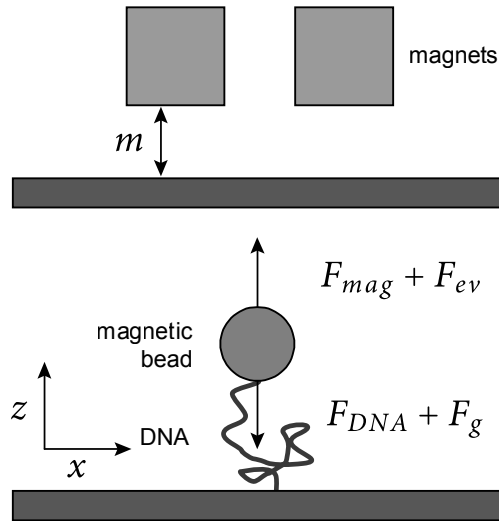


Figure 2.1: Schematic layout of the experimental geometry. The forces pulling the bead up are the magnetic force,  $F_{mag}$ , and the force resulting from excluded volume effects,  $F_{ev}$ . The gravitational force,  $F_g$ , and the force applied by the DNA,  $F_{DNA}$ , pull the bead downwards. The dimension of the drawing are not to scale.

are caused by the dominant role of Brownian motion at low forces, as well as the relatively high viscous drag on the bead, will be discussed and resolved.

## 2.2 Materials and Methods

### Magnetic Tweezers

DNA-tethered paramagnetic beads were imaged in a home built inverted microscope with a CCD camera (Pulnix TM-6710CL) at 60 frames per second. The magnet position was controlled by a stepper motor-based translation stage (M-126, Physik Instrumente) with an accuracy of 200 nm. The position of the beads was measured by real time image processing using LabView software (National Instruments) with an accuracy of 10 nm. A schematic layout of the experimental geometry is shown in Fig. 2.1. During a quasi-static force measurement, the force at each magnet position was calculated from the fluctuations of the bead in the transverse direction,  $x$ , parallel to the coverslip, and from the average height of the bead,  $z$ , normal to the coverslip [3]:

$$F = k_b T \frac{\langle z(t) \rangle}{\langle (\bar{x} - x(t))^2 \rangle} \quad (2.1)$$

During a dynamic force measurement the magnets were moved towards the bead and back at a constant speed resulting in a forward and backward trace, respectively. The position of the magnets was calculated from the position of the stepper motor.

## Magnetic Beads

Paramagnetic tosylactivated Dynabeads (Invitrogen) were coated with anti-digoxigenin antibodies (Sigma) according to the protocol suggested by the supplier.

## Sample Preparation

A clean glass coverslip was coated with a 10  $\mu\text{g}/\text{mL}$  poly-d-lysine solution (Sigma). Next, it was incubated with a polyethyleneglycol (PEG) solution containing a mixture of 20% w/v mPEG-Succinimidyl Propionic Acid (SPA)-5000 and 0.2% biotin-PEG-N-Hydroxysuccinimide (NHS)-3400 (Nektar) in sterile 0.1M  $\text{NaHCO}_3$  buffer (pH 8.5) for 3 hours at room temperature. The coverslip was then mounted on a polydimethylsiloxane (PDMS) flowcell containing a 10x4x0.4 mm flow channel, and flushed with 1 mL buffer MB (10 mM HEPES pH 7.6, 100 mM KAc, 2 mM  $\text{MgAc}_2$ , 10 mM  $\text{NaN}_3$ , and 0.1% (v/v) Tween-20 in milli-Q water). Next, 0.1 mg/mL streptavidin (Sigma) was flushed into the cell and incubated for 10 minutes. The cell was subsequently flushed with 1 mL of MB, 400  $\mu\text{L}$  2.5 ng/ $\mu\text{L}$  DNA in MB and incubated for 10 minutes, 1 mL MB, 1  $\mu\text{L}$  magnetic beads in 400  $\mu\text{L}$  MB supplemented with 0.02% (w/v) BSA (MB+) and incubated for 10 minutes and finally flushed with MB+.

## DNA and Chromatin Fibers

A construct of pBlueScript SK+ with a cloned insert containing 17 5S RNA nucleosome positioning sites was digested with HindIII and NotI. The fragment containing 17 positioning elements was purified. 1300 base pair PCR fragments (template: pBluescript K+; primers: 5'-CTAAA TTGTA AGCGT TAATA TTTTG TTAAA-3' and 5'-TATCT TTATA GTCCT GTCGG GTTTC GCCAC-3') containing either digoxigenin- or biotin-modified uracils in a ratio of 1:20 to non-modified thymine were digested with Not I and HindIII, respectively. The resulting 650 bp fragments were ligated, with an excess of 10:1, to each end of the vector fragment carrying the 17 positioning elements and used without further purification. Electrophoretic

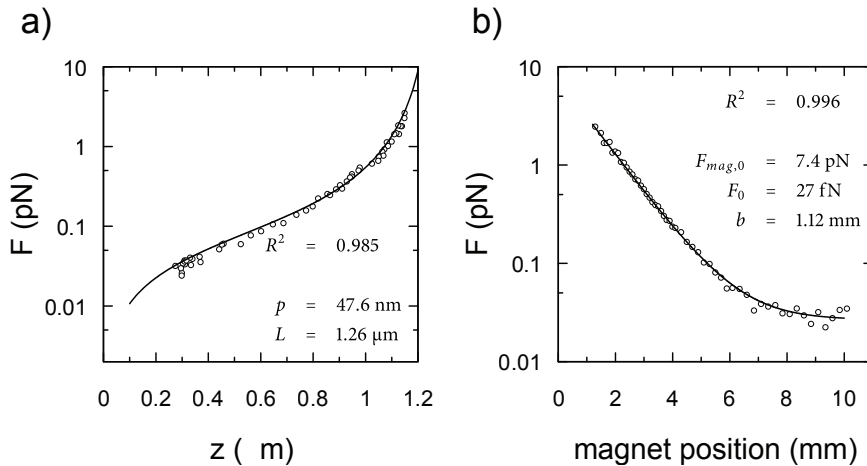


Figure 2.2: Force calibration for dynamic force spectroscopy. (a) A F-D plot of a DNA molecule obtained with quasi-static force spectroscopy (black circles) fits the WLC model (black line). (b) The force at different magnet positions (black circles) follows an exponential decay with an additional offset (black line).

gel analysis showed that all the vector fragments were ligated to the linker fragments. For nucleosome reconstitution, a salt dialysis with recombinant histone proteins was performed as described elsewhere [6]. The histone octamer to positioning site ratio was 1:1, but the yield of reconstitution was significantly smaller than 100%.

## Atomic Force Microscopy

Sub-saturated chromatin fibers were imaged with tapping mode AFM on a Nanoscope III (Veeco) after glutaraldehyde fixation and deposition on mica.

## 2.3 Validation of the method

To empirically determine the relation between force and magnet position we performed quasi-static force measurements on single DNA molecules. A typical result of these measurements is shown in Fig. 2.2a. The Force-Distance plot accurately follows the Worm Like Chain (WLC) [7]:

$$F_{DNA}(z) = \frac{k_b T}{p} \left( \frac{1}{4(1-z/L)^2} - \frac{1}{4} + \frac{z}{L} \right), \quad (2.2)$$

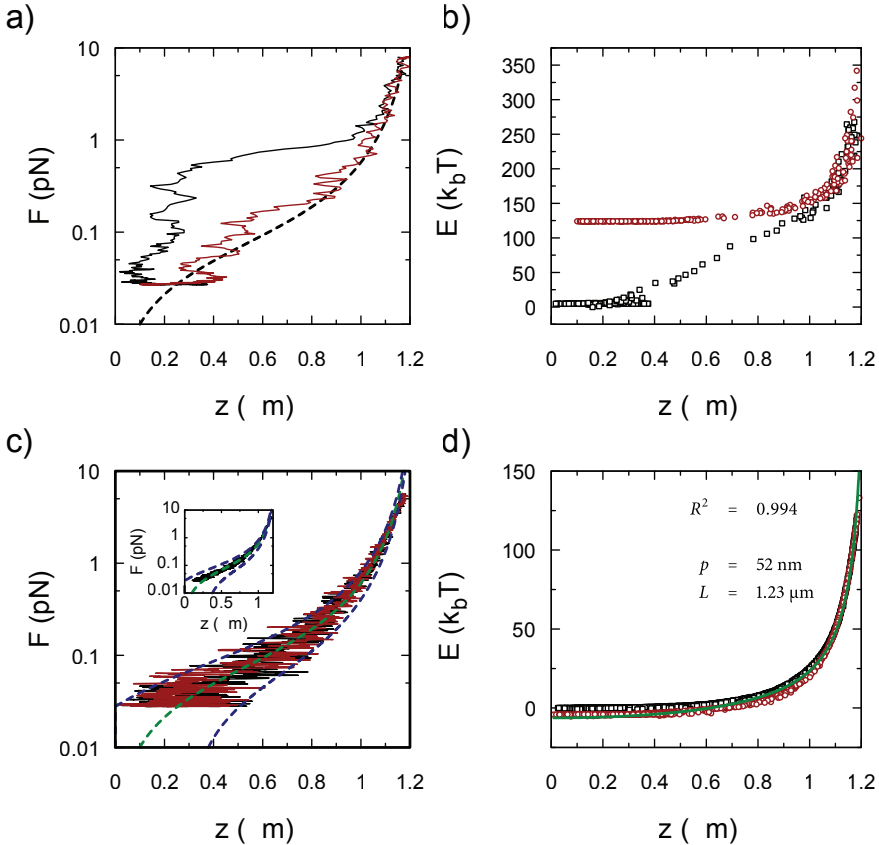


Figure 2.3: Dynamic force spectroscopy on DNA using large and small magnetic beads. (a) Dynamic force spectroscopy using  $2.8 \mu\text{m}$  beads. The forward trace (black line) and backward trace (red line) do not overlap indicating energy dissipation; the dashed black line is a WLC with a persistence length of  $52$  nm and a contour length of  $1.2 \mu\text{m}$ . Each trace was obtained in 5 seconds. (b) The work during the experiment as a function of the extension. The forward trace (black squares) and backward trace (red circles) do not overlap, indicating dissipation. (c) Dynamic force spectroscopy using  $1 \mu\text{m}$  beads. The forward trace (black line) and backward trace (red line) overlap. The dashed green line is a WLC with the persistence length and contour length taken from the fit in Fig. 2.3d. The dashed blue lines are the expected standard deviation of the Brownian noise of the bead as can be deduced from Eq. 2.2. The inset shows the average of 6 traces (black line), the noise in the traces is clearly reduced. Each trace was obtained in 5 seconds. (d) The work during the experiment as a function of the extension, the forward trace (black squares) and backward trace (red circles) overlap, indicating a fully elastic response. A WLC model was fitted to the backward trace (green line).



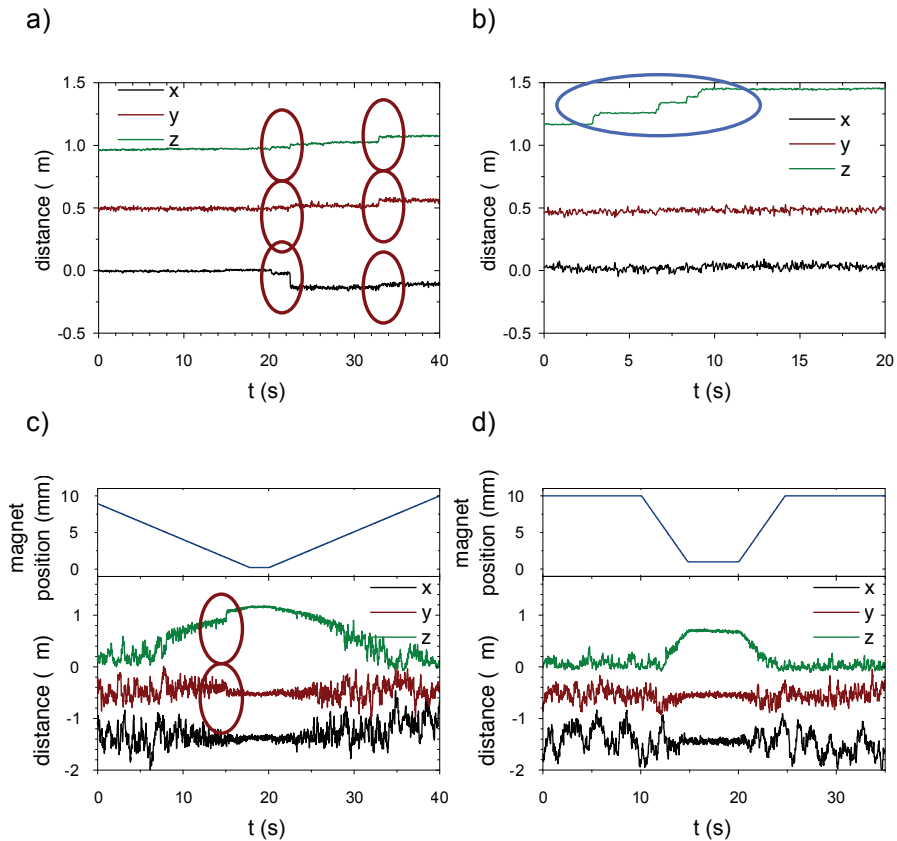


Figure 2.4: *Discrimination between disruptions of non-specific interactions with the surface and intra-molecular interactions. The time trace of a subsaturated chromatin fiber, taken at a constant force of 17 pN, shows (a) non specific surface interaction events (red circles) which were accompanied by lateral movements and (b) intra-molecular disruptions which were not accompanied by lateral movement (blue circle). (c) The time trace of a dynamic force measurement shows an instance of a rupture (red circles) which was accompanied by lateral movement. We attribute this to non-specific surface interactions. (d) The time trace of the F-D curve shown in Fig. 4b in which no lateral movement was detected.*

with thermal energy  $k_b T$ , extension  $z$ , fitted persistence length  $p = 48$  nm, and contour length  $L = 1.26$   $\mu\text{m}$ . In Fig. 2.2b we plotted the obtained force as a function of the magnet position. We found that the force,  $F_{tot}$ , decays exponentially with the magnet position, according to:

$$F_{tot} = F_{mag,0} e^{-m/b} + F_0, \quad (2.3)$$

where  $m$  is the distance between the top of the fluidic cell and the magnets as depicted in Fig. 2.1.  $F_{mag,0}$  is the maximal force,  $b$  the decay length of the magnetic force, and  $F_0$  a constant offset. In our setup  $F_{mag,0}$  was  $18 \pm 2$  fN for 2.8  $\mu\text{m}$  diameter beads and  $6 \pm 1.4$  fN for 1  $\mu\text{m}$  diameter beads. We found the decay length, which is defined by the geometry of the set-up, to be constant,  $b = 1.1 \pm 0.07$  mm. Below 100 fN the observed force is independent of the magnet position. In this regime excluded volume effects, pushing the bead away from the surface and gravity, pulling the bead down, dominate [8]. We estimated  $F_0$ , the sum of the force originating from gravity and from excluded volume effects to be approximately 31 fN, in good agreement with a fitted offset of 27 fN. During a dynamic force measurement Eq. 2.3 was used to calculate the force from the magnet position.

To test the dynamic force mode on a DNA molecule we acquired a F-D cycle shown in Fig. 2.3a. Each forward pulling trace was acquired in 5 seconds, the backward trace was acquired at the same speed. Note that this is much shorter than a quasi-static measurement like the one shown in Fig. 2.2a, which was measured in about an hour. Surprisingly, a significant hysteresis was observed between the forward (increasing force) and backward (decreasing force) trace. When compared to the WLC-fit obtained with quasi-static force spectroscopy it appeared that only at forces above 1 pN both the forward and the backward trace follow the WLC. At forces below 1 pN, however, only the backward trace matches the WLC curve. As DNA has been shown to deform elastically at forces below its melting transition, i.e. below 60 pN; [5], the origin of this hysteresis cannot be internal disruption of the DNA structure, and must therefore be attributed to external dissipation.

Non-specific interactions between the DNA and/or bead with the surface are commonly observed in these measurements, especially at low forces and might alternatively explain the observed behavior. Disruption events of such non-specific interactions are generally accompanied by a movement in the lateral direction, as shown in Fig. 2.4. In order to discriminate between surface interactions and intra-molecular interactions we used the absence of lateral movement as a selection criterion. Furthermore, by PEG passivation of the surface, the number of traces that showed lateral movement was reduced to a complete absence in DNA traces and a very small fraction in the case of chromatin fibers. Thus non-specific interactions between the tether and the surface can be discarded as the origin of the hysteresis.

Understanding the nature of the observed hysteresis is a requirement for F-D analysis of more

complex structures. Therefore, we considered the equation of motion of the tethered bead:

$$F_{DNA}(z) = F_{mag} - \gamma \frac{dz}{dt}, \quad (2.4)$$

with  $z$  the position of the bead and  $\gamma$  the drag coefficient. Inertia forces can readily be neglected. Rapid changes in magnetic force will induce an extra friction force that makes the bead lag behind. The drag coefficient  $\gamma$  is given by Stokes' law:

$$\gamma = 6\pi\eta r, \quad (2.5)$$

with bead radius  $r$  and viscosity  $\eta$ . Note that the drag coefficient at close proximity to the surface  $\gamma^*$  can be significantly larger than the drag coefficient given by Eq. 2.5 when the radius of the bead,  $r$ , is comparable to the distance between the bead and the coverslip,  $z$ , [9]:

$$\gamma^* = \left(1 + \frac{r}{z} + \frac{r}{6z + 2r}\right) \gamma \quad (2.6)$$

During a dynamic force measurement we assumed that the force on the molecule is equal to the applied magnetic force determined in a quasi-static measurement. However, from Eq. 2.4 it is clear that friction also contributes to the applied force,  $F_{fr} = \gamma \frac{dz}{dt}$ . In the case of DNA the viscous drag is mostly limited to the entropic regime where DNA behaves like a Hookian spring,  $z = \frac{F_m}{k}$  with  $k = \frac{3}{2} \frac{k_b T}{\rho L}$ , therefore, using Eq. 2.3, the relative contribution of the friction,  $F_{fr}/F_m$ , can be written as:

$$\frac{F_{fr}}{F_m} = \frac{v_{mag} \gamma^*}{bk}, \quad (2.7)$$

with  $v_{mag}$  the velocity of the magnets and  $k$  the spring constant of the tether. with , resulting in the following formula for the relative contribution of the friction:

$$\frac{F_{fr}}{F_m} = \frac{2}{3} \frac{\rho v_{mag} L \gamma^*}{bk_b T} \quad (2.8)$$

The assumption that the force on the molecule is equal to the applied magnetic force is only valid when the friction force is negligible compared to the magnetic force ( $F_{fr}/F_m \ll 1$ ). The maximum magnet velocity typically used in experiments was 2 mm/s. For 2.8  $\mu\text{m}$  diameter beads  $F_{fr}/F_m = 0.43$  which is clearly not negligible. Decreasing the bead diameter will decrease this contribution. For example the contribution of friction to the total force on 1  $\mu\text{m}$  diameter beads is much smaller ( $F_{fr}/F_m = 0.15$ ) and will lead to a more accurate F-D curve as quantified in the next paragraph. A dynamic F-D plot measured using a 1  $\mu\text{m}$  diameter bead is shown in Fig. 2.3c. In contrast to the data obtained with 2.8  $\mu\text{m}$  diameter beads (Fig. 2.3a), the data follow the WLC model accurately and no obvious hysteresis was observed between

the forward and the backward trace.

## 2.4 Energy analysis

Brownian motion of the bead causes the large fluctuations in the low force regime as demonstrated in Fig. 2.3a, making it difficult to assess any residual dissipation. Averaging of Brownian fluctuations from multiple F-D curves, reduces this effect, as shown in Fig. 2.3c, inset. However, averaging precludes the ability to resolve single ruptures that are not synchronous in repeated experiments, a major advantage of dynamic force spectroscopy. As an alternative we calculated the work done during the experiment, i.e.  $E(t) = \int_0^t F(t^*) \frac{dz}{dt^*} dt^*$ , which results in an Energy-Distance (E-D) plot as shown in Fig. 2.3d. As the Brownian motion is now integrated all fluctuations will collapse on the curve:

$$E(z) = \int_0^z F_{DNA}(z^*) dz^* = \frac{1}{4} \frac{k_b T z^2 (2z - 3L)}{\rho L (z - L)} \quad (2.9)$$

Both the forward and backward trace fit very well to Eq. 2.9 for  $p = 49$  nm and  $L_0 = 1.18$   $\mu$ m.

From the measurements we also obtained the total dissipated energy, in a single F-D cycle, which manifests itself as hysteresis in the F-D plot. After a full F-D cycle the dissipation was around  $3 k_b T$  for  $1 \mu$ m diameter beads, compared to  $130 k_b T$  for measurements with  $2.8 \mu$ m diameter beads. Alternatively, an increase of the measurement time for each trace, from 5 to 60 seconds, decreased the hysteresis on a  $2.8 \mu$ m bead (data not shown) and resulted in a dissipation of  $6 k_b T$ . These values are in close agreement with numerical solutions of Eq. 2.4, 5 and 6, for DNA with a contour length of  $1.2 \mu$ m, a persistence length of 52 nm and a measurement time corresponding to 5 seconds. For a dynamic F-D experiment these calculations resulted in a dissipation of  $147 k_b T$  for  $2.8 \mu$ m diameter beads and  $3 k_b T$  for  $1 \mu$ m diameter beads.

From these experiments we can conclude that using smaller magnetic beads i) dissipation from viscous drag was negligible i.e. the molecule is permanently in equilibrium with the magnetic force ii) non-specific interactions of the bead and/or DNA with the surface were negligible and iii) DNA extension is fully elastic at forces down to 10 fN.

In the current measurements the force was increased exponentially in time, effectively emphasizing the low force regime. With a more advanced, non-linear control of the magnet position one could also linearly ramp the force, making low force dynamic force spectroscopy MT experiments possible that are compatible with the framework developed for previous studies (2).

## 2.5 Dynamic force spectroscopy on nucleosome-nucleosome interactions

In eukaryotes DNA is condensed into chromatin. Whereas the structure of the nucleosome, the first step in DNA condensation, is known with atomic precision [10], higher order structures remain highly elusive [11]. Full understanding of higher order structure and dynamics will require detailed knowledge of all interactions between the nucleosomes. However, only rough estimates of the interaction energy are currently available due to a lack in force accuracy and the common use of chromatin reconstituted from highly heterogeneous cell extracts [12]. We recently obtained well-defined, fully saturated chromatin fibers that adopt a 30 nm fiber structure [13]. These extremely well ordered structures are stabilized by multiple nucleosome-nucleosome interactions that act in concert. Such 30 nm fibers, when measured using dynamic force spectroscopy as described in this paper, resist forces up to 4.5 pN, after which the structure unfolds cooperatively. Due to the cooperative nature of unfolding, individual interactions between nucleosomes were completely obscured in these experiments (see chapter 4 of this thesis). To resolve individual nucleosome-nucleosome interactions we performed dynamic force spectroscopy on individual sub-saturated chromatin fibers in which nucleosomes can interact but are too sparse to adapt highly condensed structures.

AFM imaging of the sub-saturated chromatin fibers reveals a large variation of the number and position of nucleosomes on each DNA template molecule, with an average number of nucleosomes per molecule of  $4 \pm 3$ , as shown in Fig. 2.5a. Some of the nucleosomes interact, causing looping of the DNA as indicated by the arrow. In Fig. 2.5b and c, F-D and E-D plots of a measurement on a single sub-saturated chromatin fiber are shown. Compared to bare DNA, Fig. 2.3c, the tether extension is significantly reduced. At an applied force of around 0.5 pN the structure ruptured to an extended length, after which the forward and backward traces overlap. In the E-D plot, we observed a total energy dissipation of  $20 k_b T$  that we attributed to the rupture of nucleosome-nucleosome interactions. The dissipated energy varied significantly between F-D cycles pointing at different interactions in each refolding cycle.

After rupture of the interactions between nucleosomes the DNA is expected to follow the WLC model, having a reduced contour length because of DNA wrapping in nucleosomes and a reduced apparent persistence length as a result of the sharp bends at the entry and exit sites of a nucleosome [14]. Indeed the backward trace in Fig. 2.5c fits well to Eq. 2.9, with  $L = 0.89 \mu\text{m}$  and  $p = 18 \text{ nm}$ . It is clear that since these two effects are correlated, a smaller contour length indicates more nucleosomes resulting in a smaller apparent persistence length. From the amount of wrapped DNA, 310 nm, it follows that this fiber contained 6 nucleosomes. The results ob-

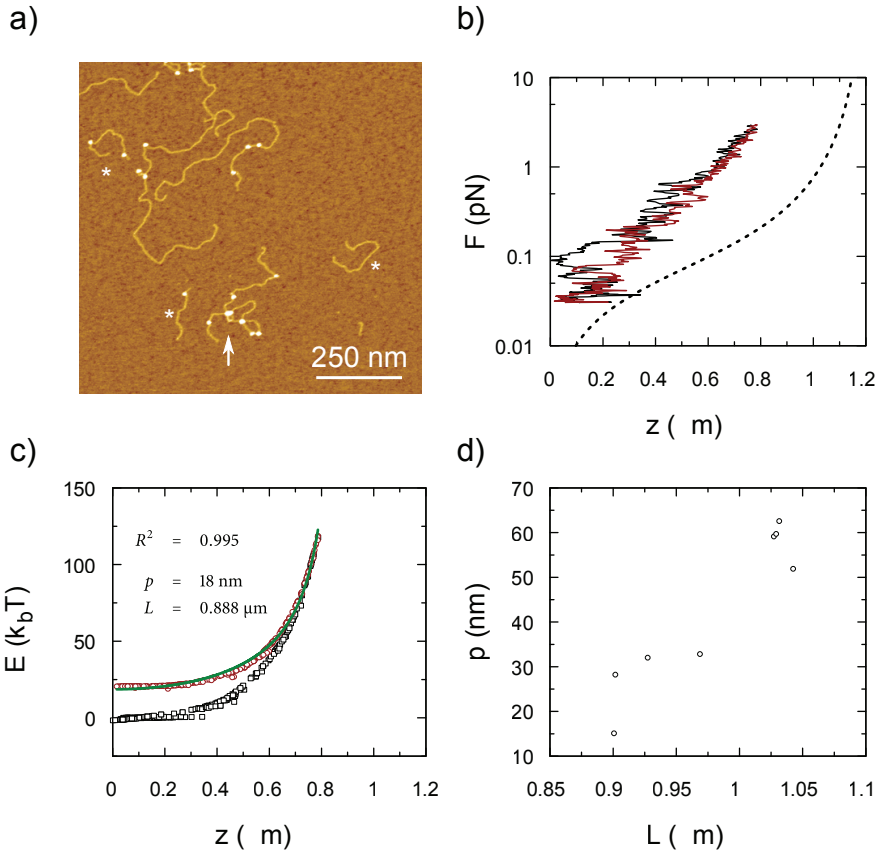


Figure 2.5: *Dynamic force spectroscopy on sub-saturated chromatin fibers* (a) AFM image of the used chromatin fibers. Possible nucleosome-nucleosome interactions are indicated by an arrow. Stars denote PCR fragments used in the MT for linking the fiber to the bead and the surface. (b) Dynamic force spectroscopy on these chromatin fibers. The forward trace (black line) and backward trace (red line) do not overlap at forces smaller than 1 pN. The dashed black line is a WLC with a persistence length of 52 nm and a contour length of 1.2  $\mu\text{m}$ , appropriate for a bare DNA tether. Each trace was obtained in 5 seconds. (c) The work during the experiment as a function of the extension. The forward trace (black squares) and backward trace (red circles) do not overlap and show an offset that can be attributed to disruption of nucleosome-nucleosome contacts. The backward trace (red circles) closely follows the WLC model (green line). (d) The fitted contour length of different sub-saturated chromatin fibers plotted versus the fitted persistence length.

tained for several molecules were further analyzed, Fig.2.5d. As expected, a clear correlation between the resulting contour length and apparent persistence length was observed. For a quantitative comparison of these traces we divided the traces into two populations, the first with a contour length larger than  $1\ \mu\text{m}$ , containing very few or no nucleosomes, and the second with a contour length smaller than  $1\ \mu\text{m}$ , containing more than 4 nucleosomes. We averaged the apparent persistence length, contour length and dissipated energy over the traces within each population. The apparent persistence length differed significantly between the two populations  $27 \pm 8\ \text{nm}$  and  $58 \pm 5\ \text{nm}$ , respectively. The average dissipated energy was higher for the population with the smaller contour length ( $16 \pm 8\ k_b T$  versus  $10 \pm 6\ k_b T$ ). However the variations in dissipated energy are large especially in the case with the larger amount of nucleosomes. This can be expected because these unstructured arrays can adopt different nucleosome-nucleosome interactions in each F-D cycle.

Recently, Mihardja et al. reported the unwrapping of DNA within a single nucleosome at forces between 2 and 4 pN [15]. At comparable pulling rates we did not observe any unwrapping of the DNA from the nucleosomes up to forces of 6 pN. When the magnets were positioned to apply a maximum force for an extended period of time we did observe unwrapping, as plotted in Fig. 2.4c, showing that we can use dynamic force spectroscopy to study transient structures that have a limited lifetime under an applied load.

## 2.6 Conclusion

In conclusion, we developed a method for fast real-time sub-piconewton dynamic force spectroscopy using magnetic tweezers. We showed that the energy dissipation due to viscous drag is dependent on bead diameter. The large Brownian fluctuations of the bead position that occur at low forces conveniently collapse on a well-defined energy-distance plot, allowing accurate analysis of dynamic force spectroscopy data and calculation of the dissipated energy. As a proof of principle, measurements on single sub-saturated chromatin fibers revealed a clear correlation between contour length and apparent persistence length. Nucleosome-nucleosome interactions that rupture at 0.5 pN with a dissipated energy in the range of 10 to  $16\ k_b T$  were observed.

## Bibliography

- [1] H. Clausen-Schaumann, M. Seitz, R. Krautbauer, and H. Gaub, "Force spectroscopy with single bio-molecules," *Current opinion in chemical biology*, vol. 4, pp. 524–30, Oct 2000.

- [2] E. A. Evans and K. Ritchie, "Dynamic strength of molecular adhesion bonds.," *Biophys. J.*, vol. 72, pp. 1541–55, Apr 1997.
- [3] T. R. Strick, J.-F. Allemand, D. Bensimon, A. Bensimon, and V. Croquette, "The elasticity of a single supercoiled dna molecule," *Science*, vol. 271, pp. 1835–7, Mar 1996.
- [4] J. Zlatanova and S. H. Leuba, "Magnetic tweezers: a sensitive tool to study dna and chromatin at the single-molecule level," *Biochem Cell Biol*, vol. 81, pp. 151–9, Jun 2003.
- [5] C. Gosse and V. Croquette, "Magnetic tweezers: micromanipulation and force measurement at the molecular level," *Biophys J*, vol. 82, pp. 3314–29, Jun 2002.
- [6] C. Logie and C. L. Peterson, "Catalytic activity of the yeast swi/snf complex on reconstituted nucleosome arrays," *EMBO J*, vol. 16, pp. 6772–82, Nov 1997.
- [7] C. Bustamante, J. F. Marko, E. Siggia, and S. Smith, "Entropic elasticity of lambda-phage dna," *Science*, vol. 265, pp. 1599–600, Sep 1994.
- [8] D. Segall, P. C. Nelson, and R. Phillips, "Volume-exclusion effects in tethered-particle experiments: bead size matters.," *Phys. Rev. Lett.*, vol. 96, p. 088306, Apr 2006.
- [9] M. Bevan and D. Prieve, "Hindered diffusion of colloidal particles very near to a wall: Revisited," *The Journal of Chemical Physics*, vol. 113, no. 3, pp. 1228–1236, 2000.
- [10] K. Luger, A. W. Mäder, R. K. Richmond, D. F. Sargent, and T. J. Richmond, "Crystal structure of the nucleosome core particle at 2.8 a resolution," *Nature*, vol. 389, pp. 251–60, Sep 1997.
- [11] D. J. Tremethick, "Higher-order structures of chromatin: the elusive 30 nm fiber," *Cell*, vol. 128, pp. 651–4, Feb 2007.
- [12] Y. Cui and C. Bustamante, "Pulling a single chromatin fiber reveals the forces that maintain its higher-order structure.," *Proc. Natl. Acad. Sci. U.S.A.*, vol. 97, pp. 127–32, Jan 2000.
- [13] V. A. T. Huynh, P. J. J. Robinson, and D. Rhodes, "A method for the in vitro reconstitution of a defined "30 nm" chromatin fibre containing stoichiometric amounts of the linker histone," *J. Mol. Biol.*, vol. 345, pp. 957–68, Feb 2005.
- [14] I. M. Kulić, H. Mohrbach, V. Lobaskin, R. Thaokar, and H. Schiessel, "Apparent persistence length renormalization of bent dna.," *Physical review. E, Statistical, nonlinear, and soft matter physics*, vol. 72, p. 041905, Dec 2005.
- [15] S. Mihardja, A. Spakowitz, Y. Zhang, and C. Bustamante, "Effect of force on mononucleosomal dynamics.," *Proc. Natl. Acad. Sci. U.S.A.*, vol. 103, pp. 15871–6, Oct 2006.



---

---

## CHAPTER 3

---

# Hidden Markov Analysis of Nucleosome Unwrapping Under Force<sup>1</sup>

### Abstract

Transient conformational changes of DNA-protein complexes play an important role in the DNA metabolism but are generally difficult to resolve. Single molecule force spectroscopy has the unique capability to follow such reactions but Brownian fluctuations in the end-to-end distance of a DNA tether can obscure these events. Here we measured the force induced unwrapping of DNA from a single nucleosome and show that hidden Markov analysis, adopted for the non-linear force-extension of DNA, can readily resolve unwrapping events that are significantly smaller than the Brownian fluctuations. The resulting probability distributions of the tether length are used to accurately resolve small changes in contour length and persistence length. The latter is shown to be directly related to the DNA bending angle of the complex. The worm like chain adapted hidden Markov analysis can be used for any transient DNA-protein complex and provides a robust method for the investigation of these transient events.

---

<sup>1</sup>This chapter is based on the article: *Hidden Markov Analysis of Nucleosome Unwrapping Under Force*, M. Kruithof and J. van Noort, accepted for publication in *Biophysical Journal*

### 3.1 Introduction

Protein-DNA complexes are transient by nature and to understand the reaction mechanisms that control DNA metabolism it is important to relate the kinetics of complex formation to the conformational changes that are associated with DNA binding. In many cases the binding of a protein induces a bend in the trajectory of the DNA as can be observed by various techniques such as gel electrophoresis, atomic force microscopy, electron microscopy, NMR and X-ray crystallography. All these techniques however require stable complexes or depend on fixation, and can not be used to resolve the structure nor the dynamics of short-lived complexes. Single molecule techniques are well equipped for this task, but the Brownian fluctuations associated with these experiments and which are intrinsic to the flexibility of the complexes sometimes dominate over structural changes. Here we use the well-known mechanical properties of DNA to resolve dynamic binding events that change the contour length and the trajectory of the DNA-protein complex in order to obtain both the kinetics of protein binding and the bending angle of such transient complexes.

In eukaryotes, nucleosomes are by far the most abundant DNA-protein complexes and many processes involving DNA are regulated by their presence. The nucleosome represents the fundamental organizational unit of chromatin. Its structure is known with atomic detail: 147 base pairs (bp) of DNA are wrapped in 1.65 turns around a histone octamer [1]. The nucleosome core particle is however not a static structure. Spontaneous nucleosome conformational changes have been reported where a stretch of DNA transiently unwraps from the histone surface [2], which allows enzymes access to the DNA that is usually occluded in the nucleosome. Various techniques have been used to study these dynamics, including fluorescence resonant energy transfer (FRET) [2, 3] and force spectroscopy [4, 5]. The latter was successfully applied to quantify force induced structural changes of the nucleosome and to determine the corresponding rates of DNA unwrapping from the histone octamer as a function of the force [4].

During force-spectroscopy experiments the extension of a DNA molecule containing a single nucleosome (Fig. 3.1a) is measured. In absence of force, the lifetime of the unwrapped conformation is much shorter than the lifetime of the wrapped conformation [4] and transient unwrapping events may be too fast, compared to the bandwidth of the tweezers, to be observed. By applying a constant force, the equilibrium shifts and the lifetime of the unwrapped conformation increases while the lifetime of the wrapped conformation decreases [6]. Force induced DNA unwrapping can be separated in two steps. At an external force of about 3 pN the first 0.65 turns of DNA unwrap from the histone core (Fig. 3.1a-b) [4]. At this force the lifetimes of the wrapped and the unwrapped conformations are similar allowing direct quantification of these lifetimes [4]. The lifetimes at zero force can be extrapolated from the force versus lifetime char-

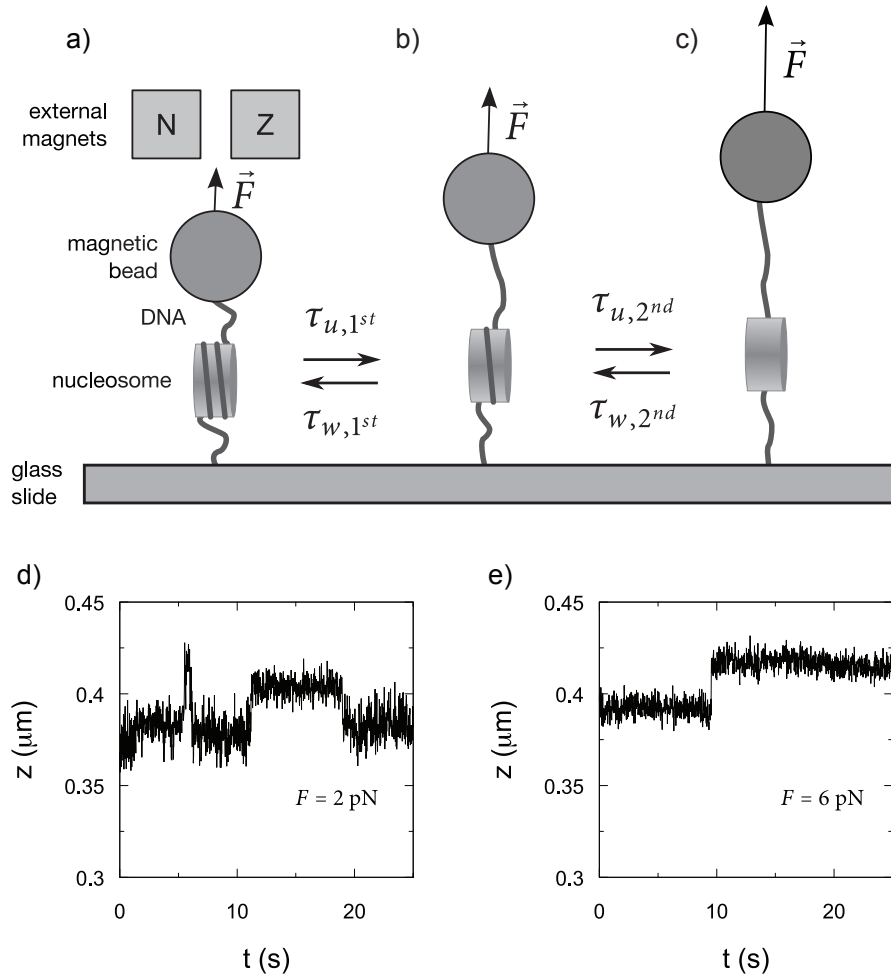


Figure 3.1: Schematic representation of a magnetic tweezers experiment on a DNA-nucleosome complex. (a) A DNA molecule containing a single nucleosome is attached between a magnetic bead and a glass coverslip. The force is controlled by changing the distance between the bead and two external magnets above the sample. DNA unwrapping from the nucleosome under force occurs in two distinct steps (a-b and b-c). Two typical examples of experimental DNA unwrapping traces at 2 pN (d) and at 6 pN (e) where unwrapping is accompanied by an increase in end-to-end distance of the DNA-nucleosome complex.

acteristic [6]. At a stretching force of 6 pN the final turn of DNA unwraps (Fig. 3.1b-c) [4, 5]. Thus during force induced unwrapping two transitions between three distinct conformations can be identified, fully wrapped, 0.65 turns unwrapped, and fully unwrapped.

The existence of these distinct conformations allows us to describe the wrapping and unwrapping of DNA from the nucleosome as a Markov process by separating the reaction path into three conformations with accompanying transition rates between them. A schematic representation for nucleosome unwrapping, as a Markov process, is depicted in Fig. 3.1. During each transition DNA wraps or unwraps, leading to step-like increases or decreases in tether length, as observed in the extension of the molecule (Fig. 3.1d and e). In such force-spectroscopy experiments, the challenge is to resolve small changes in end-to-end distance, in this case of approximately 25 nm, under conditions where thermal fluctuations of the extension of the DNA tether, may exceed these changes. Quantification of the changes in the contour length of the DNA molecule therefore requires a Hidden Markov (HM) model, which explicitly takes stochastic fluctuations of the observable into account [7, 8]. HM analysis of noisy traces has successfully been applied to various experimental data such as FRET trajectories [9] and DNA looping kinetics [10] assuming the noise to be normally distributed. It is however essential to use correct probability distributions of the different states and in case of force spectroscopy on DNA the probability distribution differs significantly from a normal distribution. In this paper, we calculate the probability distribution of the DNA end-to-end length under an external force and use this distribution in the HM analysis. This approach strongly improves the accuracy of detecting steps in constant force time traces of the DNA extension, resulting in a more accurate determination of the kinetics. Furthermore, we will show that the HM model also gives new insight into the mechanical and structural properties of the nucleosome.

## 3.2 The Probability Distribution of the End-To-End distance of a DNA-Bead System

A number of algorithms have been published to find the most likely distribution of Markov states [7, 11, 12]. We used the forward-backward algorithm [7]. The forward-backward algorithm uses the probability distribution of the various states to calculate the probability for data point  $n$  to be in each state. Data point  $n$  is then attributed to the state with the highest probability. For the first iteration an estimate of the transition probabilities and probability distributions is needed, which is typically based on simple thresholding. A new probability distribution for each state is then fitted to a histogram of the data belonging to the corresponding state. From the dwell times of the different states new lifetimes are calculated. In subsequent

iterations each data point is reassigned to a new state. Successive iterations are performed until the lifetimes and probability densities converge to a stable solution.

In many applications a normal distribution is used to describe the probability distribution of a state [9, 10]. Due to the nonlinear force-distance relation of DNA (Eq. 3.4), the end-to-end distance of a DNA molecule under constant force deviates significantly from a normal distribution. The probability distribution,  $P(z)$ , of the end-to-end distance,  $z$ , under force can be calculated from the work required to stretch the molecule,  $E(z)$ , relative to the thermal energy  $k_b T$ :

$$P(z) \propto \exp(-E(z)/k_b T). \quad (3.1)$$

$E(z)$  is obtained by integration of the force required to extend the DNA molecule, given by

$$E(z) = - \int_0^z F(s) ds. \quad (3.2)$$

In a typical tweezers-based force-spectroscopy experiment, the total force acting on the bead is

$$F(z) = F_{ext} - F_{WLC}(z) + F_{EV}(z), \quad (3.3)$$

with  $F_{ext}$  the external force applied to the bead, either from magnetic or optical trapping. The excluded volume force,  $F_{EV}(z)$ , for a freely rotating bead equals  $k_b T/z$  [13]. The excluded volume force should not be taken into account when the distance between the bead and the surface is larger than twice the radius of the bead.  $F_{WLC}$  is the force required to stretch the DNA molecule as given by the Worm-Like-Chain (WLC) model [14] with a persistence length,  $p$  and a contour length  $L$ :

$$F_{WLC}(z) = \frac{k_b T}{p} \left[ \frac{1}{4 \left(1 - \frac{z}{L}\right)^2} - \frac{1}{4} + \frac{z}{L} \right]. \quad (3.4)$$

The work needed to stretch the DNA molecule follows from Eqs. 3.2-3.4 yielding

$$E(z) = -F_{ext}z + \frac{k_b T z^2 (3L - 2z)}{4Lp(L - z)} - k_b T \ln(z). \quad (3.5)$$

Using Eqs. 3.1 and 3.5, the normalized probability distribution,  $P(z)$ , becomes

$$P(z) = \frac{\exp \left[ \frac{F_{ext}z}{k_b T} - \frac{z^2(3L-2z)}{4Lp(L-z)} + \ln(z) \right]}{\int_{-\infty}^{\infty} \exp[-E(s)/k_b T] ds}. \quad (3.6)$$

In cases where the number of states is not known *a priori*, it is possible to extend the analysis with a second iteration fitting an increasing number of states as described by McKinney et al. [9]. In the current study of DNA unwrapping from nucleosome cores however we limited our analysis to three states corresponding three probability distributions.

### 3.3 Brownian Dynamics Simulations

Thermal fluctuations of the extension of the DNA tether can be significant and may even exceed the changes in extension associated with DNA unwrapping. To test the accuracy of the above HM model, we performed Brownian dynamics simulations of time traces of DNA molecules at constant force, exhibiting fluctuations between two different states representing wrapping and unwrapping of DNA from the nucleosome. The step size,  $\Delta s$ , at given force,  $F$ , is defined as the difference between the end-to-end distance of the two states

$$\Delta s = |z_{WLC}(F, L_1, p_1) - z_{WLC}(F, L_2, p_2)| \quad (3.7)$$

with  $p_n$  and  $L_n$  the persistence and contour length of the DNA containing a single nucleosome, in state  $n$ , which not only has a different contour length but may also have a different apparent persistence length.  $z_{WLC}$  is the inverse of Eq. 3.4. Two example time traces with a different ratio between the step size and the thermal fluctuations are depicted in Fig. 3.2a. The green line shows the input fluctuations between the two states. The black line shows the simulated Brownian motion of a bead attached to a DNA molecule following the variations in the green trace. We fitted the simulated time trace by HM using the WLC probability distribution (red line) and a normal distribution (blue line). The analysis was performed at 1 pN and at 0.7 pN. In the latter case thermal fluctuations are significantly larger than the step size. The fit of the time trace that corresponds to 0.7 pN demonstrates that even small changes in end-to-end distance, which cannot be detected by simple thresholding, are readily resolved by HM analysis using a WLC distribution, but are largely overlooked when using a normal distribution.

As a figure of merit for the relative size of the end-to-end distance changes, we use the ratio between the step size and the width of the thermal fluctuation distribution. The standard deviation of the thermal fluctuations in the DNA extension  $\sigma$  (Fig. 3.2b) follows

$$\sigma(F) = \sqrt{\frac{k_b T}{k_{WLC}(F)}} = \sqrt{k_b T \cdot \left( \frac{dF_{WLC}(s)}{ds} \Big|_{s=z_{WLC}(F)} \right)^{-1}}, \quad (3.8)$$

where  $k_{WLC}$  is the stiffness of the DNA molecule at a given stretching force. Using Eq. 3.4, this

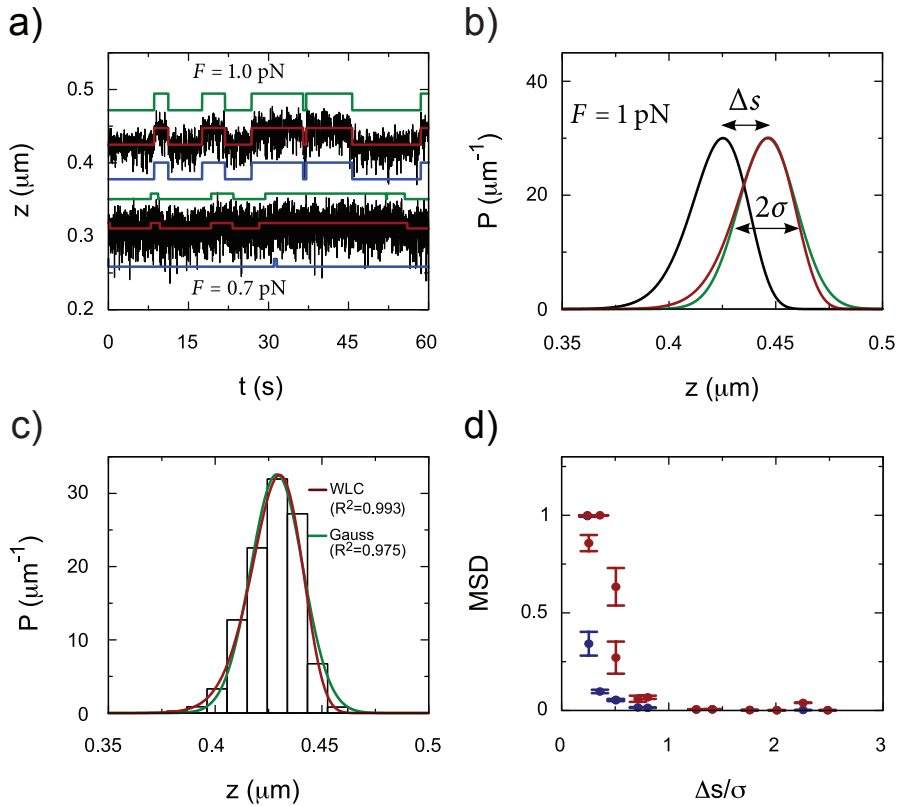


Figure 3.2: Hidden Markov fits to Brownian dynamics simulations of a DNA molecule in which transitions occur between two contour lengths. (a) Traces of simulated data (black lines), the HM fit with the WLC model (red lines), and a Gaussian model (blue lines), and the actual steps (green lines). The top trace is simulated at 1 pN for a DNA molecule, with a contour length of 500 nm, a persistence length of 52 nm and a step of 25 nm. The bottom trace is simulated at 0.7 pN for a similar molecule but with a step of 10 nm. (b) The WLC probability distributions for a DNA molecule at 1 pN, with a contour length of 500 nm (black line) and a contour length of 525 nm (red line). The stepsize,  $\Delta s$ , represents the difference in end-to-end distance between the distributions. Though the width of the WLC distribution is very similar to the width of a normal distribution,  $\sigma$ , (green line), the tails of the distributions differ significantly. (c) A simulated time trace, with a constant contour length, is binned and shown as a histogram. This histogram is fit with the WLC probability distribution at 1 pN and compared to a normal distribution. The WLC distribution describes the data much better as expressed in the  $R^2$ . (d) The MSD of the fits using a WLC probability distribution (blue circles) is compared to the MSD using a normal distribution (red circles) for different ratios between the stepsize and the thermal fluctuations. The error bars represent the spread in the MSD for 10 different traces.

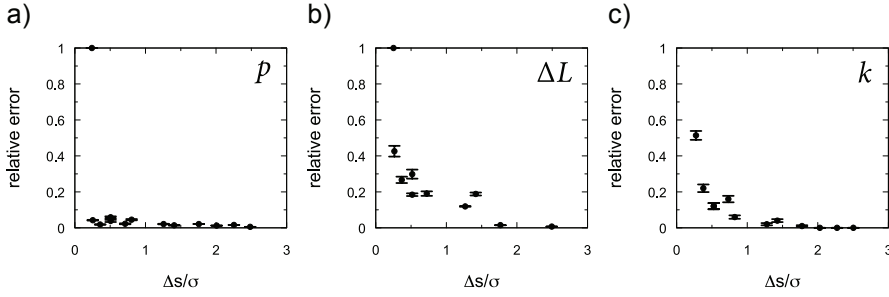


Figure 3.3: The relative errors between the HM fit and the input of the persistence length (a), stepsize (b) and lifetime (c), using a WLC distribution, with respect to the ratio between stepsize and thermal fluctuations. The error bars represent the spread in the relative error for 10 different traces.

expression can be rewritten as

$$\sigma(F) = \sqrt{\frac{2Lp(L - z_{WLC}(F))^3}{3L^3 - 6L^2z_{WLC}(F) + 6Lz_{WLC}(F)^2 - 2z_{WLC}(F)^3}}. \quad (3.9)$$

The mean squared difference (MSD) of the WLC probability distribution (Eq. 3.6) can now be compared to the MSD of a Gaussian approximation of the probability distribution  $P_G(z)$  defined as

$$P_G(z) = \frac{1}{\sigma(F)\sqrt{2\pi}} \exp\left[-\frac{(z - z_{iWLC}(F))^2}{2\sigma(F)^2}\right]. \quad (3.10)$$

An example of a histogram of a single simulated state is shown in Fig. 3.2c where both a Gaussian probability distribution and a WLC probability distribution are fitted. The  $R^2$  of the WLC distribution is smaller than the Gaussian distribution indicating that the WLC describes the simulated data better. To quantify the robustness of our method, we calculate the normalized MSD between the input time trace of the tether length and the fitted time trace of the tether length. Fig. 3.2d shows that HM analysis using the WLC probability distribution, calculated from Eq 3.6, yields a much better fit than using a normal distribution when  $\Delta s/\sigma$  becomes smaller than 1. The normalized MSD is smaller than 0.1 even for a  $\Delta s/\sigma$  of 0.25 in which case it is clear that the HM analysis using a normal distribution is unable to detect any steps. Overall, the WLC distribution detects the steps more accurately and thus yields a better fit.

Since the probability distribution of the end-to-end distance depends on the persistence length and contour length of the tether, the HM analysis not only allows detection of steps, but can also directly extract values for the persistence length and contour length from experimental, constant force, time traces. Fig. 3.3 shows the relative error in the fitted persistence length, con-



tour length and lifetime of the different states. The relative error in the fitted persistence length is on average better than 5% (Fig. 3.3a). Surprisingly, the accuracy of the detected persistence length does not depend on the ratio between the step size and the thermal fluctuations. The relative errors in the fitted contour length and lifetimes (Fig. 3.3b and c) do depend on the step-noise ratio, but are smaller than 0.2 for step size larger than 0.5 times the thermal fluctuations. Thus the HM analysis cannot only be used to extract the lifetimes of the different states but can also be used to obtain accurate measures of the mechanical properties of transient structures that have only small differences in extension relative to the thermal fluctuations.

### 3.4 Analysis of Mono-nucleosome Unwrapping Under Force

Having established the potential to measure small excursions in the end-to-end distance of DNA molecules, we analyzed the unwrapping of the first turn of DNA from single nucleosomes as observed by constant force measurements, using the HM analysis. An example time trace of the end-to-end distance of single nucleosomes in a 500 nm DNA tether measured using magnetic tweezers, is shown in Fig. 3.4a. In this time trace, measured at a constant stretching force of 2.5 pN, we observed two distinct levels that we attribute to the fully wrapped and first-turn unwrapped conformation.

Within the time of our experiments we did not observe irreversible unfolding of DNA from the nucleosome core that could be due to dissociation of histone dimers, as reported before [15]. Though the details of the experimental conditions are difficult to compare, at least two factors favour nucleosome stability in our experiments. Firstly, the 601 nucleosome positioning element that we used here has a significantly ( $3 k_b T$ ) higher stability than the natural 5S RNA and genomic chicken DNA templates [16] that were used in their study. Secondly, we carefully limited the force on our mononucleosomes to maximally 6 pN whereas Claudet *et al.* report forces up to several tens of piconewtons. After each experiment of typically 60 s the force was directly reduced to the sub-pN level. Because all length increases of the mono-nucleosome tether were reversible, we can exclude nucleosome dissociation to be associated with the length increases that we report here.

The average length of DNA that unwraps from the nucleosome ( $dL$ ), derived from the difference in contour length between the two conformations, was  $21.3 \pm 0.5$  nm ( $N = 12$ ) in good agreement with previous data [4]. The lifetimes of the wrapped ( $\tau_w$ ) and unwrapped ( $\tau_u$ ) con-

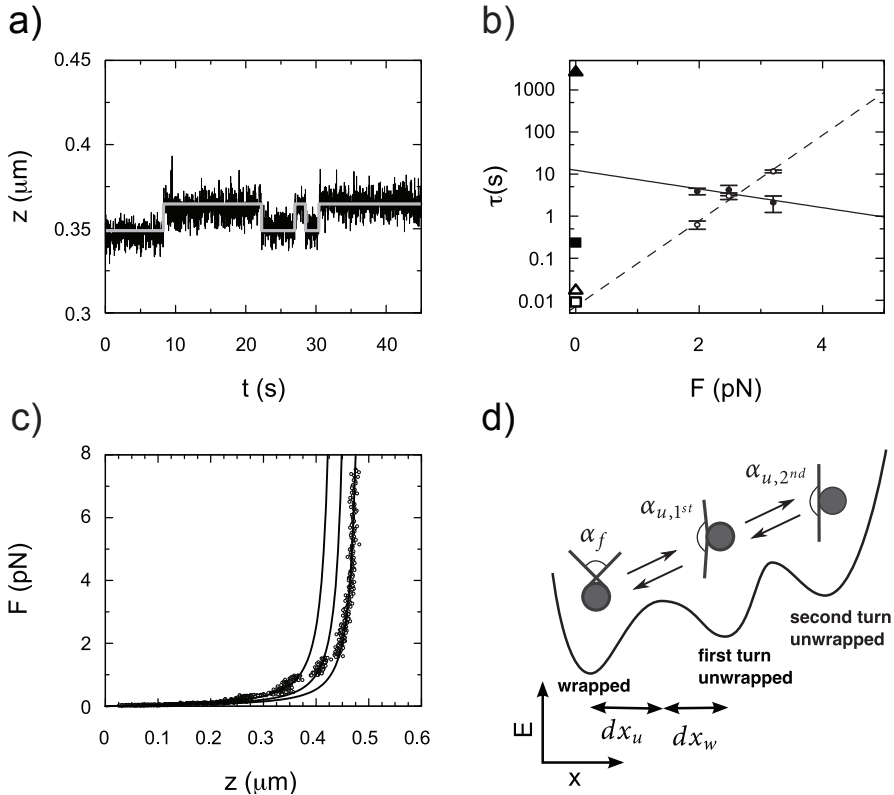


Figure 3.4: (a) Hidden Markov fit (light gray) to experimental data of nucleosome unwrapping at a force of 2.5 pN (b) The obtained lifetimes of the unwrapped conformation (dashed line and open circles) and the wrapped conformation (solid line and closed circles) of the first turn at different forces. The exponential fits are extrapolated to zero force. The black points are wrapped and unwrapped lifetimes measured using FRET [2] (closed and open square) and using optical tweezers [4] (closed and open triangle). (c) Force-extension plot of a mono-nucleosome on a 500 nm DNA fragment showing unwrapping events. The solid black lines are WLC with a contour length and persistence length taken from the HM analysis for the three different conformations. (d) Schematic overview of the exit angle of a fully wrapped,  $\alpha_f$ , first turn unwrapped,  $\alpha_{u,1st}$ , and second turn unwrapped,  $\alpha_{u,2nd}$ , nucleosome. The energy landscape (black line) shows the distances in reaction coordinates between the energy barrier and the wrapped and unwrapped conformation. The opening angles are as determined from the HM-WLC analysis

formation have been reported to depend exponentially on the applied force [6]

$$\begin{aligned}\tau_w(F) &= \tau_{0,w} e^{-Fd x_w}, \\ \tau_u(F) &= \tau_{0,u} e^{Fd x_u},\end{aligned}\tag{3.11}$$

where  $\tau_{0,w}$  and  $\tau_{0,u}$  are the lifetimes at zero force and  $d x_w$  (and  $d x_u$ ) the distance of the reaction coordinate between the initial state and the transition state (Fig. 3.4d). These distances determine the effect of the force on the lifetimes and are limited by the total unwrapping length,  $d x_u + d x_w \leq d L$ . The lifetimes of the unwrapped conformation and the wrapped conformation, obtained from our HM analysis, were fitted with Eq. 3.11 (Fig. 3.4b), resulting in a lifetime of the unwrapped conformation at zero force of  $0.007 \pm 0.001$  s and a lifetime of the wrapped conformation at zero force of  $12 \pm 5$  s. The corresponding distance in reaction coordinates to the transition state was  $10 \pm 1.4$  nm and  $2 \pm 1.3$  nm respectively.

Now that we have calculated the lifetimes of the unwrapped conformations and the wrapped conformation of the nucleosome, how do they compare to previous studies? Mihardja *et al.* [4] performed similar force-spectroscopy experiments using optical tweezers and also extrapolated the lifetimes of the unwrapped conformations and the wrapped conformation of the nucleosome at zero force from measurements at different forces. Li *et al.* [2] measured the zero-force lifetimes of nucleosome breathing directly using bulk FRET, which were later confirmed by single pair FRET [3]. The results of these studies are also plotted in Fig. 3.4b and show that the lifetime for the unwrapped conformation we find ( $0.007 \pm 0.001$  s) is in good agreement with the lifetimes obtained using FRET (0.01 s) and optical tweezers (0.0172 s). The lifetime of the wrapped conformation, however, varies significantly between the three studies. Li *et al.* reports a lifetime of the wrapped conformation of 0.25 s. The lifetime we find however, is much higher. In the FRET experiments any small amount of DNA unwrapping is detected as an unwrapping event. In contrast, in force spectroscopy only unwrapping of a full turn is detected as an unwrapping event. The small excursions that are readily observed in FRET are likely to occur more frequently than full turn unwrapping, which would explain the longer lifetime we observe for the fully wrapped conformation. A major complication in comparing these results however is the differences in post-translational modifications that may be present and that are functional in epigenetic regulation of transcription. Li *et al.* [2] and Koopmans *et al.* [3] used recombinant histones that lack such modifications whereas we and Mihardja *et al.* used histones obtained from chicken erythrocytes that have been prone to such modifications. It is likely that the modifications effect the lifetimes of both the fully wrapped and the unwrapped state. As in chicken erythrocytes chromatin is programmed to be in a transcriptionally silent state, in our histone material the equilibrium may be shifted towards the wrapped state which is consistent with a longer life time of this conformation. Another important parameter in

nucleosome folding is the presence of  $Mg^{2+}$ . The difference in concentration of  $Mg^{2+}$  between the experiments of Mihardja *et al.* (10 mM) and our experiments (2 mM) may explain this difference in the observed wrapped lifetime, since it is known that  $Mg^{2+}$  ions stabilize the nucleosome fiber structure [17]. However, we are not aware of systematic studies on mono-nucleosome stability as a function of  $[Mg^{2+}]$ . As the concentration of  $Mg^{2+}$  *in vivo* is expected to be 2 mM [18] we argue that our experiments may more closely match these conditions.

The high force transition, corresponding to unwrapping of the second turn of DNA was irreversible. Like Mihardja *et al.* [4] we only observed a single unwrapping event per force trace, indicating a free energy barrier for refolding that is substantially larger than  $k_b T$ . Only from the rate dependence of the rupture force, or from experiments at high salt conditions, it was concluded that this transition does not follow a simple two-state model. We also could not resolve this in our constant force measurements which feature a single step transition, see Fig. 3.1e. As shown in the next paragraph the distributions of the end-to-end distance in the both states accurately follow the expected distribution and thus do not give an indication for intermediate states, validating a three state HM analysis. Summarizing, the above illustrates that our HM analysis readily confirms the lifetime of the unwrapped conformation but finds a lifetime of the wrapped conformation that is in between previously reported values.

### 3.5 Structural Implications

Is it possible to use our HM analysis to extract structural properties of the DNA-nucleosome complex during the different conformations? In particular it would be informative to extract the bending angle of the transient complex. Protein-induced bending has been reported to decrease the apparent persistence length of a DNA molecule significantly. Yan *et al.* [19] showed that the force-extension behavior for a  $90^\circ$  bend in a DNA molecule can be described by a WLC with a reduced apparent persistence length. Experimental results confirm such a relation between DNA-bend angles and the apparent persistence length. For instance, force-extension experiments on HU and IHF proteins, which are known to induce a stable bend in the trajectory of a DNA molecule, yield a WLC with a decreased apparent persistence length [20, 21]. Using Euler mechanics Kulic and Schiessel [22] showed that the angle  $\alpha$ , of a kink or fixed angle loop in the trajectory of a DNA molecule reduces the apparent persistence length  $p_{app}$

$$p_{app} = p \left\{ 1 + 8 \frac{p}{L} \left[ 1 - \cos \left( \frac{\pi - \alpha}{4} \right) \right] \right\}^{-2}. \quad (3.12)$$

A renormalization of the persistence length can also be expected for a DNA molecule that contains a nucleosome since wrapping of 1.65 turns of DNA around the nucleosome induces a

loop in the DNA trajectory (Fig. 3.4d), as exemplified by the crystal structure [1]. When DNA unwraps from the nucleosome not only the contour length changes but also the opening angle of the DNA and hence the apparent persistence length.

In force spectroscopy, the persistence length of a molecule is generally extracted from its force-extension behavior by fitting Eq. 3.4 [14]. When pulling on a mono-nucleosome the two transient conformations result in abrupt changes clearly distinguishable by the stepwise increase in tether length. An example trace of a force-extension curve of a 500 nm long DNA molecule containing a single nucleosome is shown in Fig. 3.4c. Two distinct steps represent the transitions between the wrapped and the unwrapped conformation. The limited force range in which each conformation is stable severely impedes accurate fitting, resulting in a contour length of  $430 \pm 20$  nm,  $510 \pm 120$  nm, and  $500 \pm 20$  nm respectively. The corresponding apparent persistence length of the three different conformations was  $34 \pm 8$  nm,  $17 \pm 20$  nm, and  $20 \pm 11$  nm. The inaccurate fitting, due to the limited force range in which the conformation is stable, is prominent for the 0.65 turns unwrapped conformation where very limited data is available and the WLC fit cannot distinguish between this conformation and the conformation of a fully unwrapped nucleosome. Furthermore, the values for both the contour length and the apparent persistence length deviate from the values that can be expected based on the length of the DNA and the structure of the (partially unwrapped) nucleosome. Therefore, force-extension curves are of limited use for fitting structural parameters from transient complexes.

Using the HM analysis on constant force time traces, the changes in apparent persistence length can directly be extracted from the probability distribution of each conformation. The apparent persistence length before unwrapping was  $45 \pm 5$  nm ( $N = 12$ ), whereas after unwrapping of 0.65 turns of DNA the apparent persistence length became  $50 \pm 6$  nm ( $N = 12$ ). The same conformation was probed independently in time traces that featured the second transition to the fully unwrapped conformation. In this case the apparent persistence length before unwrapping of the final turn was  $51.1 \pm 0.9$  nm ( $N = 5$ ), in excellent agreement with the previous measurement and changed after unwrapping of the final turn to  $52.0 \pm 0.7$  nm ( $N = 5$ ). Note that the accuracy is far better than the results obtained by fitting the force-extension data.

Using Eq. 3.12 to calculate the exit angle for each conformation, results in  $81 \pm 40^\circ$  for the wrapped conformation,  $130 \pm 70^\circ$  and  $144 \pm 16^\circ$  after unwrapping of 0.65 turns and  $180 \pm 10^\circ$  for the fully unwrapped conformation. The relatively large uncertainties in the obtained opening angle are caused by the steep dependence of the opening angle on the apparent persistence length. Based on the crystal structure [1] of the nucleosome, the exit angle of the fully wrapped (1.65 turns of DNA) conformation is  $|180^\circ - 0.65 \cdot 360^\circ| = 54^\circ$ . After unwrapping of 21 nm

of DNA from the histone core, the length of DNA that we obtained directly from the HM analysis, 0.95 turns remain, corresponding to an exit angle of  $|180^\circ - 0.95 \cdot 360^\circ| = 162^\circ$ . When the second turn is also unwrapped, the trajectory of the DNA is likely not affected by the nucleosome resulting in an exit angle of  $180^\circ$ . These values agree well with the values of the exit angle obtained from the HM analysis. Thus, the probability distributions that can be obtained by HM analysis can be used to measure the exit angle of the DNA from constant force time traces of nucleosome (un)wrapping.

### 3.6 Conclusion

By integrating the mechanical properties of DNA into probability distributions of a HM model we developed an accurate method for quantification of DNA force spectroscopy data. The described HM model, which uses the force-extension relation described by a WLC, fits the data with a high accuracy even when thermal fluctuations exceed the step size of a conformational change. Using a normal probability distribution, HM analysis fails to resolve steps smaller than the thermal fluctuations. Detailed information about the first- and second-turn nucleosome unwrapping, e.g. lifetimes, step sizes, persistence lengths, and DNA trajectory bending angles were extracted from constant force time traces. For the first time we were able to determine the bending angles of nucleosomal DNA in solution and resolved conformations that were fully wrapped, partially unwrapped and fully unwrapped. The HM analysis allowed extrapolation to zero-force lifetimes from constant force time traces. To probe the bending angles of a DNA trajectory of transient conformations, such as DNA unwrapping from a nucleosome, using electron or atomic force microscopy or crystal data is not straightforward, if possible at all, because the nucleosomes need to be trapped in the unwrapped conformation. As no force is applied in these type of experiments, most nucleosomes are trapped in the wrapped conformation.

The method is not restricted to analysis of DNA dynamics in nucleosomes, in which the histone octamer remains bound to the DNA. Also association and dissociation of DNA binding proteins like for example repressor proteins [10], protein DNA chimeras [23], or the unfolding of RNA pseudoknots [24] are associated with changes in contour length and bending angle. Accurate assessment of the kinetics of such reactions will need to take the non-linear extension of DNA into account and the current adapted HM analysis will be equally profitable in these studies.

## Acknowledgments

We would like to thank T. van der Heijden, S. Semrau, F. Chien, M. de Jager and A. Routh for providing materials and for the helpful discussions. This work was financially supported by the ‘Nederlandse Organisatie voor Wetenschappelijk Onderzoek’ (NWO).

## Methods

### Magnetic Tweezers

DNA-tethered superparamagnetic beads were imaged in a flow cell on a home-built inverted microscope with a CCD camera (Pulnix TM-6710CL) at 60 frames per second. The magnet position was controlled by a stepper motor-based translation stage (M-126, Physik Instrumente) with an accuracy of 200 nm. The position of the beads was measured by real-time image processing using LabView software (National Instruments) with an accuracy of 4 nm [25].

Due to the transient nature of the observed conformations, the height of the bead does not remain constant during an experiment, therefore the force can not be calculated accurately from equipartition [26]. Instead, the force was calculated from the position of the external magnets and a previous calibration measurement as described elsewhere [25].

### Preparation of the DNA Construct

A PCR was performed on a modified pGem3Z plasmid with a 601 nucleosome positioning site introduced at 94 bp. The reverse primer (5'-AAACC ACCCG GGTGG GCTCA CTCAT TAGGC ACCCC-3') was modified with a single digoxigenin at the 5' end. The forward primer (5'-CCCCA TGTTG TGCAA AAAAG CGG-3') was modified with a biotin on the 5' end.

### Mono-nucleosome Preparation

5 µg of the PCR product described above, was mixed with nucleosomes purified from chicken blood in a 1 to 10 molar ratio and diluted to a total volume of 40 µL in TE (10 mM Tris-HCl pH 8.0 and 1 mM EDTA) and NaCl (2 M). Next, a salt dialysis was performed as described elsewhere [27]. The final product was dissolved in TE. The reconstitution was analysed by native polyacrylamide gel electrophoresis and Atomic Force Microscopy (Fig. 3.5). Only bare DNA and mono-nucleosomes on the 601 position were observed.

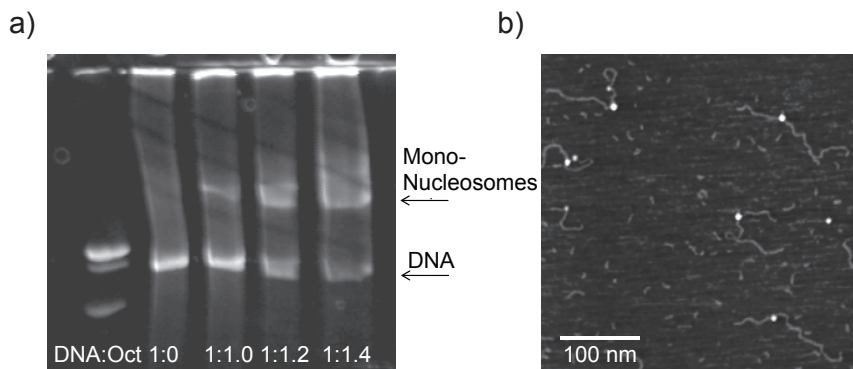


Figure 3.5: (a) Nucleosome reconstitution was analysed by native polyacrylamide gelelectrophoresis. (b) Tapping mode Atomic Force Microscopy of reconstituted mono-nucleosomes fixed in 2% glutaraldehyde in 5 mM  $MgCl_2$ , 10 mM HEPES and deposited on freshly cleaved mica.

## Flow cell Preparation

A clean glass coverslip was spincoated with a thin layer of a 1% polystyrene toluene solution. The coverslip was subsequently mounted on a polydimethylsiloxane (PDMS) flow cell containing a 10 x 4 x 0.4 mm flow channel. The flow cell interior was flushed with 10 mM HEPES (pH 7.6). Next, 0.1 mg/mL anti-digoxygenin (Roche) was introduced into the flow cell and incubated for 60 minutes at room temperature, followed by 10 minutes of incubation with blocking buffer: 10 mM HEPES (pH 7.6), 0.2% (w/v) BSA and 0.1% (v/v) Tween-20. Subsequently 8  $\mu$ L of measurement buffer (MB) 10 mM HEPES (pH 7.6), 0.02% (w/v) BSA, 2 mM magnesium acetate, 10 mM  $NaN_3$ , and 0.1% (v/v) Tween-20 was incubated with 1  $\mu$ L of 2.8  $\mu$ m superparamagnetic biotinylated Dynabeads (Invitrogen) and 1  $\mu$ L 10 ng/ $\mu$ L mono-nucleosomes for 15 minutes at room temperature to allow binding between the bead-DNA and the surface. The mixture was diluted in 400  $\mu$ L MB and incubated in the flow cell for 10 minutes. Finally the cell was flushed with MB.

## 3.7 Appendix: The Effect of Camera Filtering on the Measured Height Fluctuations of a Bead in a Trap

In this chapter we analysed the height fluctuations of a bead in a magnetic tweezers setup and calculated the mechanical properties of the tether and the lifetimes of the states of the nucleosome. However, we did not take camera filtering into account. Camera filtering occurs when the cutoff frequency of the bead fluctuations is much higher than one over the illumination



time of the camera used to measure the motion of the bead. The motion of the bead will be averaged during the illumination time of the camera and the measured height fluctuations will be smaller.

To investigate the effect of the camera filtering on our measurements, we used Brownian dynamics to simulate the motion of a bead attached to a DNA molecule in a magnetic tweezers setup. We calculated the height distribution of the unfiltered bead motion and the height distribution of the bead motion filtered by a camera. The width of the height distribution is estimated by the standard deviation of a normal distribution. We compared the persistence length and contour length obtained from the height distribution of the filtered and the unfiltered bead motion. Finally we investigated the influence of camera filtering on the results obtained in this chapter.

The cutoff frequency of the bead fluctuations is given by [26]:

$$f_c = \frac{k(F)}{2\pi\gamma^*}, \quad (3.13)$$

with  $k$  the stiffness of the tether at a given force  $F$ , for DNA given by Eq. 5.10 and  $\gamma^*$  the drag coefficient of a sphere corrected for the proximity of a wall as given by Eq. 2.6. Eq. 3.13 shows that the cutoff frequency is affected by several parameters, the stiffness of the tether, which in turn, depends on the force, the contour length and the persistence length of the DNA, and the drag coefficient, which in turn, is determined by the radius and the location of the bead. To investigate the effect of these parameters we plot the cutoff frequency of a bead attached to a DNA molecule for different forces, contour lengths and persistence lengths in Fig. 3.6. It is clear that an increase in tether length or bead size leads to a decreased cutoff frequency and an increase in persistence length leads to an increased cutoff frequency.

The timestep,  $dt$ , of the Brownian dynamics simulations performed was typically  $10^{-4} - 10^{-5}$  s. To simulate camera filtering we took the mean of the first  $\tau/dt$  points of the simulation as our first filtered point, with  $\tau$  the illumination time of the camera, the second  $\tau/dt$  points are averaged for the second point etcetera. The camera used in our experiments has a framerate of 60 Hz. We assumed that the camera shutter was continuously open resulting in an illumination time of 0.017 s.

We simulated a bead with a radius of  $1.4 \mu\text{m}$  attached to a DNA molecule with a contour length of 52 nm and a persistence length of 500 nm, similar to the bead and DNA used in the experiments in chapter 3. We simulated the motion of the bead at different forces and thus cutoff frequencies. The resulting filtered widths, contour lengths and persistence lengths compared to the unfiltered results are shown in Fig. 3.7a-c. It is evident that camera filtering has a large

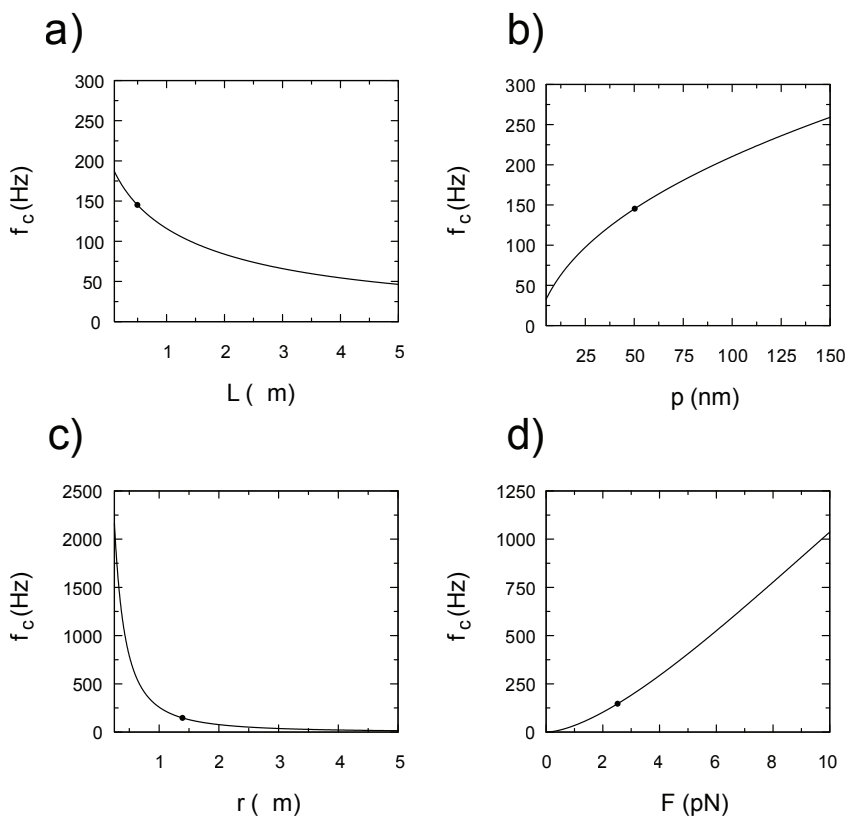


Figure 3.6: The cutoff frequency of the height fluctuations of the bead versus the contour length (a), persistence length (b), bead radius (c) and force (d) as calculated from Eq. 3.13. The dot is for a bead with a radius of  $1.4 \mu\text{m}$  attached to a DNA molecule with a contour length of  $500 \text{ nm}$  and a persistence length of  $50 \text{ nm}$  at a force of  $2.5 \text{ pN}$ .

effect on the width of the distribution. At 4 pN the filtered width is 0.4 times the input width. The effect on the fitted contour length is not big, which is to be expected since filtering does not change the average position of the bead but only the width of the fluctuations. The effect of camera filtering on the fitted persistence length is dramatic, up to a more than 60 times increase at a force of 4 pN.

What does this mean for the measured lifetimes, persistence length and contour length? Since the lifetimes do not depend on the width of the fluctuations, they are not affected by camera filtering. The contour length shows a small dependency on the force, see Fig. 3.7b, and thus the cutoff frequency of the bead. This effect, however, is within 5% of the input value of the contour length which indicates that the values obtained in chapter 3.5 are close to the real value. The measured persistence length is greatly affected by camera filtering as shown in Fig. 3.7c. In our experiments we measured a persistence length between 45 and 50 nm at a force of about 2.5 pN. By simulating a DNA molecule with different persistence lengths and plotting the resulting filtered persistence length we get an idea of the real persistence length of the DNA tether. Fig 3.7d shows that a measured persistence length of 50 nm would mean a real persistence length of about 20 nm. This large reduction in persistence length cannot be explained by the angle induced in the DNA trajectory of a single nucleosome. Even an exit angle would of 0, results in an apparent persistence length of 35 nm. However, several other explanations exist for the observed large decrease in persistence length. If we would have overestimated the force, the apparent persistence would appear to be smaller. For example, if we simulate the motion of the bead attached to a DNA molecule with a contour length of 500 nm and a persistence length of 20 nm at a force of 2.25 pN we obtain with filtering a persistence length of 46 nm. However, if we took the force to be 2.5 pN we would obtain a persistence length of 35 nm. In the simulations we did not take the residual mechanical noise and inaccuracies of the measurement of the position of the bead into account. These would increase the apparent fluctuations, thereby decreasing the measured persistence length. Furthermore, the exposure time of the camera is the value that determines the amount of filtering, if the exposure time was much smaller than the time per frame of the camera, the measured fluctuations would be smaller leading to a larger measured persistence length. The last three explanations compensate the filtering effect and could be checked by measuring bare DNA molecules and comparing the expected filtered height distribution width to the measured distribution width.

It is clear that one should carefully consider camera filtering when analysing the height fluctuations of a bead in a tweezers setup. One should make sure that the cutoff frequency of the bead motion is well below 1 over the exposure time of the camera. Fig. 3.6 shows that the cutoff frequency can be reduced by taking a larger bead or a larger molecule. However, an increased cutoff frequency would lead to a slower reaction of the bead on unwrapping events which

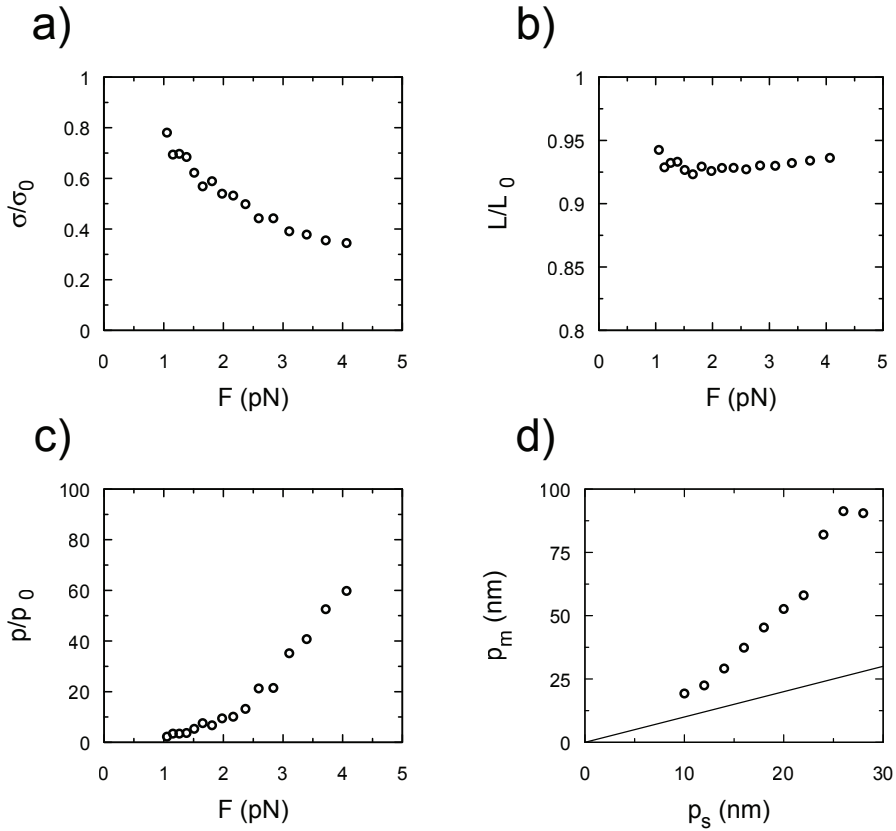


Figure 3.7: *a-c) The height distribution width, contour length and persistence length of the filtered signal of a Brownian dynamics simulation of a DNA molecule with a contour length of 500 nm and a persistence length of 52 nm, compared to the unfiltered values at different forces. d) The measured persistence length of the filtered fluctuations compared to the input persistence length of a DNA molecule with a contour length of 500 nm at a force of 2.5 pN, the solid line ( $p_m = p_s$ ) is drawn as a guide to the eye.*

may lead to missing short transitions. Furthermore one could reduce the illumination time by decreasing the exposure time of the camera or using a pulsed light source. In the case of the measurements in this chapter, the resulting lifetimes and contour lengths are not affected by the camera filtering, the resulting apparent persistence lengths from the Hidden Markov analyses, however, may be an overestimate of the real apparent persistence lengths.

## Bibliography

- [1] K. Luger, A. W. Mäder, R. K. Richmond, D. F. Sargent, and T. J. Richmond, "Crystal structure of the nucleosome core particle at 2.8 Å resolution," *Nature*, vol. 389, pp. 251–260, Sep 1997.
- [2] G. Li, M. Levitus, C. Bustamante, and J. Widom, "Rapid spontaneous accessibility of nucleosomal dna.," *Nat. Struct. Mol. Biol.*, vol. 12, pp. 46–53, Dec 2004.
- [3] W. J. A. Koopmans, T. Schmidt, and J. van Noort, "Nucleosome immobilization strategies for single-pair fret microscopy.," *ChemPhysChem*, vol. 9, pp. 2002–2009, Oct 2008.
- [4] S. Mihardja, A. Spakowitz, Y. Zhang, and C. Bustamante, "Effect of force on mononucleosomal dynamics.," *Proc. Natl. Acad. Sci. U.S.A.*, vol. 103, pp. 15871–15876, Oct 2006.
- [5] B. D. Brower-Toland, C. L. Smith, R. C. Yeh, J. T. Lis, C. L. Peterson, and M. D. Wang, "Mechanical disruption of individual nucleosomes reveals a reversible multistage release of dna," *Proc. Natl. Acad. Sci. U.S.A.*, vol. 99, pp. 1960–1965, Feb 2002.
- [6] E. A. Evans and K. Ritchie, "Dynamic strength of molecular adhesion bonds.," *Biophys. J.*, vol. 72, pp. 1541–1555, Apr 1997.
- [7] L. Rabiner, "A tutorial on hidden markov-models and selected applications in speech recognition," *P. Ieee*, vol. 77, pp. 257–286, Jan 1989.
- [8] S. R. Eddy, "What is a hidden markov model?," *Nat. Biotechnol.*, vol. 22, pp. 1315–1316, Oct 2004.
- [9] S. A. McKinney, C. Joo, and T. Ha, "Analysis of single-molecule fret trajectories using hidden markov modeling," *Biophys. J.*, vol. 91, pp. 1941–1951, Sep 2006.
- [10] J. F. Beausang, C. Zurla, C. Manzo, D. Dunlap, L. Finzi, and P. C. Nelson, "Dna looping kinetics analyzed using diffusive hidden markov model," *Biophys. J.*, vol. 92, pp. L64–L66, Apr 2007.

- [11] A. Viterbi, "Error bounds for convolutional codes and an asymptotically optimum decoding algorithm," *Ieee T. Inform. Theory*, vol. 13, pp. 260–269, Jan 1967.
- [12] L. Baum, T. Petrie, G. Soules, and N. Weiss, "A maximization technique occurring in statistical analysis of probabilistic functions of markov chains," *Ann. Math. Stat.*, vol. 41, pp. 164–171, Jan 1970.
- [13] D. Segall, P. C. Nelson, and R. Phillips, "Volume-exclusion effects in tethered-particle experiments: bead size matters.," *Phys. Rev. Lett.*, vol. 96, p. 088306, Apr 2006.
- [14] J. F. Marko and E. Siggia, "Stretching dna," *Macromolecules*, vol. 28, pp. 8759–8770, Jan 1995.
- [15] C. Claudet, D. Angelov, P. Bouvet, S. Dimitrov, and J. Bednar, "Histone octamer instability under single molecule experiment conditions.," *J Biol Chem*, vol. 280, pp. 19958–19965, May 2005.
- [16] A. Thåström, P. T. Lowary, and J. Widom, "Measurement of histone-dna interaction free energy in nucleosomes.," *Methods*, vol. 33, pp. 33–44, May 2004.
- [17] J. Widom, "Physicochemical studies of the folding of the 100 a nucleosome filament into the 300 a filament. cation dependence," *J. Mol. Biol.*, vol. 190, pp. 411–424, Aug 1986.
- [18] L. Valberg, J. Holt, E. Paulson, and J. Szivek, "Spectrochemical analysis of sodium, potassium, calcium, magnesium, copper, and zinc in normal human erythrocytes," *J. Clin. Invest.*, vol. 44, pp. 379–389, Mar 1965.
- [19] J. Yan and J. F. Marko, "Effects of dna-distorting proteins on dna elastic response," *Physical review. E, Statistical, nonlinear, and soft matter physics*, vol. 68, p. 011905, Jul 2003.
- [20] J. van Noort, S. Verbrugge, N. Goosen, C. Dekker, and R. T. Dame, "Dual architectural roles of hu: formation of flexible hinges and rigid filaments," *Proc. Natl. Acad. Sci. U.S.A.*, vol. 101, pp. 6969–6974, May 2004.
- [21] B. M. Ali, R. Amit, I. Braslavsky, A. B. Oppenheim, O. Gileadi, and J. Stavans, "Compaction of single dna molecules induced by binding of integration host factor (ihf)," *Proc. Natl. Acad. Sci. U.S.A.*, vol. 98, pp. 10658–10663, Sep 2001.
- [22] I. M. Kulić, H. Mohrbach, V. Lobaskin, R. Thaokar, and H. Schiessel, "Apparent persistence length renormalization of bent dna.," *Physical review. E, Statistical, nonlinear, and soft matter physics*, vol. 72, p. 041905, Dec 2005.

- [23] C. Cecconi, E. A. Shank, F. W. Dahlquist, S. Marqusee, and C. Bustamante, “Protein-dna chimeras for single molecule mechanical folding studies with the optical tweezers,” *Eur. Biophys. J.*, vol. 37, pp. 729–38, Jul 2008.
- [24] J.-D. Wen, M. Manosas, P. T. X. Li, S. B. Smith, C. Bustamante, F. Ritort, and I. T. Jr, “Force unfolding kinetics of rna using optical tweezers. i. effects of experimental variables on measured results,” *Biophys. J.*, vol. 92, pp. 2996–3009, May 2007.
- [25] M. Kruithof, F. Chien, M. de Jager, and J. van Noort, “Sub-piconewton dynamic force spectroscopy using magnetic tweezers,” *Biophys. J.*, vol. 94, pp. 2343–2348, Dec 2007.
- [26] C. Gosse and V. Croquette, “Magnetic tweezers: micromanipulation and force measurement at the molecular level,” *Biophys. J.*, vol. 82, pp. 3314–3329, Jun 2002.
- [27] C. Logie and C. L. Peterson, “Catalytic activity of the yeast swi/snf complex on reconstituted nucleosome arrays,” *EMBO J.*, vol. 16, pp. 6772–6782, Nov 1997.





---

---

## CHAPTER 4

---

# Single Molecule Force Spectroscopy Reveals a Highly Compliant Helical Folding for the 30 nm Chromatin Fiber<sup>1</sup>

### Abstract

The compaction of eukaryotic DNA into chromatin has been implicated in the regulation of all cellular processes whose substrate is DNA. To understand this regulation, it is essential to reveal the structure and mechanism by which chromatin fibers fold and unfold. Here, we have used magnetic tweezers to probe the mechanical properties of a single, well-defined array of 25 nucleosomes. When folded into a 30 nm fiber, representing the first level of chromatin condensation, the fiber stretched like a Hookian spring at forces up to 4 pN. Together with a nucleosome-nucleosome stacking energy of  $14 k_b T$ , four times larger than previously reported, this points to a solenoid as the underlying topology of the 30 nm fiber. Surprisingly, linker

---

<sup>1</sup>This chapter is based on the article: *Single molecule force spectroscopy reveals a highly compliant helical folding for the 30 nm chromatin fiber*, M. Kruithof, F. Chien, A. Routh, C. Logie, D. Rhodes and J. van Noort, accepted for publication in Nature Structural and Molecular Biology

histones do not affect the length or stiffness of the fibers, but stabilize fiber folding up to forces of 7 pN. Fibers with a nucleosome repeat length of 167 bp instead of 197 bp are significantly stiffer, consistent with a two-start helical arrangement. The extensive thermal breathing of the chromatin fiber that is a consequence of the observed high compliance provides a structural basis for understanding the balance between chromatin condensation and transparency for DNA transactions.

## 4.1 Introduction

The eukaryotic genome is organized into chromatin, a highly compacted structure that is now recognized to be a key regulator of all nuclear processes whose substrate is DNA, such as transcription and replication. The lowest level of DNA organization in chromatin is well known: an octamer of histone proteins wraps 146 bp of DNA in 1.65 super helical turns [1]. The linker histone organizes an additional 20 bp of DNA and is located at the entry/exit site of the DNA protruding from the nucleosome core [2]. Nucleosome cores are connected by linker DNA, typically 10 - 90 bp in length, forming nucleosomal arrays. Under physiological conditions, including divalent cations, nucleosome arrays fold into compact chromatin fibers with a diameter of about 30 nm [3, 4]. Biochemical and structural data suggest that nucleosome array folding is driven by nucleosome-nucleosome interactions, but that the path of the DNA linking adjacent nucleosomes is unknown. Therefore the structure of the 30 nm chromatin fiber remains controversial, despite three decades of intense research, with the consensus viewpoint see-sawing back and forth between a one-start solenoidal and a two-start zig-zag architecture [5-7].

One of the parameters that defines the architecture of the chromatin fiber is the length of the linker DNA, as expressed in terms of the nucleosome repeat length (NRL). *In vivo*, NRLs vary between 165-212 bp, but NRLs of 188 and 196 bp are by far the most common [8]. Short NRLs are less abundant and generally associated with transcriptionally active chromatin, found for example in yeast [9] and in neuron cells [10]. Long NRLs can be found in transcriptionally silent chromatin from chicken erythrocytes [11]. The presence or absence of the linker histone is a second parameter that affects chromatin folding and has also been implicated in transcription repression. Stoichiometric amounts of linker histone can be found in highly condensed chromatin. In yeast chromatin linker histones are relatively rare. In fact, longer NRLs correlate well with a higher abundance of linker histones [12]. Both the NRL and the presence of the linker histone control the relative positioning of successive nucleosomes in an array and hence direct the formation of higher order chromatin structures.

Recently major progress in the characterization of higher order chromatin folding has been obtained using arrays of 601 nucleosome positioning DNA [13, 14]. A 9 Å crystal structure of a tetramer of nucleosome cores, based on a 167 bp NRL array without the linker histones, [15] clearly showed folding of the two-start helix type. These measurements were supported by crosslinking experiments [16]. Electron Microscopy (EM) on fibers with NRLs between 177 and 217 bp however revealed a well-defined constant diameter of 33 nm [7]. The dimensions of these fibers, which were independent on the NRL, implied an interdigitated one-start solenoid structure. Thus, in spite of these breakthroughs, the controversy over the structure of the 30 nm fibers and the role of linker histones has not been resolved.

Here we address the question of the structure of the 30 nm chromatin fiber using single molecule force spectroscopy, which probes the extension of single chromatin fibers in solution with nm and sub-pN resolution. Previous force spectroscopy studies have focused on the high force regime, demonstrating the force induced unwrapping of all DNA from the octamer of histones at 15-25 pN [17–19]. Cui and Bustamante [20] did look into the chromatin compaction of long native chromatin fibers at low forces and showed that chromatin fibers unfold at several piconewtons. In this study we used highly homogeneous chromatin fibers of known composition whose folding has previously been carefully characterized by both sedimentation velocity and EM analyses [21, 22]. This ensures that the fibers analysed by force spectroscopy are fully compacted and allowed us to capture and to quantitatively interpret the initial stages of the unfolding pathway of chromatin fibers in much more detail. Furthermore, we explicitly take the presence and absence of stoichiometric amounts of linker histones into account and demonstrate that linker histones increase the mechanical stability of chromatin fibers. Finally, we compare 197 bp NRL arrays with 167 bp NRL arrays and show, based on their compaction and compliance, that these fibers fold into different structures consistent with a one-start and two-start helical folding.

## 4.2 Results

### Reconstitution of 601 arrays yields regular 30 nm chromatin fibers

Chromatin fibers were reconstituted using salt dialysis from chicken erythrocyte histone octamers and DNA arrays consisting of 25 tandem repeats of 167 or 197 bp 601 DNA, as described [14]. In each reconstitution, the histone DNA stoichiometry was titrated in 8 steps and analyzed using gel electrophoresis [14]. Optionally, stoichiometric amounts of linker histone were reconstituted in a second titration. Though gel electrophoresis clearly resolves the optimal reconstitution stoichiometry, resulting in the highest level of condensation (Fig. 4.1), it does not have the resolution to confirm full saturation of the DNA arrays with histone octamers. To resolve the number of nucleosomes per fiber, which is necessary for quantitative interpretation of the force spectroscopy data, individual chromatin fibers were imaged with Atomic Force Microscopy (AFM) under denaturing conditions, i.e. in absence of  $Mg^{2+}$  (Fig. 4.2a).

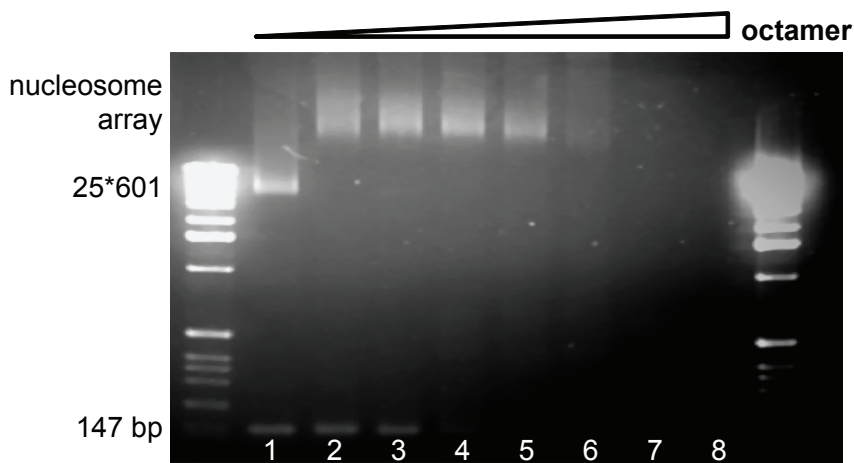


Figure 4.1: Reconstitution of nucleosomal arrays. DNA arrays containing 25\*601 nucleosome positioning elements were titrated in 8 steps with chicken erythrocyte histone octamers and mixed sequence 147 bp competitor DNA. Arrays were double-bag dialysed overnight in reconstitution buffer. 5  $\mu$ l of each sample was run on 0.9% agarose gel in 0.2 X TB buffer and stained with EtBr. Except for the experiments in Fig. 4.3, which were done with material from lane 3, all experiments were done with batches that showed the narrowest band for the nucleosomal array, in this case lane 5, pointing at optimal reconstitution.

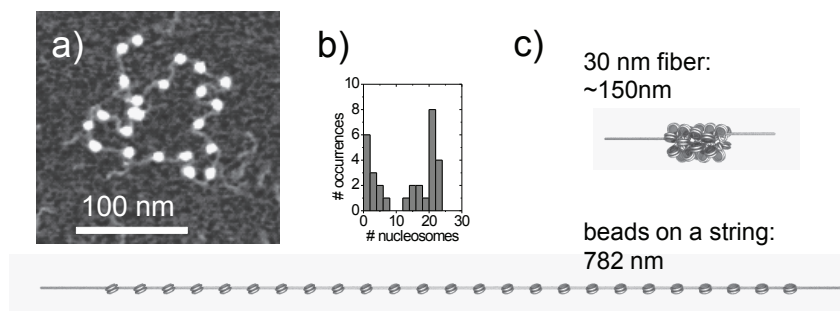


Figure 4.2: *Characterization of reconstituted chromatin fibers a) AFM image of a reconstituted fiber under denaturing conditions. b) The distribution of nucleosomes per fiber of a sub-stoichiometric reconstitution shows a bimodal distribution. c) The end-to-end length of an array containing 25 nucleosomes, folded into the 30 nm fiber and flanked by in total of 300 bp of DNA, is approximately 150 nm. When unfolded in a beads-on-a-string conformation it measures 782 nm.*

By counting the number of nucleosomes per fiber we observed a high cooperativity in nucleosome binding on the 601 arrays which was previously also reported on 5S RNA arrays [23]. The distribution of the nucleosome occupancy per fiber (Fig. 4.2b) at sub-saturating histone DNA ratios (lane 3 in Fig. 4.1) shows a bimodal distribution with populations of sparsely and densely decorated fibers. Reconstitution with a higher histone to DNA ratio (lane 5 in Fig. 4.1) yielded 99% of all 601 positioning sites in the fibers being occupied with a histone octamer. In the presence of  $Mg^{2+}$  EM inspection confirmed folding of the fibers into regular 30 nm fibers with dimensions that agree well with previously reported experiments [22]. The high regularity, known contour length, and the confirmed folding into 30 nm fibers makes this reconstituted chromatin uniquely suited for probing the forces that drive higher order chromatin folding.

### 197 bp NRL fibers stretch like a Hookian spring

A quantitative understanding of chromatin compaction requires a detailed comparison with the known dimensions of the fiber components. A single nucleosome core wraps 147 bp of DNA in a cylinder with a diameter of 11 nm and a height of 5.5 nm. The nucleosomes in a 197 bp NRL fiber without linker histones are connected by 50 bp of DNA resulting in a spacing between nucleosomes of 16.6 nm. In the absence of higher order folding the contour length of a fully reconstituted 25\*197 bp NRL beads-on-a-string fiber would be approximately 682 nm. For the total contour length of the used fibers an additional 100 nm of flanking DNA must be added, resulting in a contour length of 782 nm (Fig. 4.2c). When folded in a 30 nm fiber with a

nucleosome line density of 1.5 to 2.1 nm/nucleosome [7] the fiber adopts a length of 38–53 nm, resulting in a total contour length of approximately 150 nm.

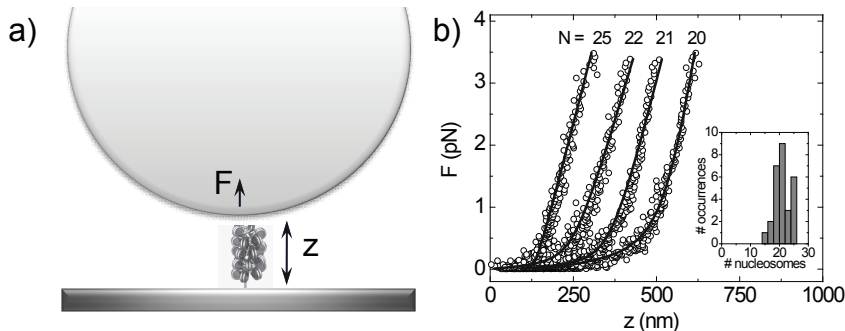


Figure 4.3: Force spectroscopy on chromatin fibers. a) Schematic drawing of a force spectroscopy experiment, not to scale. A  $1\ \mu\text{m}$  paramagnetic bead is tethered with a chromatin fiber to a microscope slide. The height of the bead represents the end-to-end distance of the fiber and is obtained from video microscopy and image processing. The force on the fiber is varied by changing the position of a pair of external magnets. b) Force-distance curves of fibers with different occupations, the solid lines were fits to Eq. 4.2. Inset: distribution of nucleosomes per fiber. Note that we discarded fibers containing small numbers of nucleosomes in this analysis.

Magnetic tweezers based dynamic force spectroscopy [24] was used to measure the extension of the fibers with nm resolution. In short, single chromatin fibers are tethered between the bottom slide of a flow cell and a  $1\ \mu\text{m}$  paramagnetic bead. The height of the tethered bead is obtained from video microscopy and image processing and represents the end-to-end distance  $z$  of the fiber (Fig. 4.3a). In a typical Force-Distance (F-D) experiment a pair of external magnets is moved down towards the flow cell in 20 s and up again, after which the experiment is repeated. Under folding conditions (100 mM KAc, 2 mM  $\text{MgAc}_2$ , 10 mM Hepes pH 7.6, room temperature) the fibers remained stable upon repeated pulling, sometimes for up to 30 F-D cycles.

At low forces, between 0.5 and 3.5 pN, all folded nucleosomal arrays that we measured, including the sub-saturated fibers that were reconstituted with low histone/DNA ratios, exhibited a linear extension (Fig. 4.3b). The F-D curves represent the stretching of both the chromatin fiber and the flanking DNA. For a more quantitative interpretation of the tether extension the contributions of the chromatin and the DNA should be separated. The mechanical properties of DNA have been well established. The force  $F(z)$ , needed to stretch a bare DNA molecule

to an end-to-end distance,  $z$ , follows a Worm Like Chain (WLC) [25, 26]:

$$F(z) = \frac{k_b T}{p} \left[ \frac{1}{4(1-z/L_0)^2} - \frac{1}{4} + \frac{z}{L_0} \right], \quad (4.1)$$

with thermal energy  $k_b T$ , contour length  $L_0$  and persistence length  $p$ . The compliance of the chromatin fiber on the other hand has not been described before. The linear part of the F-D curves (Fig. 4.3b) suggests a Hookian extension of the chromatin part of the fiber. We therefore modeled the chromatin fiber as having a rest length  $L_{30}$  and a force-induced extension that is inversely proportional to a characteristic spring constant  $k$ . This results in a total end-to-end distance of the tether of

$$z(F) = z_{WLC}(F, L_{DNA}, p_{DNA}) + L_{30} + \frac{F}{k} \quad (4.2)$$

in which  $z_{WLC}$  represents the inverse of Eq. 4.1, using the contour length  $L_{DNA}$  and persistence length  $p_{DNA}$  of the flanking DNA. The Hookian approximation proved to fit the data well (Fig. 4.3b). The large differences in the contour length of the fibers shown in Fig. 4.3b should be attributed to variations in the number of nucleosomes per fiber which was also revealed by AFM imaging of this sub-saturated chromatin batch. It was possible to relate the number of nucleosomes present in each fiber to the fitted length of the flanking DNA, which increases by 197 bp for each missing nucleosome. The resulting nucleosome density distribution (Fig. 4.3b, inset) shows good agreement with the distribution obtained by AFM imaging of the same batch (Fig. 4.2b). Even in reconstitutions with a histone octamer-DNA stoichiometry that corresponded to the highest compaction we found that 20% of the fibers missed one or two nucleosomes, consistent with a reconstitution yield of 99% of the 601 positioning sites. However, it was possible to discard all sub-saturated fibers based on the fitted length of the flanking DNA, resulting in a more homogeneous data set. Note that even without this selection all fibers feature a very similar slope in the F-D curve that is independent of the number of nucleosomes in the particular fiber.

In this paper we focus on the extensive stretching in the low force regime that provides information on the first steps in 30 nm fiber unfolding. In the low force regime all extensions of the folded chromatin fiber appeared linear. In contrast to previous force spectroscopy studies on nucleosomal arrays [19, 27, 28], which were performed at higher forces, we did not see indications of DNA unwrapping from the nucleosome. Indeed, only at forces exceeding 7 pN we observed hysteresis in the F-D curves and extensions beyond the length of the beads-on-a-string conformation (Fig. 4.4). Both non-linear features indicate concurrent fiber unfolding and DNA unwrapping. In order to preserve the higher order folding, we not only limited the



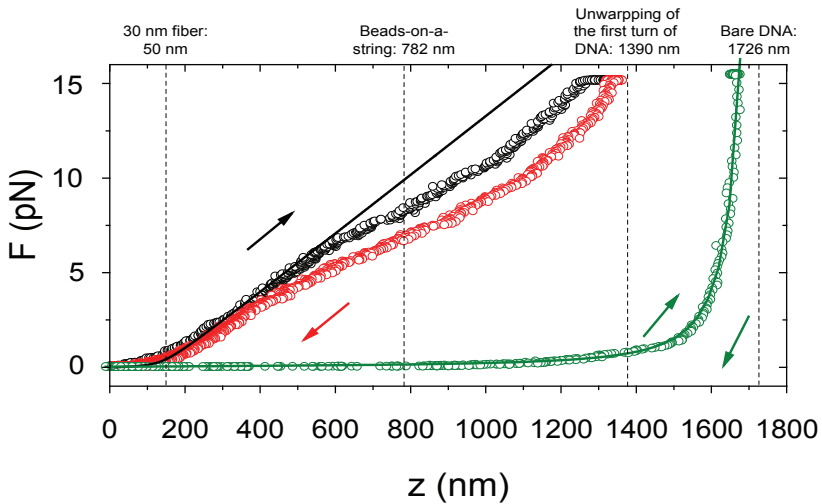


Figure 4.4: Stretching of chromatin fibers at high forces reveals DNA unwrapping. When 2.8 micrometer beads were used the maximum force in our F-D experiments increased to approximately 15 pN. Green dots show F-D curve on the DNA template alone, green line represents fit to WLC. Up to 7 pN the chromatin fiber containing H5 stretched linearly, following Hookian extension (Eq. 2). Subsequently, a non-linear length increase was observed, stretching the fiber beyond 782 nm, the contour length of a beads-on-a-string fiber. This excess length must have resulted from DNA unwrapping from the nucleosomes. The relatively high compliance of the fiber points to incomplete stacking of the nucleosomes in the fiber. This is probably due to an extended exposure to high forces during rinsing the flow cell prior to the measurement, which is inherent to the use of larger beads. At 15 pN the end-to-end distance converges to the contour length of a fiber in which one super helical turn of DNA has been unwrapped from each nucleosome. Upon reduction of the force the fiber refolded. The hysteresis in the forward and backward trace indicated that the unfolding and subsequent refolding was not in thermodynamic equilibrium. Nevertheless, folding and refolding was reversible, and could be repeated over 10 times for a single chromatin fiber.

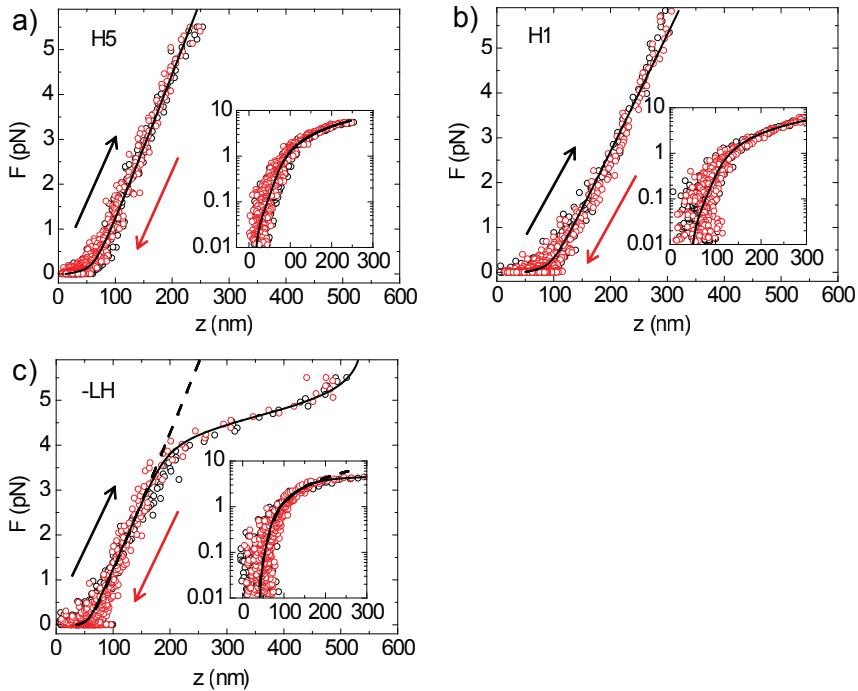


Figure 4.5: Chromatin fibers stretch like a Hookian spring, independently of the presence of linker histones. Forward (black circles) and backward (red circles) F-D curves of a) chromatin fibers containing stoichiometric concentrations of H5, b) chromatin fibers containing stoichiometric concentrations of H1. The absence of hysteresis indicated that the fibers were in thermodynamic equilibrium during the entire F-D cycle. Data were fitted to Eq. 4.2. The average fit results on multiple chromatin fibers are listed in Table 1. c) F-D curves of a fiber without linker histones, dashed line: fit to Eq. 4.2, only data up to 3 pN were included. Solid line fit to Eq. 4.5 resulting in  $\Delta G=13.2\pm 0.7 k_b T$  and  $\Delta z=12.1\pm 0.5$  nm. Insets show good fits at small forces.

maximal force to 6 pN, we also carefully optimized experimental conditions and sample handling to minimize disorder in chromatin folding. This resulted in a reproducible stiffness of the chromatin fibers, as exemplified by the very similar slopes in the F-D curves in Fig. 4.3b. We therefore conclude that the large range over which chromatin fibers exhibit Hookian extension is characteristic for the compliance of the 30 nm fiber.

### Linker histones do not affect the stiffness of a chromatin fiber

When comparing the mechanical parameters of the folded nucleosome arrays with and without linker histones (H1 or H5) we find, surprisingly, that both the stiffness and the length

were unaffected by the presence or type of linker histones (Fig. 4.5 and Tab. 4.1). As shown in Fig. 4.5a-c, the simple Hookian model accurately follows the experimental F-D relation of the chromatin fibers over 3 orders of magnitude of force. The obtained nucleosome line density varied between  $1.6 \pm 0.2$  and  $2.0 \pm 0.2$  nm/nucleosome, in good agreement with recent EM measurements [7] on this chromatin material and confirms that the nucleosome arrays were properly folded into 30 nm fibers. Importantly, the absence of hysteresis indicates thermodynamic equilibrium of all conformational changes in the time of each F-D cycle. It also appears that the interactions driving chromatin folding are not affected by the presence of linker histones, as additional contacts between the linker histones can be expected to increase the stiffness of the fiber, a feature that we did not observe. Fibers with and without linker histones could be stretched extensively, up to at least three times their rest length. Fibers with linker histones could be stretched in a linear fashion up to more than 6 pN (Fig. 4.5a and b). Thus, the presence of the linker histone stabilizes the fibers under external forces, which may relate to our earlier sedimentation velocity results that showed an increased compaction of the fiber upon inclusion of linker histones [14].

The striking difference with fibers lacking linker histones is the appearance of a force plateau at 4.5 pN (Fig. 4.5c). Contrary to high-force measurements in which concomitant DNA unwrapping from the histone core occurred (Supplementary Fig. 1), this transition did not show hysteresis and thus was fully in thermodynamic equilibrium. The end-to-end distance remained well within the length that can be expected for a beads-on-a-spring conformation, indicating that the nucleosome core particles remained fully intact. Therefore the plateau in the F-D curve of the chromatin fiber lacking linker histones should be explained by disruption of nucleosome-nucleosome interactions which are stabilized by the linker histones.

## The nucleosomes in a 30 nm fiber are arranged in a solenoidal structure

How do the measured stiffness and extension relate to the structure of the 30 nm chromatin fiber? The stiffness of an isotropic solid cylinder is defined by its Young's modulus  $E$  [29]:

$$E = \frac{kL_{30}}{2\pi R^2}. \quad (4.3)$$

Using the appropriate radius  $R = 15$  nm for a 30 nm fiber and the experimentally obtained stiffness  $k = 0.025$  pN/nm and  $L_{30} = 50$  nm results in a Young's modulus of  $0.9 \cdot 10^{-6}$  GPa, which is 6 orders of magnitude smaller than typical tabulated values of structured proteins. Furthermore, we are not aware of any bulk material that has a tensile strength that allows for stretching more than 3 times its rest length in a linear fashion, like the fibers shown in Fig. 4.5a-c that exhibit stretching from 50 nm up to more than 160 nm. Hence, it must be the *structure*

of the fiber, rather than its *isotropic elasticity* that provides its extraordinary high compliance.

Most proposed structures of chromatin folding are based on one-on-one stacking of nucleosomes [7, 30], as suggested from crystal structures [1, 15], cross linking studies [16] and EM on nucleosome core particles [31] and natively assembled nucleosome arrays [32]. The two prevailing models of the 30 nm fiber are a one-start and the two-start helix. In both these models fiber folding is driven by nucleosome stacking. The order of stacking however makes the difference between the two alternative folding conformations. In the one-start helix neighboring nucleosomes interact forming a single super helical ribbon, whilst in the two-start helix even and odd number nucleosomes stack into two parallel ribbons. A one-start helical spring composed of a single ribbon of stacked nucleosomes can be modeled as a simple helical spring yielding a stiffness of [29]:

$$k = \frac{1}{4N} \frac{Gr^4}{R^3}, \quad (4.4)$$

with  $N$  turns of a ribbon of radius  $r$  and shear modulus  $G$  defined as  $G = E/2(1 + \sigma)$ . The Poisson ratio  $\sigma$  depends on the compressibility of the material and is typically between 0.2 and 0.5. With  $\sigma = 0.2$ ,  $r = 5.5$  nm,  $N = 25/6$  and  $k = 0.025$  pN/nm a Young's modulus of  $3 \cdot 10^{-3}$  GPa was obtained. This is smaller than reported for typical proteins, but similar to the Young's modulus of elastin, a protein that has a very high elasticity due to the disordered structure of its polypeptide chains. Thus, the measured stiffness of the chromatin fiber is consistent with the elasticity of disordered proteins that act as entropic springs. Indeed the histone tails, which are disordered polypeptide chains, have been shown to be responsible for the nucleosome-nucleosome interactions [7], and may thereby determine the flexibility of the fiber.

Whereas the small stiffness that we obtained is indicative of a helical structure of the chromatin fiber, its value does not have the accuracy to discriminate between one or two start configurations. The total length of the Hookian regime in the F-D curve is more informative in this respect. Fibers containing 25 nucleosomes without linker histones could be stretched up to 160 nm (Fig. 4.5), corresponding to 6.4 nm per nucleosome. The stretching of a solenoidal structure of 25 nucleosomes is schematically depicted in Fig. 4.6a and b. Upon pulling, a solenoidal structure can stretch into a continuous stack of nucleosomes, represented by the stack-of-coins structure of the maximally extended fiber (Fig. 4.6c). The distance between the nucleosomes in such an arrangement can easily be spanned by the protruding histone tails that add to the 5.5 nm height of the nucleosome core [1]. If the nucleosomes in the fiber were to be arranged in a two-start structure [15], stretching of the two parallel ribbons up to 160 nm would exceed the height of a nucleosome by a factor of over 2, prohibiting physical contacts between the NCP's even when their extruding tails would be fully stretched. Thus the Hookian behavior of the fiber, its length, its compliance and its transition to a beads-on-a-string struc-

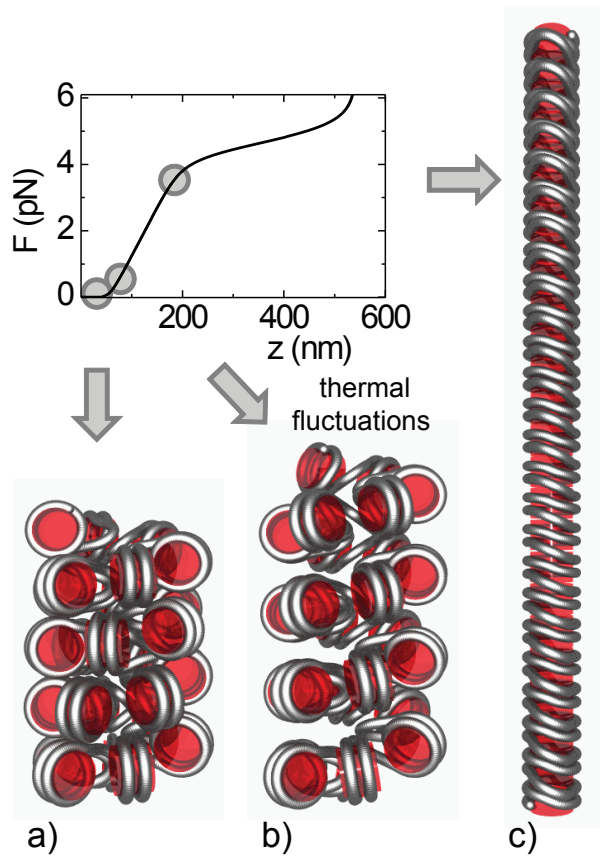


Figure 4.6: Schematic representations of chromatin fiber conformations at different forces a)  $F = 0$  pN, representing the most condensed conformation of the fiber. b) The extension at 0.4 pN is equivalent to the expected average extension due to thermal fluctuations. c) Fully extended chromatin fiber at 4 pN. The height of 25 stacked nucleosomes matches the observed maximum extension of the fiber before rupture.

ture provide quantitative support for the 30 nm chromatin fiber to be organized in a solenoidal, one-start topology [22].

### Quantification of the nucleosome-nucleosome interaction energy

Because chromatin higher order folding is driven by nucleosome stacking the high tensile strength that we obtained can only be provided by strong interactions between the nucleosomes. To understand chromatin higher order folding it is therefore essential to obtain an accurate number on the interaction energy between stacking nucleosomes. In a previous force spectroscopy study Cui and Bustamante [20] reported a nucleosome-nucleosome interaction energy of  $3.8 k_b T$ , which seems rather low to maintain stacking at forces of several piconewtons. However, this value was obtained in absence of  $Mg^{2+}$ , which is known to be required for the folding and stability of chromatin higher structures [33, 34]. We therefore tested whether  $Mg^{2+}$  depletion would affect the force required to disrupt the higher order structure by flowing in a buffer lacking magnesium acetate. Fibers without linker histones exhibited a significant decondensation after depletion of  $Mg^{2+}$ , as shown in Fig. 4.7a. The decondensation of the fibers was reversible upon replenishment with buffer containing  $Mg^{2+}$ . Upon repeated unfolding and refolding of the fibers we observed a gradual decrease in both condensation and hysteresis (Fig. 4.7b). The hysteresis represents the total work involved with the ruptures that occur in the fiber during the F-D cycle and was quantified by numerical integration. Interestingly, the hysteresis only decreased when the fiber was held in an extended conformation and we therefore plotted the interaction energy as a function of the time the chromatin fiber was held in a stretched conformation. The resulting mono-exponential decay of the hysteresis is characteristic of first order reaction kinetics. This reaction, having an off-rate of  $0.01 s^{-1}$ , might be attributed to the dissociation of  $Mg^{2+}$  from the fiber. Independent of its physical origin however, it is clear that  $Mg^{2+}$  depletion gradually decreases the interactions that maintain higher order folding and that an accurate assessment of the interaction strength should therefore include the transient effects related to stretching the fiber.

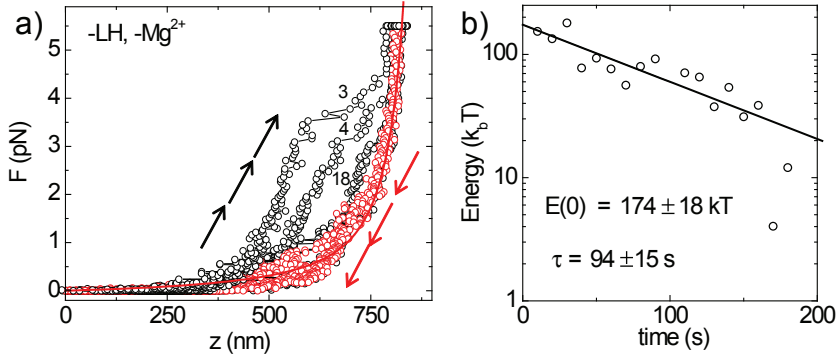


Figure 4.7:  $Mg^{2+}$  stabilizes nucleosome stacking. a) Upon depletion of  $Mg^{2+}$  hysteresis was observed in F-D curves of chromatin fibers without linker histones. Multiple F-D cycles obtained from a single fiber are shown, their order indicated by the numbers next to the curves. The fibers without linker histones initially ruptured at 3.5 pN and did not fully refold upon repeated F-D cycles. Backward traces (red dots) were fitted with two WLC in series i.e. Eq. 4.2 with  $\alpha$  set to 1 and  $p_{DNA}$  fixed to 50 nm (red line). Fitting the three remaining free parameters resulted in  $p_{BoS}=17.6\pm 2.0$  nm,  $L_{BoS} = 691\pm 70$  nm,  $L_{DNA} = 125\pm 72$  nm and  $R^2 = 0.97$ . b) The hysteresis in successive F-D cycles decreased exponentially with the time the fiber was held in an extended conformation.

What is the interaction energy when partial rupture of the fiber is taken into account? From the first F-D curve after  $Mg^{2+}$  depletion we estimated, based on the extension at low force, that approximately half of the fiber already unfolded during buffer exchange. Taking this partial unfolding into account yields a free energy of nucleosome stacking of approximately  $15 k_b T$  per nucleosome pair. After a large number of F-D cycles the hysteresis entirely disappears, which is indicative of the absence of any higher order structure, see Fig. 4.7a. The resulting beads-on-a-string fiber is expected to follow a single WLC with a reduced contour length  $L_{BoS}$  due to DNA wrapping around the histone core and a reduced persistence length  $p_{BoS}$  due to the sharp kinks in the trajectory of the DNA path [35]. We obtained a good fit with  $p_{BoS}=17.6\pm 2.0$  nm, approaching the value previously reported [20]. The obtained contour lengths  $L_{BoS} = 691\pm 70$  nm and  $L_{DNA} = 125\pm 72$  nm show good agreement with the expected dimensions of the fiber as schematically depicted in Fig. 4.2. Not only these contour lengths but also the reduced apparent persistence length relative to DNA demonstrates that no DNA unwrapping from the nucleosome cores has occurred as a reduced apparent persistence length points at kinks in the DNA trajectory [35]. DNA exits in an angle of approximately 50 degrees from the core particle. Unwrapping leads to a much larger opening angle and as a result the apparent persistence length approaches that of DNA (see Chapter 3 of this thesis). In conclu-

sion, these experiments both explain the low value for nucleosome-nucleosome interaction energy reported previously [20] and highlight the essential role of  $Mg^{2+}$  ions in stabilizing nucleosome-nucleosome stacking interactions.

## $Mg^{2+}$ stabilizes nucleosome stacking under physiological conditions

Can the force plateau in the presence of  $Mg^{2+}$  also be attributed to nucleosome unstacking? After having established that the beads-on-a-string fiber accurately follows a WLC, we can now quantify the changes in fiber length during forced disruption under more physiological conditions that include  $Mg^{2+}$ . The interaction energy can be calculated in a straight forward manner [20] by multiplying the length increase at the force plateau (from 200 to 500 nm) with the force (4.5 pN), which are both obtained from Fig. 4.5c and dividing it by the number of nucleosome pairs (24), resulting in  $14 k_b T$ . For a more accurate assessment we need to take the compliance of both the folded fiber and the flanking DNA into account by expanding Eq. 4.2 with an expression for the extension of the ruptured fiber. Using the length of the flanking DNA and a linear combination of the fraction of unstacked nucleosomes  $\alpha$ , in equilibrium with the fraction of stacked nucleosomes  $(1 - \alpha)$  the F-D curve should follow:

$$z(F) = z_{WLC}(F, L_{DNA}, p_{DNA}) + [1 - \alpha(F)] z_{30}(F, L_{30}, k) + \alpha(F) z_{WLC}(F, L_{BoS}, p_{BoS}), \quad (4.5)$$

with

$$\alpha(F) = \left[ 1 + \exp\left(\frac{\Delta G - F\Delta z}{k_b T}\right) \right]^{-1}, \quad (4.6)$$

in which  $\Delta G$  represents the free energy of nucleosome stacking, and  $\Delta z$  the length increase upon nucleosome unstacking. A similar expression was recently derived for force induced structural transitions in polysaccharides [36]. To reduce the number of free variables  $p_{BoS}$  and  $L_{BoS}$  were fixed to the values obtained from fitting fibers lacking higher order structure, as shown in Fig. 4.7a and that are consistent with those reported by Cui and Bustamante [20].  $p_{DNA}$  is well documented and was fixed to 50 nm, which was reproduced in the F-D curve of bare DNA, shown in Suppl. Fig. 2. The remaining five variables i.e.  $L_{DNA}$ ,  $L_{30}$ ,  $k$ ,  $\Delta G$  and  $\Delta z$  were used to fit the F-D curve shown in Fig 4.5C. Eqs. 4.5 and 4.6 accurately describe the full F-D cycle, including the transition observed at 4.5 pN. The length increase upon nucleosome unstacking of 13.4 nm approaches the expected length of 50 bp of linker DNA that should be added upon unstacking of a pair of nucleosomes. The free energy of nucleosome stacking corresponded to  $13.8 k_b T$ , matching the value obtained from extrapolation of the non-equilibrium disruption of chromatin fibers in absence of  $Mg^{2+}$ , see Fig. 4.7b. It is also in close agreement with our previous measurements on the interaction energy between individual nucleosomes



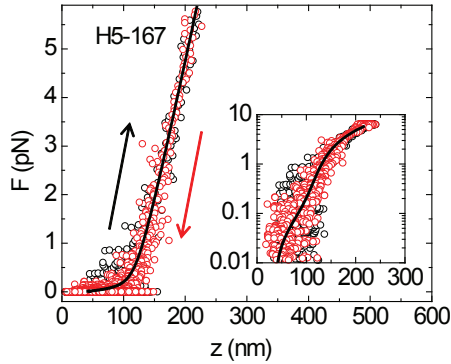


Figure 4.8: 167 bp repeat length fibers are longer and stiffer. F-D curve of a 167 bp repeat length nucleosome array. The fiber behaves qualitatively similar to 197 bp repeat length fibers, showing Hookian extension in both the forward (black) and the backward trace (red). The fit to Eq. 4.2, black line, however reveals less condensation and a higher stiffness.

in a DNA fiber sparsely decorated with nucleosomes [24]. The large interaction energy and the excellent fit to the two state model of Eq. 4.5, supports the interpretation of our data in terms of one-on-one stacking of nucleosomes. Thus, all the details of the F-D profile of the chromatin fibers can be quantitatively understood in terms of the rupture of stacked nucleosomes in a solenoidal chromatin fiber.

### 167 bp NRL chromatin fibers are longer and stiffer, consistent with a two-start helix

The most compelling evidence for a two-start helical organization of chromatin fibers comes from cross linking [16] and crystallography [15] data on 167 bp NRL chromatin arrays. Visualization by EM revealed however that such fibers have a smaller diameter and a significantly larger length compared to 197 bp NRL fibers. This suggests a different folding, i.e. a two start helix [21]. To test this hypothesis we reconstituted 25\*167 NRL fibers, and measured their compliance (Fig.4.8). Compared to the 25\*197 bp NRL fibers all 25\*167 bp NRL fibers were longer at 0.5 pN and stretched less at 6 pN force. Thus, independent of any structural interpretation, the slopes of the F-D curves were all higher than those of the 25\*197 bp NRL fibers. Though the fibers exhibited more heterogeneity and non-specific sticking to the flow cell, indicating more disorder, the F-D curves also feature a linear extension that was fitted to Eq. 4.2. The average stiffness of the 25\*167 bp NRL fibers appeared to be 2.7 times larger than the stiffness of the

Table 4.1: *The mechanical parameters that define chromatin structure. Average and standard error of mean of the fitting parameters to Eq. 4.2 for chromatin fibers containing H5, H1 and lacking linker histone, selected to contain 25 nucleosomes. <sup>a</sup>Fit was limited to the Hookian range i.e.  $F < 3$  pN. <sup>b</sup>F-D curves of fibers without linker histones fitted to Eq. 4.5 using  $p_{Bos} = 17$  nm, as obtained from Fig. 4.7a and  $p_{DNA} = 50$  nm.*

Linker histone	NRL (bp)	$k$ (pN/nm)	$L_{30}$ (nm)	$L_{DNA}$ (nm)	$\Delta G$ ( $k_b T$ )
H5	197	$0.019 \pm 0.004$	$50 \pm 6$	$50 \pm 6$	-
H1	197	$0.028 \pm 0.001$	$40 \pm 4$	$60 \pm 8$	-
none <sup>a</sup>	197	$0.023 \pm 0.003$	$66 \pm 16$	$54 \pm 12$	-
none <sup>b</sup>	197	$0.021 \pm 0.003$	$72 \pm 17$	$40 \pm 10$	$13.8 \pm 0.5$
H5	167	$0.052 \pm 0.013$	$79 \pm 21$	$78 \pm 23$	-
Linker histone	NRL (bp)	$\Delta z$ (nm)	$N$	$\langle R^2 \rangle$	
H5	197		10	0.88	
H1	197		7	0.85	
none <sup>a</sup>	197		3	0.80	
none <sup>b</sup>	197	$13.4 \pm 0.7$	3	0.93	
H5	167		7	0.77	

25\*197 bp NRL fibers (Tab. 4.1). Like the EM data we find an increased length of 25\*167 bp NRL fibers [21]. The increase in stiffness is consistent with the nucleosomes being arranged into two twisted ribbons of half the length, which would quadruple the stiffness. We found a relative increase of only 2.7 together with a smaller  $R^2$  of the fit and a larger rest length of the fiber. All these observations hint at increased disorder relative to the 25\*197 bp NRL fibers. Further quantification, however, requires more advanced analysis (Chien *et al.*, in preparation). Importantly, if the stiffness that we report would originate from stretching an isotropic rod instead of a double helical stack, pulling the longer and thinner 125\*67 bp NRL fibers would yield a decreased instead of an increased stiffness. Therefore the F-D measurements on the 25\*167 bp NRL chromatin fibers confirm that these fibers are arranged in two twisted stacks, consistent with a two-start helix.

### 4.3 Discussion

Single molecule force spectroscopy provides a unique way to probe the interactions that drive chromatin folding. By using well-defined chromatin arrays it was possible to analyze F-D curves using the framework of classical mechanics, allowing for detailed quantitative interpretation with nm and sub-pN resolution. Because chromatin fibers were not stained, dried, surface deposited or exposed to extreme buffer conditions, the fibers could adopt their thermodynamically most favorable conformation. This allowed us to probe higher order chromatin

structure directly, under physiological conditions and without preparation artifacts. Furthermore, it was possible to reproduce F-D curves on each individual fiber, confirming thermodynamic equilibrium, and to unequivocally verify the presence of each nucleosome in the fiber. The possibility to manipulate fibers individually and to select specific fibers is unique to single-molecule techniques and warrants new possibilities for revealing the heavily debated structure of chromatin fibers.

The single molecule force spectroscopy experiments agree well with recent EM and sedimentation velocity data that established a linker histone-dependent compaction of 197 bp NRL arrays into a 30-nm chromatin fibers [21]. 167-bp NRL arrays displayed a limited linker histone-dependent compaction, resulting in thinner fibers. All methods indicate that the linker histone stabilizes the higher order structure, which in the case of force spectroscopy shows as a higher rupture force. The current data go beyond the sedimentation velocity and EM analysis since they provide direct evidence for the topology of both types of fibers. Furthermore, by fitting the F-D curves to a Hookian model we show that the presence of linker histones does not result in more compact fibers in absence of force, but instead increases the tensile strength of the fiber. The high compliance and the rupture of nucleosome stacking at 4 pN that we report here may translate into differences in overall compaction when measured by sedimentation velocity or EM as the centrifugal forces and the forces involved with surface deposition may be sufficient to induce partial unstacking of the nucleosomes. Since single molecule force spectroscopy can separate force induced extension from differences in rest length it can give a more accurate value for the nucleosome packing density of the highly compliant chromatin fibers.

By looking at the total contour length of the fiber under conditions with and without  $Mg^{2+}$  we showed that no DNA was unwrapped from the histone core at forces below 7 pN. The later may seem surprising when compared to pulling experiments on single nucleosomes which feature unwrapping of 60 bp at 3 pN and full unwrapping at 6 pN [37]. It appears however that the embedding of a nucleosome in an array of nucleosomes stabilizes the wrapped conformation. This is consistent with the finding that full unwrapping in the context of a nucleosomal array requires 15-25 pN [17–19], significantly more than in the mono-nucleosome experiment. *In vivo*, nucleosomes are always flanked by neighbouring nucleosomes, which stresses the relevance of this higher tensile strength.

Does the high compliance of the condensed chromatin fiber have any physiological relevance? Even these highly regular, strongly condensed fibers featured an extraordinary small stiffness, which results in large thermal fluctuations in their extension, following equipartition theorem:

$$\frac{1}{2}kz^2 = \frac{1}{2}k_b T \quad (4.7)$$

The root-mean-squared amplitude of these fluctuations at room temperature exceeds 10 nm

for a fiber consisting of 25 nucleosomes. Thus the low stiffness of the 30 nm fiber allows for thermal fluctuations of about 20% of its length, but larger fluctuation will also occur. Fig. 4.6b shows that the nucleosomal DNA in fibers stretched to such extensions is relatively well exposed. Thus the breathing of the folded structure without unstacking of the nucleosomes that is the consequence of the observed high compliance can be of biological importance since it provides eukaryotic cells with the opportunity to combine structural transparency with a high compaction of chromatin.

In recent work Poirier *et al.* [38] studied the enzymatic accessibility of nucleosomal DNA in homogeneous arrays similar to the arrays used here but with a 177 bp NRL. By comparison of the digestion rates of target sites in a mononucleosome with the same sites within a nucleosomal array they found that nucleosome organization into chromatin fibers changes the accessibility of nucleosomal DNA only modestly. The relative accessibility varied from  $\sim 3$ -fold decreases to  $\sim 8$ -fold increases. Linker DNA however was severely occluded compared to bare DNA. The relatively open structure of the fiber that we report here is clearly required for this surprising finding. The increase in accessibility, that points to enhanced unwrapping of the nucleosomal DNA, may reduce the bending of the linker DNA that is characteristic for one-start helical folding of the fiber. The amplitude of the thermal fluctuations is however insufficient to render enzymatic access to the linker DNA that remains in the central region of the fiber. Hence both studies support the picture of a dynamic, flexible chromatin fiber that has a relatively open structure.

How do our findings on reconstituted model fibers relate to the structure of native chromatin? Although for any species and cell type the linker DNA length is variable, it varies around a characteristic distinct length. Analysis of nucleosome repeat lengths found in nature showed broad maxima at 167, 177, 188, 197 bp [8, 39], providing evidence that linker lengths are quantized and satisfy the equation  $147 \text{ bp} + 10n$ , where  $n$  is an integer number. Recent genome-wide analysis of nucleosome positions in the yeast genome [40] also provide evidence for well defined linker DNA lengths. Our model fibers reflect the dominant NRL distributions found in nature. Previous studies [14, 21] confirmed that the model fibers used in our study have the same folding pathway and dimensions as native chromatin fibers. Furthermore, EM analysis has shown that model fibers with NRLs of 177, 187, 197 and 207 bp form the same structure, tolerating a wide range of linker DNA lengths. The 167 NRL nucleosome array of which a tetramer was crystallized and was shown to fold in a two-start helix [15], features different dimensions [21]. This finding was substantiated by our current data comparing 167 and 197 bp fibers. It is likely that *in vivo* a number of structures will coexist because of heterogeneity in NRL. However, to decipher what these structures are requires model fibers with defined NRLs and histone content as used in this study.

Another important finding in our experiments is that the nucleosome-nucleosome interaction energy is 4 times higher than reported before [20]. It is known that not only  $Mg^{2+}$  but also an ionic strength of at least 50 mM is required for the stability of chromatin folding [14, 41]. The experiments of Cui and Bustamante were performed at 40 mM NaCl and in absence of  $Mg^{2+}$  and it is therefore likely that under those conditions only partially compacted fibers were measured. We have shown that in absence of  $Mg^{2+}$  we could reproduce this smaller interaction energy in the entire fiber, but that it is indeed accompanied by defects in nucleosome stacking. A higher ionic strength and the presence of  $Mg^{2+}$  is also expected to better approach the ionic conditions *in vivo* and our findings underscore the necessity to study chromatin structure under conditions that are representative of its natural environment.

The high interaction energy also has implications for the values used in computational chromatin fibre modeling. A small interaction energy has been the basis to model the higher order structure of chromatin, which generally favors zig-zag conformations [42–44]. A net free energy of nucleosome-nucleosome interaction of  $14 k_b T$ , as we report here, implies that the interactions between nucleosomes can accommodate much more DNA bending than previously thought. This will yield very different outcomes in structural computations and may favor helical folding over a zig-zag structure. Whereas in the zig-zag model the linker length directly determines the diameter of the fiber, EM measurements show that this is not the case [22]. Thus the question remains, what determines the diameter of the fiber? Recent theoretical modeling suggests tight packing of nucleosomes as the mechanism determining the diameter of 30 nm fibres [45]. The high interaction energy that we report here definitely supports such a suggestion, but we also show that the stacking of nucleosomes is quite flexible. From our measurements on different NRLs it is clear though that the length of the linker DNA remains a major parameter in organizing chromatin.

A nucleosome-nucleosome interaction of  $14 k_b T$  corresponds to an equilibrium constant for unstacking of  $10^{-6}$ , i.e. in equilibrium one of every million nucleosomes is unstacked. An interaction this strong implies that an active mechanism to disrupt nucleosome-nucleosome interactions is required if DNA is to be unpacked. One such mechanism can be the specific modification of histone residues. A prime candidate for such a modification is acetylation of K16 in the N-terminal tail of H4 [46] which is located in a region of the H4 tail that makes specific contacts with the surface of H2A-H2B on an adjacent nucleosome, as seen in the crystal structure of nucleosome cores [1]. This provides a physical mechanism for epigenetic control of transcription.

A possibly equally important physical mode of control is the variation of linker length between the nucleosomes. Our results confirm that the topology of the fiber, but not the mode of stacking the nucleosomes, is dependent on the NRL. It is well established that transcriptionally ac-

tive nuclei, found for example in yeast and neurons, often feature short linker lengths [47]. The relatively high disorder that we found in 167 bp NRL fibers, in combination with the previously reported smaller condensation, may be intrinsic to the chromatin structure of short NRLs as a consequence of increased bending of the linker DNA compared to 197 bp NRL fibers. The free energy of nucleosome stacking in the 197 bp NRL fibers that we report here represents the net free energy in the context of a chromatin fiber. It is the sum of the attractive stacking interaction between the nucleosomes and the energetic penalty for bending the linker DNA between them. Because the histone composition and the buffer conditions were identical in the two different NRL arrays that we measured, it must be the linker DNA that changed the interactions that drive overall fiber folding. An increased DNA bending in short NRL fibers would explain a decrease of the free energy of nucleosome stacking which in turn results in a more open chromatin structure. It may therefore be the decreased stacking probability rather than the alternative topology of short NRL chromatin that is functionally relevant for transcription control.

The physical origin and the extend of distorted stacking of nucleosomes is currently under investigation. The highly regular chromatin fibers used in this study provide a reference for comparison with fibers that bear the wide variety of histone composition, NRL, post-transcriptional modifications and other marks that are abundantly present in native chromatin. On top of these variations in chromatin composition, chromatin *in vivo* is continuously subject to forces that are generated by chromatin remodelers, RNA and DNA polymerases and other DNA based molecular motors. The magnitude of these forces is hard to estimate but these DNA based molecular motors typically have a stalling force of 10-25 pN [19, 48]. Thus it is clear that all the force induced structural rearrangements reported here are within the realm of the nuclear DNA machinery. Overall, our findings not only provide strong evidence for a one-start helical topology of the 30 nm fiber but also provide quantitative parameters that characterize the highly dynamic organization of chromatin.

## Methods

### DNA and chromatin fibers

25 repeats of a 197 bp 601 DNA sequence were produced in several cloning steps, using the low-copy-number vector pETcoco-1 (Novagen). DNA was linearized by XhoI and NheI digestion, and filled in dUTP-digoxigenin at the XhoI end and dUTP-biotin at the NheI end. Chromatin fibers were reconstituted through salt dialysis with competitor DNA (147 bp) and histone octamers purified from chicken erythrocytes. A second salt dialysis was performed

for incorporating linker histones H5 or H1 [14].

## Flow cell

A clean cover slip was coated with poly-d-lysine (Sigma), and then with a mixture of poly-ethyleneglycol (PEG) containing 20% w/v mPEG-Succinimidyl Propionic Acid (SPA)-5000 and 0.2% biotin-PEG-N-Hydroxysuccinimide (NHS)-3400 (Nektar). The coverslip was then mounted on a poly-di-methylsiloxane (PDMS, Dow Corning) flow cell containing 10x40x0.4 mm flow channel. Further surface preparation was performed inside the channel with specific binding of 0.1 mg/ml streptavidin (Sigma) for 10 minutes.

## Sample preparation

The flow cell was flushed with 1 ml measurement buffer (MB) (10 mM HEPES pH 7.6, 100 mM KAc, 2 mM MgAc<sub>2</sub>, 10 mM NaN<sub>3</sub>, 0.1% (v/v) Tween-20, (+) 0.02% (w/v) BSA), followed by 0.1 µg chromatin fibers diluted in 250 µl MB for 10 min, and subsequently with 1 ml MB, then 40 µg 1 µm paramagnetic beads (DYNAL MyOne) coated with anti-digoxigenin (Roche) and diluted in 250 µl MB (+). After 10 min incubation, the cell was rinsed by 1 ml MB (+) at flow rate of 5 µl/s.

## Magnetic tweezers

Chromatin fiber-tethered paramagnetic beads were imaged in a home built inverted microscope. Force extension curves were generated using dynamic force microscopy as described [24]. Contrary to previous experiments on chromatin fibers with optical tweezers that act as a position clamp [19, 20, 27], magnetic tweezers are operated as a force clamp. Rupture events will thus appear as an increase in extension rather than a decrease in force, which produces the characteristic spikes in F-D curves obtained with optical tweezers.

## Acknowledgments

We would like to thank T. Richmond, H. Schiessel, and T. Schmidt, and J. Widom for the helpful discussions. This work was financially supported by the “Nederlandse Organisatie voor Wetenschappelijk Onderzoek” (NWO) and the European Science Foundation (ESF).

## Bibliography

- [1] K. Luger, A. W. Mäder, R. K. Richmond, D. F. Sargent, and T. J. Richmond, "Crystal structure of the nucleosome core particle at 2.8 Å resolution," *Nature*, vol. 389, pp. 251–60, Sep 1997.
- [2] R. T. Simpson, "Structure of the chromatosome, a chromatin particle containing 160 base pairs of dna and all the histones.," *Biochemistry*, vol. 17, pp. 5524–5531, Dec 1978.
- [3] F. Thoma, T. Koller, and A. Klug, "Involvement of histone h1 in the organization of the nucleosome and of the salt-dependent superstructures of chromatin," *J. Cell. Biol.*, vol. 83, pp. 403–427, Nov 1979.
- [4] J. Widom and A. Klug, "Structure of the 300Å chromatin filament: X-ray diffraction from oriented samples," *Cell*, vol. 43, pp. 207–213, Nov 1985.
- [5] J. Widom, "Toward a unified model of chromatin folding," *An. Rev. Biophys. and Biophys. Chem.*, vol. 18, pp. 365–395, Jan 1989.
- [6] D. J. Tremethick, "Higher-order structures of chromatin: the elusive 30 nm fiber," *Cell*, vol. 128, pp. 651–654, Feb 2007.
- [7] P. J. J. Robinson and D. Rhodes, "Structure of the '30 nm' chromatin fibre: a key role for the linker histone," *Curr. Opin. Struct. Biol.*, vol. 16, pp. 336–343, Jun 2006.
- [8] K. E. van Holde, *Chromatin*. Springer-Verlag, New York, 1989. Chromatin.
- [9] I. Freidkin and D. J. Katcoff, "Specific distribution of the *saccharomyces cerevisiae* linker histone homolog hho1p in the chromatin.," *Nucleic Acids Res*, vol. 29, pp. 4043–4051, Oct 2001.
- [10] E. C. Pearson, D. L. Bates, T. D. Prospero, and J. O. Thomas, "Neuronal nuclei and glial nuclei from mammalian cerebral cortex. nucleosome repeat lengths, dna contents and h1 contents.," *Eur J Biochem*, vol. 144, pp. 353–360, Oct 1984.
- [11] D. L. Bates and J. O. Thomas, "Histones h1 and h5: one or two molecules per nucleosome?," *Nucleic Acids Res*, vol. 9, pp. 5883–5894, Nov 1981.
- [12] C. L. Woodcock, A. I. Skoultchi, and Y. Fan, "Role of linker histone in chromatin structure and function: H1 stoichiometry and nucleosome repeat length.," *Chromosome Res*, vol. 14, no. 1, pp. 17–25, 2006.



- [13] P. T. Lowary and J. Widom, "New dna sequence rules for high affinity binding to histone octamer and sequence-directed nucleosome positioning," *J. Mol. Biol.*, vol. 276, pp. 19–42, Feb 1998.
- [14] V. A. T. Huynh, P. J. J. Robinson, and D. Rhodes, "A method for the in vitro reconstitution of a defined "30 nm" chromatin fibre containing stoichiometric amounts of the linker histone," *J. Mol. Biol.*, vol. 345, pp. 957–968, Feb 2005.
- [15] T. Schalch, S. Duda, D. F. Sargent, and T. J. Richmond, "X-ray structure of a tetranucleosome and its implications for the chromatin fibre," *Nature*, vol. 436, pp. 138–141, Jul 2005.
- [16] B. Dorigo, T. Schalch, A. Kulangara, S. Duda, R. R. Schroeder, and T. J. Richmond, "Nucleosome arrays reveal the two-start organization of the chromatin fiber," *Science*, vol. 306, pp. 1571–1573, Nov 2004.
- [17] M. L. Bennink, S. H. Leuba, G. H. Leno, J. Zlatanova, B. G. de Groot, and J. Greve, "Unfolding individual nucleosomes by stretching single chromatin fibers with optical tweezers," *Nat Struct Biol*, vol. 8, pp. 606–610, Jul 2001.
- [18] C. Claudet, D. Angelov, P. Bouvet, S. Dimitrov, and J. Bednar, "Histone octamer instability under single molecule experiment conditions," *J Biol Chem*, vol. 280, pp. 19958–19965, May 2005.
- [19] B. D. Brower-Toland, C. L. Smith, R. C. Yeh, J. T. Lis, C. L. Peterson, and M. D. Wang, "Mechanical disruption of individual nucleosomes reveals a reversible multistage release of dna," *Proc. Natl. Acad. Sci. U.S.A.*, vol. 99, pp. 1960–1965, Feb 2002.
- [20] Y. Cui and C. Bustamante, "Pulling a single chromatin fiber reveals the forces that maintain its higher-order structure," *Proc. Natl. Acad. Sci. U.S.A.*, vol. 97, pp. 127–132, Jan 2000.
- [21] A. Routh, S. Sandin, and D. Rhodes, "Nucleosome repeat length and linker histone stoichiometry determine chromatin fiber structure," *Proc Natl Acad Sci U S A*, vol. 105, pp. 8872–8877, Jul 2008.
- [22] P. J. J. Robinson, L. Fairall, V. A. T. Huynh, and D. Rhodes, "Em measurements define the dimensions of the "30-nm" chromatin fiber: evidence for a compact, interdigitated structure," *Proc. Natl. Acad. Sci. U.S.A.*, vol. 103, pp. 6506–6511, Apr 2006.
- [23] F. J. Solis, R. Bash, J. Yodh, S. M. Lindsay, and D. Lohr, "A statistical thermodynamic model applied to experimental afm population and location data is able to quantify dna-histone binding strength and internucleosomal interaction differences between acetylated and unacetylated nucleosomal arrays," *Biophys J*, vol. 87, pp. 3372–3387, Nov 2004.

- [24] M. Kruithof, F. Chien, M. de Jager, and J. van Noort, "Sub-piconewton dynamic force spectroscopy using magnetic tweezers," *Biophys. J.*, vol. 94, pp. 2343–2348, Dec 2008.
- [25] J. F. Marko and E. Siggia, "Stretching dna," *Macromolecules*, vol. 28, pp. 8759–8770, Jan 1995.
- [26] C. Bustamante, J. F. Marko, E. Siggia, and S. Smith, "Entropic elasticity of lambda-phage dna," *Science*, vol. 265, pp. 1599–1600, Sep 1994.
- [27] M. Bennink, S. H. Leuba, G. H. Leno, J. Zlatanova, B. G. de Grooth, and J. Greve, "Unfolding individual nucleosomes by stretching single chromatin fibers with optical tweezers.," *Nat. Struct. Biol.*, vol. 8, pp. 606–610, Jun 2001.
- [28] J. Bednar, R. A. Horowitz, S. A. Grigoryev, L. M. Carruthers, J. C. Hansen, A. J. Koster, and C. L. Woodcock, "Nucleosomes, linker dna, and linker histone form a unique structural motif that directs the higher-order folding and compaction of chromatin," *Proc. Natl. Acad. Sci. U.S.A.*, vol. 95, pp. 14173–14178, Nov 1998.
- [29] J. Howard, *Mechanics of Motor Proteins and the Cytoskeleton*. Sinauer Associates Inc, Massachusetts, 2001.
- [30] H. Wong, J.-M. Victor, and J. Mozziconacci, "An all-atom model of the chromatin fiber containing linker histones reveals a versatile structure tuned by the nucleosomal repeat length," *PLoS ONE*, vol. 9, p. e877, Jan 2007.
- [31] J. Dubochet and M. Noll, "Nucleosome arcs and helices," *Science*, vol. 202, pp. 280–286, Oct 1978.
- [32] J. Dubochet, M. Adrian, P. Schultz, and P. Oudet, "Cryo-electron microscopy of vitrified sv40 minichromosomes: the liquid drop model," *EMBO J.*, vol. 5, pp. 519–528, Mar 1986.
- [33] M. d'Erme, G. Yang, E. Sheagly, F. Palitti, and C. Bustamante, "Effect of poly(adenosine)ribosylation and  $Mg^{2+}$  ions on chromatin structure revealed by scanning force microscopy," *Biochemistry*, vol. 40, pp. 10947–10955, Sep 2001.
- [34] R. Strick, P. L. Strissel, K. Gavrilov, and R. Levi-Setti, "Cation-chromatin binding as shown by ion microscopy is essential for the structural integrity of chromosomes," *J. Cell. Biol.*, vol. 155, pp. 899–910, Dec 2001.
- [35] I. M. Kulić, H. Mohrbach, V. Lobaskin, R. Thaokar, and H. Schiessel, "Apparent persistence length renormalization of bent dna," *Phys. Rev. E*, vol. 72, pp. 041905–041910, Dec 2005.

- [36] R. G. Haverkamp, A. T. Marshall, and M. A. K. Williams, "Model for stretching elastic biopolymers which exhibit conformational transformations," *Phys. Rev. E*, vol. 75, pp. 021907–021914, Jan 2007.
- [37] S. Mihardja, A. J. Spakowitz, Y. Zhang, and C. Bustamante, "Effect of force on mononucleosomal dynamics.," *Proc Natl Acad Sci U S A*, vol. 103, pp. 15871–15876, Oct 2006.
- [38] M. G. Poirier, M. Bussiek, J. Langowski, and J. Widom, "Spontaneous access to dna target sites in folded chromatin fibers.," *J. Mol. Biol.*, vol. 379, pp. 772–786, Jun 2008.
- [39] J. Widom, "A relationship between the helical twist of dna and the ordered positioning of nucleosomes in all eukaryotic cells," *Proc. Natl. Acad. Sci. U.S.A.*, vol. 89, pp. 1095–1099, Feb 1992.
- [40] J.-P. Wang, Y. Fondufe-Mittendorf, L. Xi, G.-F. Tsai, E. Segal, and J. Widom, "Preferentially quantized linker dna lengths in *saccharomyces cerevisiae*," *PLoS Comput Biol*, vol. 4, no. 9, p. e1000175, 2008.
- [41] D. L. Bates, P. J. Butler, E. C. Pearson, and J. O. Thomas, "Stability of the higher-order structure of chicken-erythrocyte chromatin in solution.," *Eur J Biochem*, vol. 119, pp. 469–476, Oct 1981.
- [42] G. Wedemann and J. Langowski, "Computer simulation of the 30-nanometer chromatin fiber.," *Biophys J*, vol. 82, pp. 2847–2859, Jun 2002.
- [43] J. Sun, Q. Zhang, and T. Schlick, "Electrostatic mechanism of nucleosomal array folding revealed by computer simulation.," *Proc Natl Acad Sci U S A*, vol. 102, pp. 8180–8185, Jun 2005.
- [44] N. Kepper, D. Foethke, R. Stehr, G. Wedemann, and K. Rippe, "Nucleosome geometry and internucleosomal interactions control the chromatin fiber conformation.," *Biophys J*, vol. 95, pp. 3692–3705, Oct 2008.
- [45] M. Depken and H. Schiessel, "Nucleosome shape dictates chromatin fiber structure," *Biophys J*, vol. In press, 2008.
- [46] P. J. J. Robinson, W. An, A. Routh, F. Martino, L. Chapman, R. G. Roeder, and D. Rhodes, "30 nm chromatin fibre decompaction requires both h4-k16 acetylation and linker histone eviction.," *J Mol Biol*, vol. 381, pp. 816–825, Sep 2008.
- [47] J. O. Thomas and R. J. Thompson, "Variation in chromatin structure in two cell types from the same tissue: a short dna repeat length in cerebral cortex neurons.," *Cell*, vol. 10, pp. 633–640, Apr 1977.

- [48] M. D. Wang, M. J. Schnitzer, H. Yin, R. Landick, J. Gelles, and S. M. Block, “Force and velocity measured for single molecules of rna polymerase.,” *Science*, vol. 282, pp. 902–907, Oct 1998.

---

---

## CHAPTER 5

---

# Thermal Fluctuations of Neighbouring Nucleosomes increase Nucleosome Stability<sup>1</sup>

### Abstract

Nucleosomes play a fundamental role in DNA compaction. For a greater understanding of processes that involve protein DNA interaction it is therefore imperative to determine physical properties such as the interaction energy between the DNA and the histone core. These properties are generally studied using force spectroscopy. DNA unwraps in two steps from the histone core. Experiments on single nucleosomes and nucleosomes in a fiber revealed an unexpected difference of the unwrapping force of the unwrapping of the first turn and unwrapping of the second turn. The unwrapping forces for a single nucleosome were much smaller, 3 pN for the first turn and 6 pN for the second turn, than those for a nucleosome in a fiber, 6 pN and 18 pN respectively. Here we modeled a nucleosome-DNA-bead system, used in force spectroscopy experiments, as spheres and springs. We found that the thermal fluctuations of neighbouring nucleosomes stabilized the nucleosome thereby increasing the unwrapping force for a nucleosome in a fiber. This effect shows that results obtained for single nucleosomes cannot simply be extrapolated to a system containing more than 1 nucleosome.

---

<sup>1</sup>A manuscript based on this chapter has been submitted for publication.

## 5.1 Introduction

Chromatin structure plays a fundamental role in the regulation of nuclear processes such as DNA transcription, replication, recombination, and repair. The basic repeating unit of chromatin, the nucleosome core particle, organizes 147 bp of DNA in 1.65 left-handed superhelical turns around an octamer of four core histones [1–3]. The nucleosome is a dynamic entity in which the DNA transiently unwraps from the histone core. *In vitro* linear nucleosome arrays fold into a fiber of 30 nm diameter [4, 5]. The mechanical stability of single nucleosomes [6] (Chapter 3 of this thesis) as well as chromatin fibers [7–16] (Chapter 4 of this thesis) have been intensively studied by force spectroscopy. Such measurements on single nucleosomes show unwrapping of the first turn of DNA, occurring at 3 pN, and unwrapping of the second turn at 6 pN [6] (Chapter 3 of this thesis). In contrast, experiments on chromatin fibers did not show unwrapping of the first turn of DNA until the force is increased to 6 pN (Chapter 4 of this thesis). Similarly, unwrapping of the second turn of DNA from a nucleosome embedded in chromatin occurs at forces much higher ( $F > 15$  pN) than for a single nucleosome ( $F > \sim 6$  pN) [9]. Since some of these experiments were performed at constant force, the striking difference between the unwrapping forces of single nucleosomes and fibers cannot be explained by the difference in loading rate, which determines the unwrapping force in non-equilibrium conditions [17]. The large differences in unwrapping forces warrants a closer inspection of the (un)wrapping dynamics of nucleosomes under force before extrapolation to the *in vivo* DNA organisation of chromatin fibers can be made.

To investigate the apparent discrepancies in unwrapping forces between the different structures we will first analyse the unwrapping of single nucleosomes with and without a tether to a surface. From this analysis we will see that a nucleosome tethered to a surface is subject to force fluctuations. To calculate the effect of the force fluctuations it is necessary to include the geometry of the fiber and the mechanical coupling generally used in these experiments: a DNA molecule attached to a fixed surface on one end and a bead on the other end. With the description of this system we fit experimental data obtained by Mihardja *et al.* [6] and find that the energy landscape is asymmetric. Which, in combination with the force fluctuations and the large change in stiffness of the DNA during unwrapping, drives the nucleosome into the wrapped state. When we compare single nucleosomes to nucleosomes in fibers we find that the force fluctuations that the nucleosome experiences in the fibers is much larger than the fluctuations in a force spectroscopy experiment on a single nucleosome. Since larger force fluctuations drive the nucleosome towards the wrapped state, a nucleosome in a fiber will unwrap at a higher force. This phenomenon is similar to the mechanism of thermal ratchets in which stochastic fluctuations can drive an object in a specific direction if the energy landscape would be asymmetric.

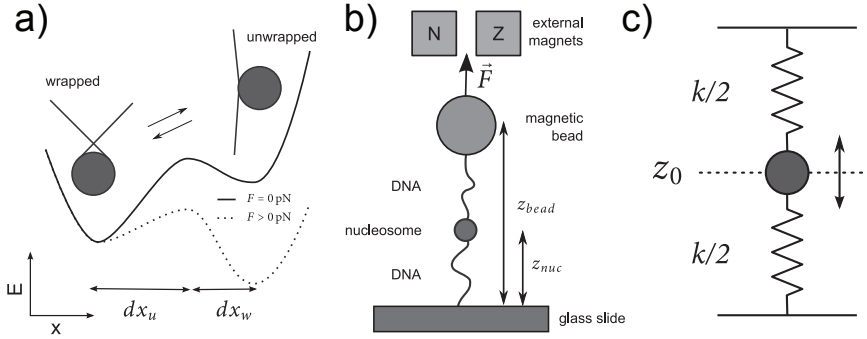


Figure 5.1: (a) Schematic overview of the energy landscape (black line) shows the distances in reaction coordinates between the wrapped and unwrapped state and the transition state. Increasing the force tilts the energy landscape (dashed line) and changes the height of the energy barrier. (b) A schematic overview of a mononucleosome in a magnetic tweezers setup. (c) A model of a nucleosome tethered to a surface. The nucleosome (dark grey sphere) fluctuates around a position  $z_0$  and is attached on both ends to two springs with spring constant  $k/2$ .

## 5.2 A Model for a Single Nucleosome Under Force

Let us first consider a single nucleosome in solution. A simple model for the energy landscape for unwrapping of the nucleosome is depicted by the solid line in Fig. 5.1a, where a nucleosome in the unwrapped state is separated from the wrapped state by an energy barrier  $E_b$ . The lifetime,  $\tau_0$ , of a state (wrapped or unwrapped) of the nucleosome in free solution is [17, 18]

$$\tau_0 = \frac{1}{\omega_0} \exp\left(\frac{E_b}{k_b T}\right), \quad (5.1)$$

with  $\omega_0$  a frequency factor and  $k_b T$  the thermal energy. Because the DNA ends are free to move, the motion of the nucleosome does not affect the energy landscape of unwrapping. This changes, however, when the nucleosome is tethered to a fixed surface. Any movement of the nucleosome will change the tension in the tether, thereby applying a force to the DNA exiting from the nucleosome. This force will tilt the energy landscape (Fig. 5.1a dashed line) and changes the height of the energy barrier. To quantify the effect of the change in height of the energy barrier on the dynamics of the DNA of a nucleosome, we describe the dependence of the lifetime of a state  $i$  of the nucleosome on a force  $F$  by an Arrhenius-like expression

$$\tau_i(F) = \tau_{0,i} \exp\left(-\frac{F a_i}{k_b T}\right), \quad (5.2)$$

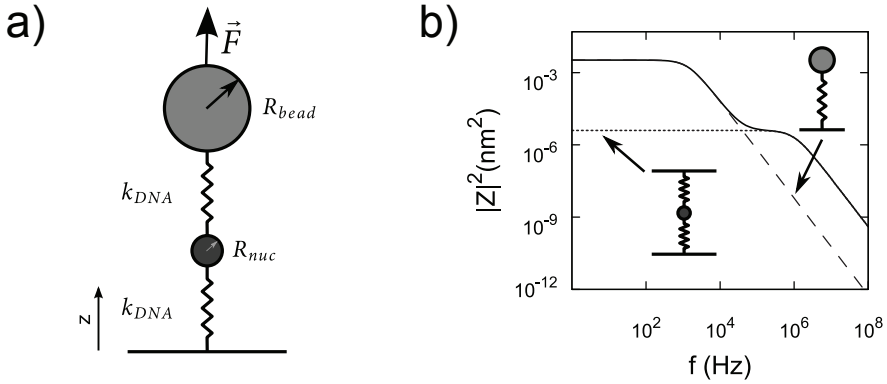


Figure 5.2: Modeling nucleosome thermal motion. (a) The magnetic bead and the nucleosome are modeled as spheres, the radius of the bead is  $1\ \mu\text{m}$  and the radius of the nucleosome  $11\ \text{nm}$ . The DNA is modeled as a spring, with a spring constant calculated from Eq. 5.10 using a contour length of  $500\ \text{nm}$ , a persistence length of  $52\ \text{nm}$  at a force of  $3\ \text{pN}$ . (b) The model for the power spectral density (PSD) of the nucleosome (solid line) can be approximated by the sum of the PSD of the bead (dashed line) and the PSD of the nucleosome if it was attached between two fixed points (dotted line).

with  $a_i$  the distance in reaction coordinates between state  $i$  and the transition state.

During a force spectroscopy experiment the force on the nucleosome is generally applied by tethering the nucleosome between a bead and a surface and then applying a force to the bead using a focused laser (optical tweezers) or a pair of magnets (magnetic tweezers) as depicted in Fig. 5.1b. The bead will be subject to thermal fluctuations, changing the tension in the tether and contributing to the force fluctuations on the nucleosome. A full description of the mechanics of the system should take the motion of the bead during a force spectroscopy experiment into account. Let us consider the equations of motion of a DNA-nucleosome-bead system as shown in Fig. 5.1b. We model both the magnetic bead and the nucleosome as spheres and the connecting DNA as springs, as depicted in Fig. 5.2a. The equations of motion of the whole system become

$$\begin{aligned} m_{nuc} \frac{d^2 z_{nuc}}{dt^2} &= -z_{nuc} k_{DNA} - \gamma_{nuc} \frac{dz_{nuc}}{dt} + (z_{bead} - z_{nuc}) k_{DNA} + F_{nuc} \\ m_{bead} \frac{d^2 z_{bead}}{dt^2} &= -(z_{bead} - z_{nuc}) k_{DNA} - \gamma_{bead} \frac{dz_{bead}}{dt} + F_{bead} + F_{ext}, \end{aligned} \quad (5.3)$$

with  $m$  the respective masses,  $z$  the positions, and  $\gamma$  the drag coefficients of the nucleosome and the bead.  $F_{bead}$  and  $F_{nuc}$  are the Brownian forces on the bead and the nucleosome.  $k_{DNA}$  is the spring constant of the DNA and  $F_{ext}$  the external force on that the tweezers apply on



the bead. In case of magnetic tweezers  $F_{ext}$  is a constant force, in case of optical tweezers  $F_{ext} = k_{trap}(z_{bead} - z_{trap})$ . The system is overdamped ( $Re \ll 1$ ) thus inertia can readily be neglected,  $m \frac{d^2 z}{dt^2} = 0$ . Since we are interested in fluctuations around a steady state, we solve the Fourier transform of the equations of motion

$$\begin{aligned} 0 &= -Z_{nuc}k_{DNA} - 2\pi i\gamma_{nuc}Z_{nuc}f + (Z_{bead} - Z_{nuc})k_{DNA} + \mathcal{F}_{nuc} \\ 0 &= -(Z_{bead} - Z_{nuc})k_{DNA} - 2\pi i\gamma_{bead}Z_{bead}f + \mathcal{F}_{bead} + \mathcal{F}_{ext}, \end{aligned} \quad (5.4)$$

with  $Z_{bead}$  and  $Z_{nuc}$  the Fourier transform of  $z_{bead}$  and  $z_{nuc}$ ,  $\mathcal{F}$  the Fourier transform of the Brownian force, and  $f$  the frequency. The Fourier transform of the external force,  $\mathcal{F}_{ext}$ , is constant for magnetic tweezers and only contributes at  $f = 0$ :  $\mathcal{F}_{ext} = F_{ext}\delta(f)$ . For optical tweezers in position clamp mode, the position of the trap remains constant leading to  $\mathcal{F}_{ext} = k_{trap}(z_{trap}\delta(f) + Z_{bead})$ . The drag coefficients of the bead and the mononucleosome depend on their radius,  $R$ , and the kinematic viscosity,  $\eta$ , as defined by Stokes' law

$$\gamma = 6\pi\eta R. \quad (5.5)$$

From fluctuation dissipation theorem, it follows that the Brownian force appears as white noise in the spectrum [19]:

$$|\mathcal{F}|^2 = 24\pi k_b T \eta R. \quad (5.6)$$

The stiffness of a tether can be calculated from

$$k(F) = \left. \frac{dF(s)}{ds} \right|_{s=z(F)}, \quad (5.7)$$

with  $F(s)$  the force needed to stretch the tether to an extension  $s$  and  $z(F)$  the extension of the tether at a constant force  $F$ , which is the inverse of  $F(s)$ . If DNA is taken to be the tether, the force needed to extend a DNA molecule with a persistence length  $p$  and a contour length  $L$  is given by the Worm-Like-Chain (WLC) model [20]

$$F_{WLC}(z) = \frac{k_b T}{p} \left[ \frac{1}{4\left(1 - \frac{z}{L}\right)^2} - \frac{1}{4} + \frac{z}{L} \right]. \quad (5.8)$$

At large forces ( $F > 5$  pN) the elastic stretching of the DNA molecule cannot be neglected [21]. The elastic stretching spring constant of a DNA molecule is

$$k_{ES} = \frac{K_0}{L}, \quad (5.9)$$

with  $K_0$  the stretching modulus of DNA. Thus the spring constant of a DNA molecule for the

full force range is given by a entropic spring (Eq. 5.7) and an elastic spring (Eq. 5.9) in series

$$k_{DNA}(F) = \frac{k_{ES}k_{WLC}(F)}{k_{ES} + k_{WLC}(F)}, \quad (5.10)$$

with  $k_{WLC}(F)$  and  $k_{elastic}(F)$  from Eqs. 5.7 and 5.8. The spring constant of a DNA molecule depends on the external force, the contour length and the persistence length of the molecule.

We first compute the power spectral density (PSD) of the motion of the nucleosome-bead system. The PSD shows that in the case of a constant external force of 3 pN, at low frequencies ( $f < 10^4$  Hz) the bead dominates the motion of the nucleosome (Fig. 5.2b). At high frequencies ( $f \gg 10^4$  Hz) the motion of the bead gets dampened out due to its larger radius and the nucleosome behaves like a sphere attached between two fixed points.

The solutions for the PSD of the nucleosome of Eq. 5.4 can be split into two contributions, the bead without nucleosome,  $|Z_{bead,sol}(F)|^2$ , and the nucleosome without bead,  $|Z_{nuc,sol}(F)|^2$  (Fig. 5.2b)

$$|Z_{nuc,tot}(F)|^2 = |Z_{bead,sol}(F)|^2 + |Z_{nuc,sol}(F)|^2. \quad (5.11)$$

The average fluctuations in position of the nucleosome are calculated from the PSD using

$$\sigma_z^2 = \int_{-\infty}^{\infty} |Z(F)|^2 df. \quad (5.12)$$

Leading to the contribution of the bead to the thermal motion of the nucleosome

$$\sigma_{z,bead}^2(F) = \frac{k_b T}{k_{DNA}(F) + k_{trap}}, \quad (5.13)$$

with  $k_{DNA}(F)$  the stiffness of the entire DNA molecule that links the nucleosome to the bead and the surface and  $k_{trap}$  the stiffness of an optical trap (for magnetic tweezers and an optical trap in constant force mode  $k_{trap} = 0$ ). For the PSD contribution of the nucleosome we get

$$\sigma_{z,nuc}^2 = \frac{k_b T}{k_{DNA,1}(F) + k_{DNA,2}(F)}, \quad (5.14)$$

with  $k_{DNA,1}(F)$  the stiffness of the DNA below the nucleosome, and  $k_{DNA,2}(F)$  the stiffness of the DNA above the nucleosome.

### 5.3 The Effect of Thermal Motion on Wrapping Dynamics

When the energy landscape is rocked back and forth the lifetimes change continuously, leading us to calculate the average lifetime of state  $i$  from the average rate constant,  $k = 1/\tau$ , using Eq. 5.2 [22, 23]

$$\begin{aligned}
 \langle \tau_i (F(t)) \rangle &= \langle k_i (F(t)) \rangle^{-1} \\
 &= \tau_{0,i} \left\langle \exp \left[ \frac{F(t)a_i}{k_b T} \right] \right\rangle^{-1} \\
 &= \tau_{0,i} \left( \int_{-\infty}^{\infty} P(F_0, \sigma_F^2) \exp \left[ \frac{F a_i}{k_b T} \right] dF \right)^{-1} \\
 &= \tau_i (F_0) \exp \left[ -\frac{a_i^2}{2(k_b T)^2} \sigma_F^2 \right],
 \end{aligned} \tag{5.15}$$

with  $P(F_0, \sigma_F^2)$  the probability distribution of the force fluctuations, which is normally distributed around the average force  $F_0$  with a variance of  $\sigma_F^2$ . From Eq. 5.15 we see that the lifetime of each state is decreased due to the force fluctuations. More importantly, if the energy landscape is asymmetric ( $a_u \neq a_w$ ), the lifetime of the state with the shortest distance to the transition state decreases less than the lifetime of the other state, driving the nucleosome towards this state. Furthermore, we see from Eq. 5.15 that this effect becomes stronger with increasing force fluctuations. Since the nucleosome is subject to thermal motion, the energy landscape of the nucleosome will constantly tilt back and forth. Thus the (un)wrapping of a nucleosome can be described as a rocked thermal ratchet [24–26].

As we have seen the thermal motion of the nucleosome can be split into two components, each component results in a force to the DNA of the nucleosome. The average contributions to the force caused by each component is calculated from Eqs. 5.13 and 5.14

$$\sigma_F^2 = k^2 \sigma_z^2 = k_b T k. \tag{5.16}$$

Thus, the stiffness of the tether,  $k$ , is the only variable which determines the force fluctuations. Using Eq. 5.10 we find that the force fluctuations grow with increasing force and decreasing contour length.

Combining Eqs. 5.13, 5.14, 5.15, and 5.16, we get for the average lifetime of a state of the nucleosome

$$\begin{aligned}
 \langle \tau_i (F, t) \rangle &= \tau_i (F) \exp \left[ -\frac{a_i^2 (k_{DNA,1,i}(F) + k_{DNA,2,i}(F))}{2k_b T} \right] \\
 &\times \exp \left[ -\frac{a_i^2 (k_{DNA,i}(F) + k_{trap})}{2k_b T} \right].
 \end{aligned} \tag{5.17}$$

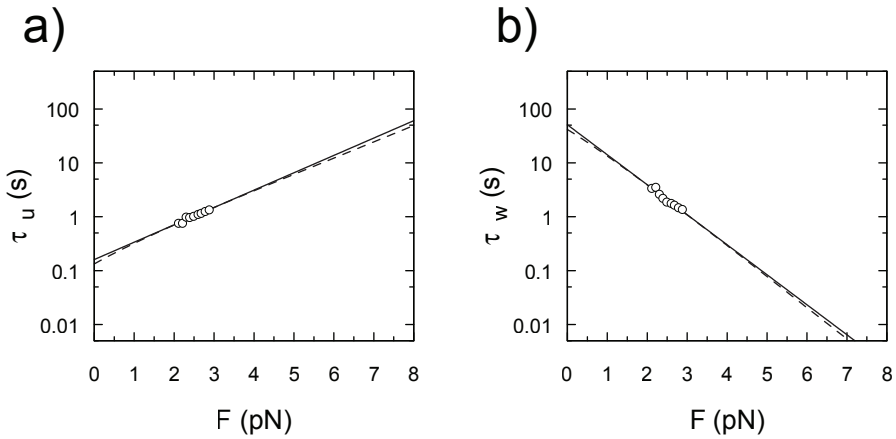


Figure 5.3: (a) The unwrapped lifetime fit with a simple exponential (solid line) and the force-fluctuation corrected model (dashed line). (b) The wrapped lifetime fit with a simple exponential (solid line) and the force-fluctuation corrected model (dashed line).

Eq. 5.17 describes the lifetime of the wrapped or unwrapped state of a single nucleosome tethered between a surface and a bead as depicted in Fig. 5.1b, which we can use to fit the force-lifetime curve obtained from single molecule force spectroscopy experiments.

## 5.4 Comparison With Experiments on Mononucleosomes

Let us use Eq. 5.17 to extract the distance between the wrapped and unwrapped state and the transition state from single molecule force spectroscopy experiments. Mihardja *et al.* [6] measured mononucleosome (un)wrapping dynamics under constant force using optical tweezers. Since the lifetime depends exponentially on the stiffness which in turn depends on the contour length and the apparent persistence length of the tethering DNA we need to carefully consider the DNA-nucleosome-bead geometry. In the experiments of Mihardja *et al.* [6], the length of DNA, before unwrapping, on one side of the nucleosome was 375 nm and on the other side 785 nm leading to a total contour length of 1160 nm. Furthermore, it was shown that a kink or bend in the DNA, induced by a nucleosome, reduces the apparent persistence length of the DNA [27–30] (Chapter 3 of this thesis). The dimensions in this particular experiment result in a reduced apparent persistence length of 48 nm (Chapter 3 of this thesis) compared to 52 nm for DNA that does not contain a kink.

The fits of the data to Eq. 5.17 are depicted in Fig. 5.3a and b. In this case the corrected model (Eq. 5.15, blue line) deviates only marginally from a simple exponential model (red line) which

does not take the compliance of the tethers and the Brownian motion of the bead and nucleosome into account. The fit resulted in a distance between the unwrapped state and the transition state  $a_u = 4.19 \pm 0.06$  nm, and a lifetime of the unwrapped state at zero force  $\tau_u = 0.135 \pm 0.004$  s. For the distance between the wrapped state and the transition state we got  $a_w = 4.02 \pm 0.04$  nm and a wrapped lifetime of  $\tau_w = 41.6 \pm 1.5$  s, resulting in an equilibrium constant of  $K = \frac{\tau_w}{\tau_u} = 380$  for wrapping in absence of force, this large equilibrium constant in absence of force confirms that the nucleosome is a very stable structure. Mihardja *et al.* found a lifetime of the unwrapped state of  $\tau_u = 0.017$  s and a lifetime of the wrapped state of  $\tau_w = 2600$  s. They fit their data with an equation that accounts for the decreased hop size they see with increasing force, which explains the difference between their results and our results. However we did not see this behavior in our experiments on mononucleosomes (see Chapter 3 of this thesis). This counter intuitive approach results in an improbable large lifetime of the wrapped state. Li *et al.* [31] measured the zero-force lifetimes of nucleosome breathing directly using bulk FRET. They observed a wrapped lifetime of 0.25 s and an unwrapped lifetime of 0.01 s. Our lifetimes are much larger, which might be explained since we extrapolate force induced full turn unwrapping events whilst the FRET experiments look at smaller unwrapping lengths.

Though the data show a slight asymmetry in the energy landscape of unwrapping, the difference is only marginal. Similar to a rocked thermal ratchet, the force fluctuations decrease the lifetimes of each state but due to the asymmetry in the energy landscape the lifetime of one state will decrease more than the other which will drive the nucleosome towards the state with the smallest distance to the transition state, in this case the wrapped state. The larger these fluctuations, the more the nucleosome gets driven towards the wrapped state, showing that force fluctuations actually stabilize the nucleosome.

## 5.5 Contributions of Neighbouring Nucleosomes

Now that the distances between the wrapped, the unwrapped and the transition state are known for a single nucleosome, let us consider the motion of a single nucleosome within an array of nucleosomes tethered between a glass surface and a bead. The presence of neighbouring nucleosomes will result in additional force fluctuations. These additional force fluctuations can be calculated from the relative motion of a neighbour and the stiffness of the DNA between the nucleosome and its neighbour. Fig. 5.4 shows the relative contribution of the neighbours on the force fluctuations of a nucleosome. Since a nucleosome at the end of a fiber has a different configuration of neighbours as a nucleosome at the center of a fiber, the force fluctuations

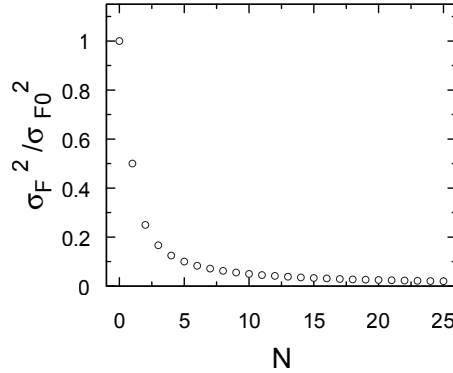


Figure 5.4: *The contribution of neighbour  $N$  to the force fluctuations of a nucleosome relative to the fluctuations of the nucleosome.*

the nucleosomes feel will be different. This situation is similar as described before (Eq. 5.11), but now the fluctuations of neighbouring nucleosomes add to the motion of the nucleosome resulting in a sum over all neighbours

$$\sigma_{z,neigh,i}^2 = \sum_j \frac{k_b T}{k_{DNA,neigh,j}(F)}, \quad (5.18)$$

where we estimate the stiffness of the DNA between the nucleosomes,  $k_{DNA,neigh}(F)$ , using Eq. 5.10.

Using Eqs. 5.13, 5.14, 5.15, 5.16, and 5.18 we get for the average lifetime of a state of the nucleosome in a fiber

$$\begin{aligned} \langle \tau_i(F, t) \rangle &= \tau_i(F) \exp \left[ -\frac{a_i^2 (k_{DNA,1}(F) + k_{DNA,2}(F))}{2k_b T} \right] \\ &\times \exp \left[ -\frac{a_i^2 k_{DNA}(F)}{2k_b T} \right] \exp \left[ -\frac{a_i^2}{2k_b T} \sum_j k_{DNA,neigh,j}(F) \right]. \end{aligned} \quad (5.19)$$

We need to carefully look at the contour and apparent persistence length of the DNA in the fiber. The fibers used in our experiments (Chapter 4 of this thesis) contain 25 nucleosomes. The distance between the nucleosomes is 17 nm and the total contour length of the fiber is 782 nm. The distance between the two neighbours of a nucleosome is therefore 34 nm. After unwrapping, the length of DNA between the nucleosome and its neighbour becomes longer (29 nm) as well as the distance between the neighbours (58 nm). As shown before for the mononucleosome, the loop induced by the nucleosome in the DNA causes a change in apparent persistence length. We expect this effect to be much larger for a fiber since more nucleosomes are present.

The change in apparent persistence length due to a loop in the DNA can be calculated from the exit angle of the DNA wrapped around the nucleosome [30]. If we take for the exit angle  $\alpha = 81^\circ$  (Chapter 3 of this theses) we get for the apparent persistence length  $p = 5$  nm. However, in measurements on chromatin fibers in the beads-on-a-string configuration we see a apparent persistence length of 10 nm (Chien *et al.* unpublished work). This difference might be explained because the relation between the apparent persistence length and the exit angle assumes freely rotating DNA ends which is not the case for a fiber. We took the apparent persistence length found in our previous measurements of 10 nm before unwrapping in an array of nucleosomes. After unwrapping, the exit angle is much larger  $\alpha = 144^\circ$  resulting in a apparent persistence length of 50 nm. Due to the difference in opening angle, the apparent persistence length before unwrapping is smaller than the apparent persistence length after unwrapping which, combined with the larger contour length between nucleosomes after unwrapping, leads to a change in the compliance of the fiber.

## 5.6 Second Turn Unwrapping

The lifetimes of the second turn unwrapping can also be calculated using Eq. 5.17 for a single nucleosome and Eq. 5.19 for a nucleosome in a fiber. Again we need to consider the the contour and apparent persistence length of the DNA in the fiber. For the second turn, the distance between the nucleosomes is 41 nm. After unwrapping, the length of DNA between the nucleosome and its neighbour becomes longer (66 nm). Again the loop induced by the nucleosome in the DNA causes a change in apparent persistence length. For the second turn the change in persistence length is much less than for the first turn, since the angle is closer to  $180^\circ$ . If we take for the exit angle  $\alpha = 144^\circ$  (see Chapter 3 of this thesis) we get for the apparent persistence length  $p = 48$  nm. Furthermore, we need to know the distance between the wrapped and unwrapped state and the transition state. Brower-Toland *et al.* [9] calculated the distance between the wrapped state and the transition state to be 3.2 nm. Because the second turn of the nucleosome does not rewrap during force spectroscopy experiments [6, 9, 12] the distance between the unwrapped state and the transition state is not known. We chose the distance between the unwrapped state and the transition state such that it would lead to an unwrapping of the second turn of a single nucleosome at 6 pN as reported by Mihardja [6] resulting in a distance of 4.3 nm.

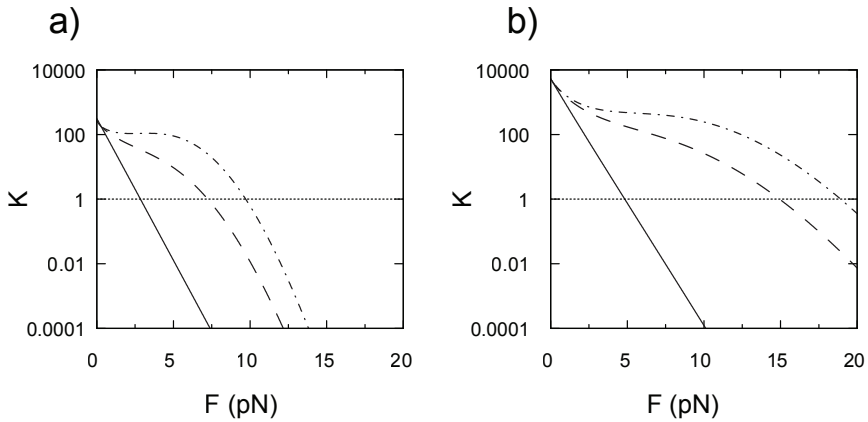


Figure 5.5: (a) The ratio between the corrected wrapped lifetime and the corrected unwrapped time of the first turn for a mononucleosome (solid line), a nucleosome in the center a fiber (dash dotted line) and a nucleosome at the end of a fiber (dashed line). The transition between wrapped and unwrapped state occurs near the force where the ratio crosses 1. (b) The ratio between the corrected wrapped lifetime and the corrected unwrapped time of the second turn for a mononucleosome (solid line), a nucleosome in the center of a fiber (dash dotted line) and a nucleosome at the end of a fiber (dashed line). The transition between wrapped and unwrapped state occurs near the force where the ratio crosses 1.

## 5.7 Rupture Forces Depend on Force Fluctuations

Now that we can calculate the lifetimes of a nucleosome in a fiber, we can compare the lifetimes in a fiber to the lifetimes in a mononucleosome. We define the unwrapping force as the force at which the wrapping equilibrium constant is 1. When this equilibrium constant is larger than 1, the nucleosome spends most of its time in the wrapped state. The reverse holds when the equilibrium constant is smaller than 1. When the equilibrium constant is 1, wrapping and unwrapping occurs at the same rate. These wrapping and unwrapping events of the first turn of DNA can directly be observed in constant force time traces. The wrapping equilibrium constant, as calculated from Eq. 5.17 is depicted in Fig. 5.5a for a mononucleosome and for a fiber. The figure shows unwrapping occurring at a force of 3 pN for mononucleosome and 6 pN for a nucleosome embedded in a fiber. This exactly reproduces values reported in previous measurements [6, 9, 12] (Chapter 3 and 4 of this thesis). Furthermore it is interesting to see that a nucleosome in the center of the fiber has an even larger rupture force than a nucleosome at the end of the fiber.

The quantitative model shows that when the energy landscape of the unwrapping is asymmetric, with  $a_u > a_w$ , force fluctuations drive the nucleosome towards the wrapped state and



therefore increase the unwrapping force. Because the lifetimes depend exponentially on the distance between the state and the transition state, even a small asymmetry can have a large effect on the unwrapping force. The change in stiffness of the DNA during unwrapping also pushes the nucleosomes into the wrapped state and for the unwrapping of the first turn this effect dominates the change in unwrapping force. Since a nucleosome in a fiber is much closer to its neighbours the coupling with the fluctuations of the neighbouring nucleosomes causes the force fluctuations to be much higher, stabilizing the nucleosome and thereby increasing the unwrapping force.

The same argument holds for the unwrapping force of the second turn, as is depicted in Fig. 5.5b where the equilibrium constant of a single nucleosome is equal to 1 at 6 pN and the equilibrium constant for a nucleosome in a fiber is equal to 1 at a much higher force (20 pN), which explains the large differences between the unwrapping force of fibers [9] and mononucleosomes [6] in force spectroscopy experiments. Here the change in stiffness is much less and the asymmetry plays the dominant role. Again a nucleosome in the center is more stable than a nucleosome at the end of the fiber.

This effect implies that the nucleosomes unwrap cooperatively because if a nucleosome is fully unwrapped the length of DNA between it and a neighbouring nucleosome suddenly increases. This will decrease the force fluctuations for that nucleosome, which in turn will destabilizes the next nucleosome and so forth. Furthermore, as mentioned before, since a nucleosome at the end of a fiber is less stable than a nucleosome in the center, unwrapping is much more likely to start at the ends of the fiber.

The change in equilibrium constant due to the stiffness of the DNA attached to a nucleosome is important in any experiment where a nucleosome is attached to a surface with a small tether. Since the size of the tether is directly related to the extend of the force fluctuations, small tether lengths may drive the nucleosome into the wrapped state, even in absence of force. The lifetimes found in such experiments are underestimates of the lifetime of a nucleosome in solution, though the equilibrium is shifted towards the open state.

Although such tethering seems artificial, they give a more accurate description of the behavior of nucleosomes *in vivo*, since there the distance between a nucleosome and its neighbour is generally small, in the order of 20 nm [32]. It is imperative to take the effect of the force fluctuations into account when general conclusions are made about the *in vivo* situation from measurements on single nucleosomes. Recent theory and simulations on the unfolding of RNA hairpins shows a similar trend where an increased stiffness of the tether decreases the lifetime of the folded state [33]. The arrest force of RNA polymerase, a typical DNA interacting motor protein in a cell, is 15 pN at room temperature [34], Fig. 5.3c shows that at those forces the wrapping equilibrium constant for a fiber differs significantly from the equilibrium constant

of a mononucleosome. This effect stabilizes the nucleosome but at the same time makes it more open, since the fluctuations between the conformations increase due to the decreased lifetimes.

## 5.8 Conclusion

We have shown that force induced unwrapping of a tethered nucleosome should be described by a rocked energy landscape in analogy with a thermal ratchet. This rocking decreases the lifetimes of both the wrapped and the unwrapped state. Furthermore, the asymmetry in the energy landscape of nucleosome unwrapping drives the nucleosome towards the wrapped state. The asymmetry and the change in stiffness during unwrapping results in the large difference in unwrapping force that is observed between force spectroscopy experiments on fibers and mononucleosomes. It also shows that careful consideration is in order if one wants to extrapolate information from experiments on mononucleosomes to the *in vivo* case where nucleosomes are always embedded in chromatin. The neighbouring nucleosomes pick up thermal fluctuations since the length of the DNA between the nucleosome and its neighbours is an important parameter.

## Bibliography

- [1] J. T. Finch, L. C. Lutter, D. Rhodes, R. S. Brown, B. Rushton, M. Levitt, and A. Klug, "Structure of nucleosome core particles of chromatin," *Nature*, vol. 269, pp. 29–36, Sep 1977.
- [2] T. J. Richmond, J. T. Finch, B. Rushton, D. Rhodes, and A. Klug, "Structure of the nucleosome core particle at 7 Å resolution," *Nature*, vol. 311, pp. 532–7, Jan 1984.
- [3] K. Luger, A. W. Mäder, R. K. Richmond, D. F. Sargent, and T. J. Richmond, "Crystal structure of the nucleosome core particle at 2.8 Å resolution," *Nature*, vol. 389, pp. 251–60, Sep 1997.
- [4] H. G. Davies and J. V. Small, "Structural units in chromatin and their orientation on membranes," *Nature*, vol. 217, pp. 1122–5, Mar 1968.
- [5] H. Ris and D. F. Kubai, "Chromosome structure," *Annu Rev Genet*, vol. 4, pp. 263–94, Jan 1970.

- [6] S. Mihardja, A. Spakowitz, Y. Zhang, and C. Bustamante, "Effect of force on mononucleosomal dynamics.," *Proc. Natl. Acad. Sci. U.S.A.*, vol. 103, pp. 15871–6, Oct 2006.
- [7] A. Bancaud, N. C. e Silva, M. Barbi, G. Wagner, J.-F. Allemand, J. Mozziconacci, C. Lavelle, V. Croquette, J.-M. Victor, A. Prunell, and J.-L. Viovy, "Structural plasticity of single chromatin fibers revealed by torsional manipulation.," *Nat. Struct. Mol. Biol.*, vol. 13, pp. 444–50, Apr 2006.
- [8] M. Bennink, S. H. Leuba, G. H. Leno, J. Zlatanova, B. G. de Groot, and J. Greve, "Unfolding individual nucleosomes by stretching single chromatin fibers with optical tweezers.," *Nat. Struct. Biol.*, vol. 8, pp. 606–10, Jun 2001.
- [9] B. D. Brower-Toland, C. L. Smith, R. C. Yeh, J. T. Lis, C. L. Peterson, and M. D. Wang, "Mechanical disruption of individual nucleosomes reveals a reversible multistage release of dna," *Proc. Natl. Acad. Sci. U.S.A.*, vol. 99, pp. 1960–5, Feb 2002.
- [10] B. D. Brower-Toland, D. A. Wacker, R. M. Fulbright, J. T. Lis, W. L. Kraus, and M. D. Wang, "Specific contributions of histone tails and their acetylation to the mechanical stability of nucleosomes," *J. Mol. Biol.*, vol. 346, pp. 135–46, Feb 2005.
- [11] C. Claudet and J. Bednar, "Pulling the chromatin.," *The European physical journal. E, Soft matter*, vol. 19, pp. 331–7, Mar 2006.
- [12] Y. Cui and C. Bustamante, "Pulling a single chromatin fiber reveals the forces that maintain its higher-order structure.," *Proc. Natl. Acad. Sci. U.S.A.*, vol. 97, pp. 127–32, Jan 2000.
- [13] G. J. Gemmen, R. Sim, K. A. Haushalter, P. C. Ke, J. T. Kadonaga, and D. E. Smith, "Forced unraveling of nucleosomes assembled on heterogeneous dna using core histones, nap-1, and acf.," *J. Mol. Biol.*, vol. 351, pp. 89–99, Jul 2005.
- [14] S. H. Leuba, M. A. Karymov, M. Tomschik, R. Ramjit, P. Smith, and J. Zlatanova, "Assembly of single chromatin fibers depends on the tension in the dna molecule: magnetic tweezers study.," *Proc. Natl. Acad. Sci. U.S.A.*, vol. 100, pp. 495–500, Jan 2003.
- [15] M. Kruithof, F. Chien, M. de Jager, and J. van Noort, "Sub-piconewton dynamic force spectroscopy using magnetic tweezers," *Biophys J*, vol. 94, pp. 2343–2348, Dec 2007.
- [16] J. Yan, T. Maresca, D. Skoko, C. Adams, B. Xiao, M. Christensen, R. Heald, and J. F. Marko, "Micromanipulation studies of chromatin fibers in xenopus egg extracts reveal atp-dependent chromatin assembly dynamics.," *Mol Biol Cell*, Nov 2006.
- [17] E. A. Evans and K. Ritchie, "Dynamic strength of molecular adhesion bonds.," *Biophys. J.*, vol. 72, pp. 1541–55, Apr 1997.

- [18] P. Hänggi, P. Talkner, and M. Borkovec, “Reaction-rate theory: fifty years after kramers,” *Rev. Mod. Phys.*, vol. 62, p. 251, Apr 1990.
- [19] C. Gosse and V. Croquette, “Magnetic tweezers: micromanipulation and force measurement at the molecular level,” *Biophys J*, vol. 82, pp. 3314–29, Jun 2002.
- [20] J. F. Marko and E. Siggia, “Stretching dna,” *Macromolecules*, vol. 28, pp. 8759–8770, Jan 1995.
- [21] C. Bouchiat, M. D. Wang, J.-F. Allemand, T. R. Strick, S. M. Block, and V. Croquette, “Estimating the persistence length of a worm-like chain molecule from force-extension measurements,” *Biophys J*, vol. 76, pp. 409–13, Jan 1999.
- [22] K. S. Shanmugan and A. M. Breipohl, “Random signals: Detection, estimation and data analysis,” *John Wiley & Sons, Inc.*, p. 38, 1988.
- [23] H.-J. Lin, Y.-J. Sheng, H.-Y. Chen, and H.-K. Tsao, “Forced dissociation of a biomolecular complex under periodic and correlated random forcing,” *The Journal of chemical physics*, vol. 128, p. 084708, Feb 2008.
- [24] M. Magnasco, “Forced thermal ratchets,” *Phys. Rev. Lett.*, vol. 71, pp. 1477–1481, Sep 1993.
- [25] R. Bartussek, P. Haenggi, and J. Kissner, “Periodically rocked thermal ratchets,” *Europhys Lett*, Jan 1994.
- [26] R. D. Astumian, “Thermodynamics and kinetics of a brownian motor,” *Science*, vol. 276, pp. 917–22, May 1997.
- [27] J. Yan and J. F. Marko, “Effects of dna-distorting proteins on dna elastic response,” *Physical review. E, Statistical, nonlinear, and soft matter physics*, vol. 68, p. 011905, Jul 2003.
- [28] J. van Noort, S. Verbrugge, N. Goosen, C. Dekker, and R. T. Dame, “Dual architectural roles of hu: formation of flexible hinges and rigid filaments,” *Proc. Natl. Acad. Sci. U.S.A.*, vol. 101, pp. 6969–74, May 2004.
- [29] B. M. Ali, R. Amit, I. Braslavsky, A. B. Oppenheim, O. Gileadi, and J. Stavans, “Compaction of single dna molecules induced by binding of integration host factor (ihf),” *Proc. Natl. Acad. Sci. U.S.A.*, vol. 98, pp. 10658–63, Sep 2001.
- [30] I. M. Kulić, H. Mohrbach, V. Lobaskin, R. Thaokar, and H. Schiessel, “Apparent persistence length renormalization of bent dna,” *Physical review. E, Statistical, nonlinear, and soft matter physics*, vol. 72, p. 041905, Dec 2005.

- [31] G. Li, M. Levitus, C. Bustamante, and J. Widom, "Rapid spontaneous accessibility of nucleosomal dna.," *Nat. Struct. Mol. Biol.*, vol. 12, pp. 46–53, Dec 2004.
- [32] J. Widom, "A relationship between the helical twist of dna and the ordered positioning of nucleosomes in all eukaryotic cells," *Proc. Natl. Acad. Sci. U.S.A.*, vol. 89, pp. 1095–9, Feb 1992.
- [33] C. Hyeon, G. Morrison, and D. Thirumalai, "Force-dependent hopping rates of rna hairpins can be estimated from accurate measurement of the folding landscapes," *Proc Natl Acad Sci USA*, vol. 105, pp. 9604–9, Jul 2008.
- [34] Y. X. Mejia, H. Mao, N. R. Forde, and C. Bustamante, "Thermal probing of e. coli rna polymerase off-pathway mechanisms," *J. Mol. Biol.*, vol. 382, pp. 628–37, Oct 2008.



---

# Summary

Animals and plants are built from a large number of cells. These cells continuously respond to signals from outside and inside the cell by producing various kinds of proteins. The blueprints of these proteins are stored in genes. The genes, in cells with a nucleus, are carried in chromosomes: threadlike structures in the nucleus of a cell that become visible when the cell, upon dividing, condenses these structures. Chromosomes consist of roughly two parts: proteins, that take care of the condensation and DNA, carrying the genetic information of the cell. Without this condensation, the DNA in a human cell would never fit into the nucleus. During a cell division, DNA is compacted even more. The condensation has to be done in an orderly fashion so that the chromosomes can be replicated correctly at each cell division. Besides the compaction, the DNA still needs to be accessible for the expression of genes. The activity of genes can even be controlled by regulation of the DNA compaction. For a complete understanding of the regulation of DNA compaction, we need to understand, at molecular detail, not only the structure but also the dynamics of the compaction of DNA. At the first level of compaction, DNA winds around specific proteins, called histones. The DNA-histone complex is called a nucleosome. Another species of histone proteins, called linker histones are known to constrict the DNA exiting the nucleosome, thereby stabilizing the structure of the nucleosome. Under physiological conditions, arrays of nucleosomes fold into compact fibers called chromatin fibers. The transient structure of nucleosomes and the interaction between nucleosomes in a chromatin fiber, plays an important role in the compaction of DNA. We chose to use force spectroscopy, because this technique makes it possible to study the structure and dynamics of nucleosomes at the level of single molecules.

In chapter 2 we introduced a simple method for dynamic force spectroscopy using magnetic tweezers. This method allows application of sub-piconewton force on single molecules, by calibration of the applied force from the distance between a pair of magnets and a magnetic sphere, which is used to apply a force to a molecule. Initial dynamic force spectroscopy ex-

---

periments on DNA molecules revealed a large hysteresis in the force-extension curve. This hysteresis was caused by viscous drag on the magnetic bead making it impossible to measure the weak interactions between DNA and nucleosomes. Smaller beads decreased this hysteresis sufficiently to reveal intra-molecular interactions at sub-piconewton forces. Compared to typical quasi-static force spectroscopy our method is significantly faster, allowing the real time study of transient structures and reaction intermediates. As a proof of principle nucleosome-nucleosome interactions on a sub-saturated chromatin fiber were analyzed.

In chapter 3 we investigated the Brownian fluctuations of the magnetic sphere in a magnetic tweezers experiment. We measured the force induced unwrapping of DNA from a single nucleosome. We showed that hidden Markov analysis, adopted for the non-linear force-extension of DNA, can readily resolve unwrapping events that are significantly smaller than the Brownian fluctuations. The probability distribution of the height of the magnetic bead was used to accurately resolve small changes in contour length and persistence length of a DNA molecule containing a nucleosome. The latter is shown to be directly related to the DNA bending angle of the complex. The adapted hidden Markov analysis can be used for any transient DNA-protein complex and provides a robust method for the investigation of these transient events.

In chapter 4 we used magnetic tweezers to probe the mechanical properties of a single, well-defined array of 25 nucleosomes folded into a chromatin fiber. We found that the fiber stretched linearly like a Hookian spring to more than three times its starting length at forces up to 4 pN. This unexpected large extension points to a solenoid as the underlying topology of the chromatin fiber. Surprisingly, linker histones do not affect the length or stiffness of the fibers. They do stabilize the fiber at forces up to 7 pN. Fibers with a nucleosome repeat length of 167 basepairs instead of 197 basepairs are significantly stiffer, consistent with a two-start helical arrangement. The extensive thermal breathing of the chromatin fiber that is a consequence of the observed high compliance provides a structural basis for understanding the balance between compaction of DNA to fit into the cell core and the transparency of DNA to allow proteins to access the genetic information of the cell.

In chapter 5 we investigated the unexpected difference in the force needed for the unwrapping of the first turn and unwrapping of the second turn of nucleosomes in experiments on single nucleosomes and nucleosomes in a fiber. The forces needed to unwrap a single nucleosome were much smaller, 3 pN for the first turn and 6 pN for the second turn, than those for a nucleosome in a fiber, 6 pN and 18 pN respectively. We modeled a nucleosome-DNA-bead system, used in force spectroscopy experiments, as spheres and springs. We found that the thermal fluctuations of neighbouring nucleosomes stabilized the nucleosome thereby increasing the unwrapping force for a nucleosome in a fiber. This effect shows that results obtained for single nucleosomes cannot simply be extrapolated to a system containing multiple nucleosomes.



---

# Samenvatting

Dieren en planten bestaan uit een groot aantal cellen. Deze cellen reageren voortdurend op signalen van buiten en binnen de cel door diverse soorten eiwitten te maken. De bouwtekeningen van deze eiwitten zijn opgeslagen in de genen van de cel. De genen in cellen met een celkern bevinden zich in zogenaamde chromosomen: draadachtige structuren in de celkern die zichtbaar worden wanneer de cel, tijdens het delen, deze structuren condenseert. De chromosomen bestaan ruwweg uit twee onderdelen: eiwitten, die zorgen voor condensatie en DNA, de drager van de genetische informatie van de cel. Zonder condensatie zou het DNA van een menselijke cel nooit in de celkern passen. Bij een celdeling moet het DNA nog meer worden gecondenseerd. De condensatie moet op een ordelijke manier gebeuren zodat de chromosomen correct worden gedupliceerd bij iedere celdeling. Behalve dat het DNA compact moet zijn, moet het, voor de werking van de genen, nog wel toegankelijk zijn voor eiwitten. De cel moet het DNA dus kunnen opvouwen en weer ontvouwen. Dit opvouwen en ontvouwen kan zelfs gebruikt worden door de cel om de activiteit van de genen te reguleren. Voor een volledig inzicht in opvouwen en ontvouwen van DNA, moeten wij, in moleculair detail, niet alleen de structuur maar ook de dynamica van het opvouwen van DNA begrijpen. Op het eerste niveau van compactie, wikkelt DNA twee keer om specifieke eiwitten, histonen genaamd. Het DNA-histon complex wordt een nucleosoom genoemd. Een ander histon, het zogenaamde linker histon, bindt aan het DNA dat uit het nucleosoom komt, waardoor de structuur van het nucleosoom wordt gestabiliseerd. Onder fysiologische omstandigheden vouwt een lange ketting van nucleosomen zich tot een compacte vezel, die bekend staat als een chromatine vezel. De steeds veranderende structuur van nucleosomen en de interactie tussen nucleosomen in een chromatine vezel speelt een belangrijke rol in het opvouwen en ontvouwen van DNA. Wij hebben gekozen voor het gebruik van krachtspectroscopie omdat deze techniek het mogelijk maakt om de structuur en de dynamica van de nucleosomen op het niveau van enkele moleculen te bestuderen.

---

In hoofdstuk 2 introduceerden wij een eenvoudige methode om dynamische krachtspectroscopie op enkele moleculen uit te voeren, met behulp van een magnetisch pincet. Deze methode maakt het mogelijk om krachten kleiner dan een piconewton uit te oefenen op enkele moleculen, door de kracht te kalibreren aan de afstand tussen de magneten en de magnetische bolletjes waaraan wordt getrokken door het magnetische pincet. Bij de eerste dynamische krachtspectroscopie experimenten op DNA moleculen zagen wij een grote hysteresis in de kracht-uitrekkingscurve. Deze hysteresis werd veroorzaakt door de weerstand die het magnetische bolletje ondervond in water en zou het onmogelijk maken de zwakke interacties tussen DNA en eiwitten te meten. Kleinere bolletjes verminderden deze weerstand en dus de hysteresis waardoor het mogelijk werd intramoleculaire interactie te bestuderen bij krachten kleiner dan een piconewton. Onze methode is significant sneller dan de gebruikelijke quasi-statische krachtspectroscopie waardoor het mogelijk wordt snel veranderende structuren en tussenproducten van reacties te bestuderen. Als een eerste bewijs van onze methode hebben we de nucleosoom-nucleosoom interacties van niet volledig bezet chromatine geanalyseerd.

In hoofdstuk 3 onderzochten wij de Brownse beweging van het magnetisch bolletje in een magnetisch pincet. Wij bestudeerden het krachtsafhankelijke ontwikkelen van DNA van enkele nucleosomen met statische krachtspectroscopie. We lieten zien dat met verborgen Markov analyse, aangepast voor het niet-lineaire uitrekkings gedrag van DNA, lengteveranderingen in het DNA tijdens het ontwikkelen gemakkelijk geanalyseerd kan worden zelfs als die lengteveranderingen beduidend kleiner zijn dan de Brownse bewegingen. De waarschijnlijkheidsdistributie van de hoogte van het magnetische bolletje werd gebruikt om de contourlengte en persistentielengte van het DNA molecuul met een nucleosoom nauwkeurig te bepalen. Wij lieten zien dat de persistentielengte direct gerelateerd is aan de buigingshoek van het DNA dat uit het nucleosoom komt. De aangepaste verborgen Markov analyse kan voor ieder snel veranderend DNA-eiwit complex worden gebruikt en is een robuuste methode voor het onderzoek aan deze snel veranderende complexen.

In hoofdstuk 4 bestudeerden wij de mechanische eigenschappen van een reeks van 25 nucleosomen, gevouwen tot een chromatine vezel met behulp van een magnetisch pincet. De vezel rekte lineair, als een Hookse veer, uit tot meer dan drie keer de startlengte bij krachten tot 4 pN. Deze onverwacht grote uitrekking toont aan dat een chromatine vezel een enkele spiraal als onderliggende structuur heeft. Verrassend genoeg beïnvloeden linker histonen de lengte of de stijfheid van de vezels niet. Ze stabiliseerden de vezel wel tot krachten van 7 pN. De chromatine vezels met 167 baseparen DNA tussen de nucleosomen in plaats van 197 baseparen waren beduidend stijver en rekten minder ver uit, overeenkomend met twee in elkaar grijpende spiralen als structuur. De uitgebreide thermische ademhaling van de chromatine vezel, die een gevolg is van de waargenomen hoge flexibiliteit, vormt een basis voor het evenwicht tussen de

compactie van DNA om in de celkern te passen en de openheid van het DNA om uitgelezen te worden door eiwitten.

In hoofdstuk 5 onderzochten wij het onverwachte verschil tussen experimenten op enkele nucleosomen en nucleosomen in een chromatine vezel, in de kracht die nodig is voor het ontwikkelen van de eerste en de tweede wikkeling van het DNA in een nucleosoom. De benodigde kracht voor het ontwikkelen voor een enkele nucleosoom was veel kleiner, 3 pN voor de eerste wikkeling en 6 pN voor de tweede wikkeling, dan die voor nucleosoom in een vezel, respectievelijk 6 pN en 18 pN. Wij modelleerden het nucleosoom-DNA-bol systeem, zoals gebruikt is in de krachtspectroscopie experimenten, als bollen en veren. Wij vonden dat de thermische bewegingen van naburige nucleosomen een nucleosoom in een vezel stabiliseerden, waardoor de benodigde kracht voor het ontwikkelen ervan werd verhoogd. Dit effect toont aan dat de resultaten die voor enkele nucleosomen worden verkregen niet eenvoudig uit te breiden zijn naar een systeem dat meer dan één nucleosoom bevat.



---

# Curriculum Vitae

Maarten Kruithof was born in 1980 in Andernach, Germany. In 1998 he finished his second education at the Rijnlands Lyceum in Oegstgeest. In that same year he started his studies in applied physics at the University of Technology in Delft. After finishing his undergraduate studies he started working on the conductive properties of glass nanofluidic channels under the mentorship of Prof. Dr. C. Dekker. He also spend several months in the group of Prof. Dr. G. Whitesides at Harvard in Cambridge, USA. Here he created a system for microfluidic valving. in 2004 he received his MSc at the University of Technology in Delft.

From June 2004 till September 2008 he was affiliated to Leiden University as a PhD student. Here he joined the research group of Dr. Ir. J van Noort where he worked on magnetic tweezers based studies on nucleosomes and chromatin. During this period he was responsible for organising the biweekly seminar of the biophysics and monos groups. Furthermore, he lectured in the exercise classes belonging to an undergraduate course in classical mechanics.

From November 2008 he he joined the computer vision and statistics group of TNO Industry and technology where he does research on the analyses of camera images .



---

## List of Publications

Surface-charge-governed ion transport in nanofluidic channels, D. Stein, M. Kruithof and C. Dekker, *Physical Review Letters*, 2004, **93** (3): 035901

Torque-actuated valves for microfluidics, D.B. Weibel, M. Kruithof, S. Potenta, S.K. Sia, A. Lee, G.M. Whitesides, *Analytical Chemistry*, 2005, **77** (15): 4726-4733

Subpiconewton Dynamic Force Spectroscopy Using Magnetic Tweezers, M. Kruithof, F. Chien, M. de Jager and J. van Noort, *Biophysical Journal*, 2008, **94** (6): 2343-2348

Hidden Markov Analysis of Nucleosome Unwrapping Under Force, M. Kruithof and J. van Noort, accepted for publication in *Biophysical Journal*, 2009

Single molecule force spectroscopy reveals a highly compliant helical folding for the 30 nm chromatin fiber, M. Kruithof, F. Chien, A. Routh, C. Logie, D. Rhodes and J. van Noort, *Nature Structural and Molecular Biology*, 2009, May: online

